NASA CR-134901

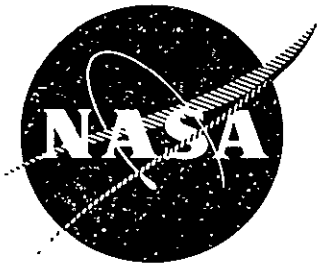

Optimization Of An Oxide Dispersion Strengthened Ni-Cr-Al Alloy For Gas Turbine Engine Vanes

D.L. Klarstrom and R. Grierson

October, 1975

Stellite Division

Cabot Corporation

Kokomo, Indiana

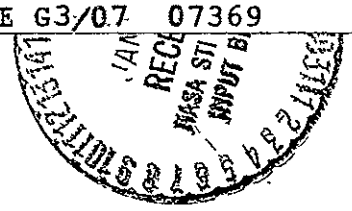

prepared for

NATIONAL AERONAUTICS AND SPACE ADMINISTRATION

NASA Lewis Research Center

Contract NAS 3-17806

Final Report

1. Report No.	2 Government Accession No.	3. Recipient's Catalog No.
NASA CR-134901		

4. Title and Subtitle	5 Report Date
Optimization of an Oxide Dispersion Strengthened Ni-Cr-Al Alloy for Gas Turbine Engine Vanes	October, 1975
	6. Performing Organization Code

7. Author(s)	8. Performing Organization Report No.
D. L. Klarstrom R. Grierson	
	10. Work Unit No.

9. Performing Organization Name and Address	11. Contract or Grant No.
Stellite Division Cabot Corporation 1020 W. Park Avenue Kokomo, IN 46901	NAS3-17806
	13. Type of Report and Period Covered

12. Sponsoring Agency Name and Address	13. Type of Report and Period Covered
	Contractor Report/Final
National Aeronautics and Space Administration Washington, D.C. 20546	14. Sponsoring Agency Code

15. Supplementary Notes

Project Manager: John D. Whittenberger, Materials and Structures Division
NASA-Lewis Research Center, Cleveland, Ohio 44135

16 Abstract

The investigation was carried out to determine the optimum alloy within the Ni-16Cr-Al-Y_2O_3 system for use as a vane material in advanced aircraft tas turbine engines. Six alloys containing nominally 4%, 5% and 6% Al with Y_2O_3 levels of 0.8% and 1.2% were prepared by mechanical attrition. Six small-scale, rectangular extrusions were produced from each powder lot for property evaluation. The approximate temperatures for incipient melting were found to be 1658°K (2525°F), 1644°K (2500°F) and 1630°K (2475°F) for the 4%, 5% and 6% aluminum levels, respectively. With the exception of longitudinal crystallographic texture, the eight extrusions selected for extensive evaluation either exceeded or were close to mechanical property goals. Major differences between the alloys became apparent during dynamic oxidation testing, and in particular during the 1366°K (2000°F)/500 hour Mach 1 tests carried out by NASA-Lewis. An aluminum level of 4.75% was subsequently judged to be optimum based on considerations of dynamic oxidation resistance, susceptibility to thermal fatigue cracking and melting point. An alloy of the selected aluminum content was then scaled up in the form of two full size, rectangular extrusions. The powder making method and the oxide content were modified in an effort to achieve the required combination of strength and low modulus texture in the extrusion direction. Two full size extrusions of experimental powders containing nominal additions of 0.9 Ta and 1.8 Ta for control of carbide formation were also produced. The tantalum-free extrusions were found to have stresses for 100 hour lives at 1366°K (2000°F) of 82.7 MPa (12 ksi) in the longitudinal direction and 34.5 MPa (5 ksi) in the transverse direction. An evaluation of texture in these two materials indicated that the longitudinal modulus of elasticity varied from the desired low range near the short ends of the rectangular cross section to an unacceptably high range at the center. It is concluded from these results that further experimentation is required to define an optimum heat treatment. The incorporation of tantalum into the alloy system for control of carbide formation was determined to be undesirable due to the detrimental effects of tantalum on melting point and texture development.

17. Key Words (Suggested by Author(s))	18. Distribution Statement
Mechanical Properties Oxide Dispersion Strengthened High Temperature Alloy Nickel-Chromium-Aluminum Alloy Mechanically Attrited Alloy Oxidation Resistant Alloy	Unclassified - Unlimited

19. Security Classif. (of this report)	20. Security Classif. (of this page)	21. No. of Pages	22. Price*
Unclassified	Unclassified		

* For sale by the National Technical Information Service, Springfield, Virginia 22151

TABLE OF CONTENTS

FIGURES

FIGURES (continued)

FIGURES (continued)

FIGURES (continued)

TABLES

TABLES (continued)

SUMMARY

The purpose of this investigation was to determine the optimum alloy composition, in terms of gas turbine vane applications, within the Ni-16Cr-Al-Y_2O_3 system and to produce this optimized material in the form of extruded vane blanks. The parameter used to define the optimum composition was primarily the material's dynamic oxidation resistance.

The program was composed of three tasks. In Task I, six alloys containing nominal aluminum contents of 4%, 5% and 6% with oxide levels of 0.8% and 1.2% were produced as mechanically attrited powders. These powders were characterized in terms of particle size, shape and chemical homogeneity. In Task II, six small scale, rectangularly shaped extrusions were produced from each powder lot in order that the dynamic oxidation resistance and the mechanical and physical properties of the various compositions could be evaluated.

The major differences noted between the alloys became apparent during dynamic oxidation testing, and especially during the 1366°K (2000°F)/500 hour Mach 1 tests carried out by NASA-Lewis. This test indicated that both the nominally 5% Al and nominally 6% Al materials had similar, and excellent, dynamic oxidation resistance while the nominally 4% Al materials had the least oxidation resistance of the three aluminum levels. Based upon these data and the fact that thermal fatigue cracking was more extensive in the highest Al content material, a 4.75% level was judged to be optimum.

A study of the recrystallization behavior of the extrusions revealed that a rapid heat treatment which consisted of placing the material directly into a furnace set at the recrystallization temperature was required to give a fully recrystallized grain structure. Unfortunately, this procedure resulted in longitudinal elastic moduli that were unacceptably high in all of the extrusions. For this reason, the optimum oxide level and processing conditions could not be identified.

In spite of the difficulty in obtaining a low modulus texture in the longitudinal direction, eight of the small scale extrusions were selected for further property evaluation in order to define an optimum aluminum content. No composition was judged to be clearly superior in terms of mechanical properties. All materials either exceeded or were close to 1366°K (2000°F) stress rupture strength goals of 100 hours at a stress of 82.7 MPa (12 ksi) in the longitudinal direction and 41.4 MPa (6 ksi) in the transverse direction.

The above results indicated that an aluminum level of 4.75% would provide excellent resistance to dynamic oxidation with low susceptibility to thermal fatigue cracking and the melting point of the selected composition would be at or above 1644°K (2500°F). This Al level was, therefore, chosen for use in the production of the full scale vane blanks.

In Task III, the 4.75% Al composition was scaled up in two full size, rectangularly shaped extrusions. Based on Stellite experience, the powder making method and the oxide level were modified in an effort to achieve the required combination of stress rupture strength and low, longitudinal elastic modulus. Two experimental heats containing nominal additions of 0.9% Ta and 1.8% Ta for control of carbide formation were also produced and extruded. Complete recrystallization was obtained in all of the extrusions using a slow heat treatment which consisted of heating the materials from 1477°K (2200°F) to 1616°K (2450°F) over a period of approximately 2 hours, holding for 1 hour at the maximum temperature, then cooling down. Modulus values determined from longitudinal pins taken near the short sides of the rectangular cross sections were in the desired low range (∿137.9 GPa or 20 x 10^6 psi) for the two tantalum-free extrusions and unacceptably high (∿200 GPa or 29 x 10^6 psi) for the two tantalum-containing extrusions. A further evaluation of grain structure and texture using macroetched transverse sections indicated that both of the tantalum containing materials possessed a core of large grains having a non-<100> texture. The two tantalum-free extrusions were found to have some non-<100> grains scattered through the cross section but more heavily concentrated near the center. The temperature ranges for melting in the tantalum-free and tantalum containing alloys were determined to be 1650-1655°K (2510-2520°F) and 1633-1639°K (2480-2490°F), respectively. Results of 1366°K (2000°F) stress rupture tests indicated that the tantalum-free extrusions had strength capabilities of 100 hours at 82.7 MPa (12 ksi) in the longitudinal direction and 34.5 MPa (5 ksi) in the transverse. The tantalum containing extrusions had longitudinal strengths of 50 hours at 82.7 MPa (12 ksi) and transverse strengths of greater than 100 hours at 34.5 MPa (5 ksi) but less than 100 hours at 41.4 MPa (6 ksi).

From these results it is concluded that the scaled up tantalum free extrusions have properties which either exceed or are close to those listed in section 1 of this report as being the objectives of this program. Further optimization of oxide level and heat treatment is necessary, however.

It is also concluded that the incorporation of tantalum to the alloy system for carbide control is not desirable due to the detrimental effects of tantalum on melting point and texture development.

INTRODUCTION

This investigation was undertaken to determine the optimum alloy composition, in terms of aluminum and oxide contents, within the Ni-16Cr-Al-Y_2O_3 system. The proposed application of such an alloy would be as a vane material in advanced aircraft gas turbine engines.

The materials studied represent a third generation of dispersion strengthened nickel-base alloys. The first two generations, represented by Ni-ThO_2 and Ni-20Cr-ThO_2, possessed excellent mechanical properties, but their resistance to high temperature, dynamic oxidation was limited. The third generation alloys overcame this deficiency by the inclusion of aluminum. However, it is known that the addition of aluminum complicates the response of these materials to thermomechanical processing and makes the obtaining of the required mechanical properties more difficult. This was regarded as the main problem to be solved in the program.

The initial work on the dispersion strengthening of the Ni-Cr-Al matrix was carried out, under NASA sponsorship, by Fansteel, Inc. (ref. 1). The alloy, which contained ThO_2 as the dispersoid, was first produced as a powder by means of a chemical process then consolidated by hot extrusion. In 1972 Fansteel ended its activities in dispersion strengthened materials and sold its patents in the area to Cabot Corporation. Concurrent with the Fansteel work on Ni-Cr-Al-ThO_2 alloys, the Stellite Division of Cabot Corporation began carrying out studies on a similar alloy with a nominal composition of Ni-16Cr-4Al-Y_2O_3 (HAYNES Developmental alloy 8077). The alloy was produced as a powder by means of mechanical attrition and then consolidated by hot extrusion. The work carried out in the current investigation was intended to build on both these previous efforts.

The primary objective of the program was to develop an ODS Ni-Cr-Al vane alloy capable of meeting the following property goals:

High temperature strength - Stress for a 100-hour life at 1366°K (2000°F) of 82.7 MPa (12 ksi) parallel to the extrusion direction and 41.4 MPa (6 ksi) in the long transverse direction.

Oxidation resistance - Less than 0.076 mm (0.003 inch) metal recession after a 500-hour exposure to high velocity gas (Mach 1) at 1366°K (2000°F) under cyclic test conditions.

Crystal texture - Low modulus texture with the <100> crystallographic direction parallel to the extrusion direction.

Ductility - Minimum of 5 percent tensile elongation at 1366°K (2000°F).

Fabricability - Alloy powder directly extrudable to vane blank or shape.

Stability - Dispersed phase stability comparable to commercial Ni-Cr-ThO_2 alloys.

Melting point - >1630°K (2475°F)

The program was composed of three technical tasks. In Task I, powders were prepared by mechanical attrition which contained nominal aluminum levels of 4%, 5% and 6% and Y_2O_3 levels of 0.8% and 1.2% making a total of six compositions. The nature of these powders was evaluated. In Task II, the powders were extruded at temperatures of 1255°K, 1311°K and 1366°K (1800°F, 1900°F and 2000°F) with nominal reduction ratios of 9:1 and 16:1 at each temperature, yielding a total of 36 extrusions. After an initial screening examination of the response of the extrusions to furnace recrystallization heat treatments, eight extrusions were selected for a detailed examination of mechanical properties and dynamic oxidation resistance. This work provided the basis for the production of four scaled-up extrusions in Task III. A detailed evaluation was carried out on the full size extrusions.

TASK I - PRODUCTION OF INITIAL POWDERS

Attrition of Powders

Six alloy powder compositions were prepared by mechanical attrition in approximately 36.3 kg (80 pound) lots using a 100S attritor. The target compositions of the six alloys are listed in Table I along with compositional limits recommended by Stellite. After attrition, each powder lot was screened and only the -30 mesh fraction was characterized and used.

Analysis of Attrited Powders

The actual chemical analyses of the six powder lots are listed in Table 2. Except for oxygen, the analyses for all elements were carried out by Stellite using techniques which are standard for superalloys. The oxygen analyses were performed by the Sterling Forest Laboratory of Union Carbide using the technique of fast neutron activation. As was anticipated, the powders were slightly different from the target compositions. However, agreement with the recommended compositional limits was quite good. Powder contaminants such as carbon, iron, nitrogen and sulfur were all at levels well below the maximum values recommended.

The particle size distribution of each powder lot was determined using a 454 gm (1 pound) sample of the -30 mesh fraction. The sieve nalysis was performed using screens having mesh Nos. 60, 120, 200, 250 and 325 (U.S. Standard series). The results are summarized in Table 3. The powders were relatively coarse typically 40-50% of the sample weight in the mesh size range of -30/+60. All lots had 98-99% of their total weight in the range of -30/+200. The attrited powder shapes were observed in two ways: (a) samples of each powder lot were mounted in copper Bakelite and examined optically and (b) samples of the powder were viewed using a scanning electron microscope. Photomicrographs of typical shapes observed are

TABLE 1

TARGET COMPOSITIONS AND RECOMMENDED COMPOSITIONAL LIMITS FOR TASK I POWDER LOTS

(Weight Percent)

Target Compositions

(a) Ni-16Cr-4Al-0.8Y_2O_3

(b) Ni-16Cr-4Al-1.2Y_2O_3

(c) Ni-16Cr-5Al-0.8Y_2O_3

(c) Ni-16Cr-5Al-1.2Y_2O_3

(d) Ni-16Cr-6Al-0.8Y_2O_3

(e) Ni-16Cr-6Al-1.2Y_2O_3

Recommended Compositional Limits

Element	Nominal Level	Limits
Chromium	16	15-17
Aluminum	4	3.7-4.2
Aluminum	5	4.7-5.2
Aluminum	6	5.7-6.2
Iron	0	Less than 1.5
Yttrium	0.95 (1.2 yttria)	0.8-1.1
Yttrium	0.63 (0.8 yttria)	0.5-0.7
Oxygen (total)	0.25 (1.2 yttria)	Less than 0.5
Oxygen (total)	0.17 (0.8 yttria)	Less than 0.4
Carbon	0	0.1 max.
Sulfur	0	0.01 max.

TABLE 2

CHEMICAL ANALYSES OF TASK I ATTRITED POWDERS

Wt. %	AT-196	AT-197	AT-198	AT-199	AT-200	AT-201
Al	4.16	4.18	4.82	5.00	5.69	6.09
C	.043	0.044	0.04	0.04	0.06	0.06
Cr	15.65	15.65	15.65	15.73	15.46	15.46
Fe	0.35	0.34	0.30	0.42	0.55	0.53
N	0.019	0.022	0.020	0.023	0.023	0.021
Ni	78.74	78.74	77.72	77.52	77.36	76.09
O (ppm)	3835	4340	4575	4390	4355	4945
S	<0.002	<0.002	<0.002	<0.002	<.002	<0.002
Y	0.64	0.80	0.86	0.74	0.66	0.80

Nominal Compositions:

AT-196	Ni-16Cr-4Al-0.8Y_2O_3
AT-197	Ni-16Cr-4Al-1.2Y_2O_3
AT-198	Ni-16Cr-5Al-1.2Y_2O_3
AT-199	Ni-16Cr-5Al-0.8Y_2O_3
AT-200	Ni-16Cr-6Al-0.8Y_2O_3
AT-201	Ni-16Cr-6Al-1.2Y_2O_3

TABLE 3

PARTICLE SIZE ANALYSES OF -30 MESH TASK I ATTRITED POWDERS
(454 gm sample weight)

U.S. Mesh No.	AT-196		AT-197		AT-198		AT-199		AT-200		AT-201	
	Wt. %	Cum. %	Wt. %	Cum. %	Wt. %	Cum. %	Wt. %	Cum. %	Wt. %	Cum. %	Wt. %	Cum. %
60	67.8	67.8	47.6	47.6	52.9	52.9	54.9	54.9	47.9	47.9	40.0	40.0
100	27.3	95.2	38.2	85.7	34.6	87.4	36.4	91.3	41.0	88.9	44.6	84.6
200	4.2	99.3	12.5	98.2	10.8	98.2	8.1	99.5	10.0	98.9	13.6	98.2
270	0.2	99.6	0.9	99.1	0.9	99.1	0.2	99.7	0.7	99.6	0.9	99.1
325	0.2	99.8	0.4	99.6	0.4	99.6	0.2	99.9	0.2	99.8	0.4	99.6
-325	0.2	100.0	0.4	100.0	0.4	100.0	0.1	100.0	0.2	100.0	0.4	100.0

Nominal Compositions: Ni-16Cr-

AT-196	4% Al, 0.8% Y_2O_3
AT-197	4% Al, 1.2% Y_2O_3
AT-198	5% Al, 1.2% Y_2O_3
AT-199	5% Al, 0.8% Y_2O_3
AT-200	6% Al, 0.8% Y_2O_3
AT-201	6% Al, 1.2% Y_2O_3

presented in Figures 1-4. The samples photographed represent the extremes in aluminum and oxide levels.

The metallographically prepared samples of each powder lot were also checked for chemical homogeneity using an electron microprobe. Several randomly selected particles of each mount were examined. Typical elemental scans for each powder lot are given in Figures 5-10. Occasional areas of concentration or depletion of the various elemental components, including the contaminant iron, were observed. For the most part, however, the area scans indicated that the powders were relatively homogeneous.

TASK II - ALLOY DEFINITION AND PROCESS DEVELOPMENT

Extrusion of Initial Powders

Six extrusion billets were prepared for each powder lot using the can design illustrated in Figure 11. Each billet contained approximately 1.8 kg (4 pounds) of -30 mesh powder. The cans were vibrated during loading to ensure that the fill density was as high as possible with uncompacted powder. Warm evacuation of the cans was carried out at 589°K (600°F) until the pressure stabilized at 3.33 Pa (25 μm). The temperature of the furnace was then raised to 1033°K (1400°F) and evacuation continued until a stable 3.33 Pa (25 μm) pressure level had again been achieved. The extrusion billets were then removed from the furnace, and the evacuation tubes were mechanically welded shut.

The 36 billets containing the Task I powders were extruded at Nuclear Metals, Inc., West Concord, Massachusetts, using a 12.46 MN (1400 ton) press equipped with a 7.78 cm (3.063 inch) liner. The extrusions were carried out through two rectangular dies intended to provide nominal reduction ratios of 9:1 and 16:1. The dies were uncoated tool steel containing 90 degree included angle integral entrance cones. Extrusions of each powder lot were carried out at each reduction ratio at temperatures of 1255°K, 1311°K and 1366°K (1800°F, 1900°F and 2000°F). The ram speed was 254 cm/min (100 in/min). A coating of Polygraph* was applied to the billets to minimize oxidation during furnace heat-up. On extrusion, Lube-A-Tube** lubricant was applied to the die and liner. The follower block employed was a graphite-mild steel assembly. A summary of the extrusion data is presented in Table 4.

Evaluation of Task II Extrusions

Oxygen Analysis

As a check for oxygen pick-up accompanying extrusion consolidation, a sample of one extruded bar from each powder composition was submitted for oxygen

---

* T. M. United International Research, Hauppauge, New York

** T. M. G. Whitfield Richards, Philadelphia, Pennsylvania

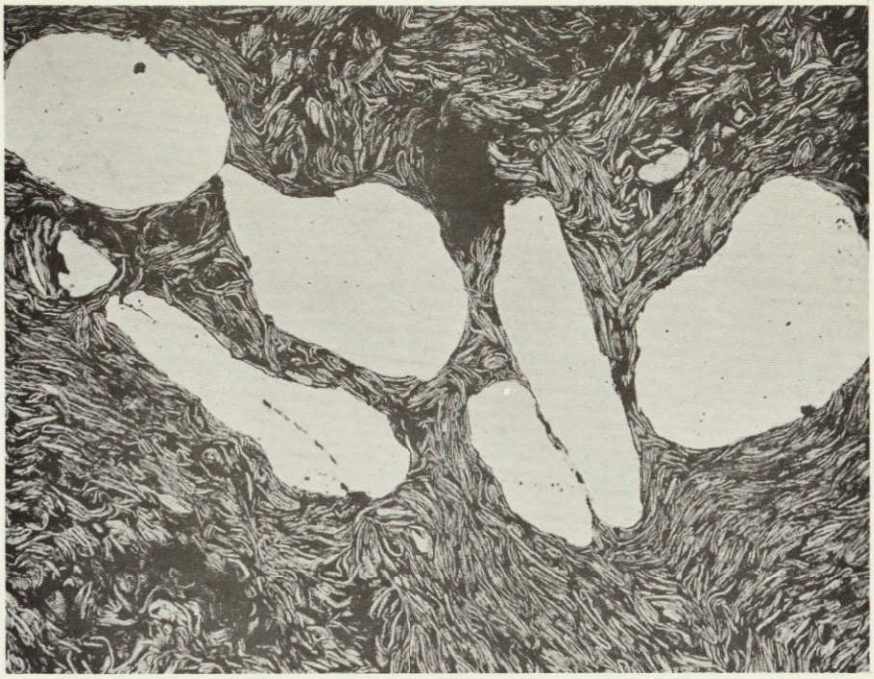

Figure 1: Heat No. AT-197 as-attrited powder - as polished - 100X

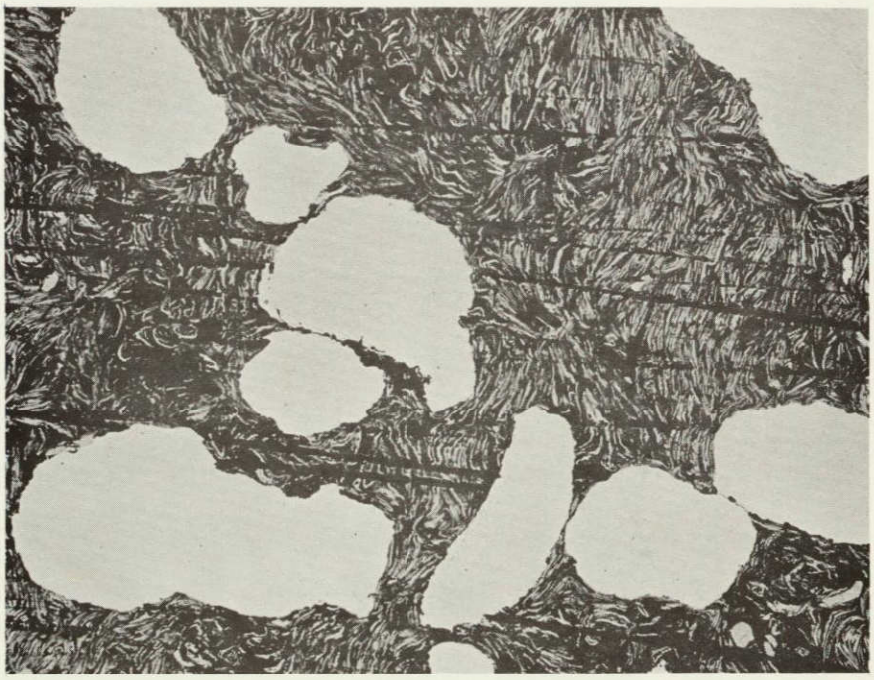

Figure 2: Heat No. AT-200 as-attrited powder - as polished - 100X

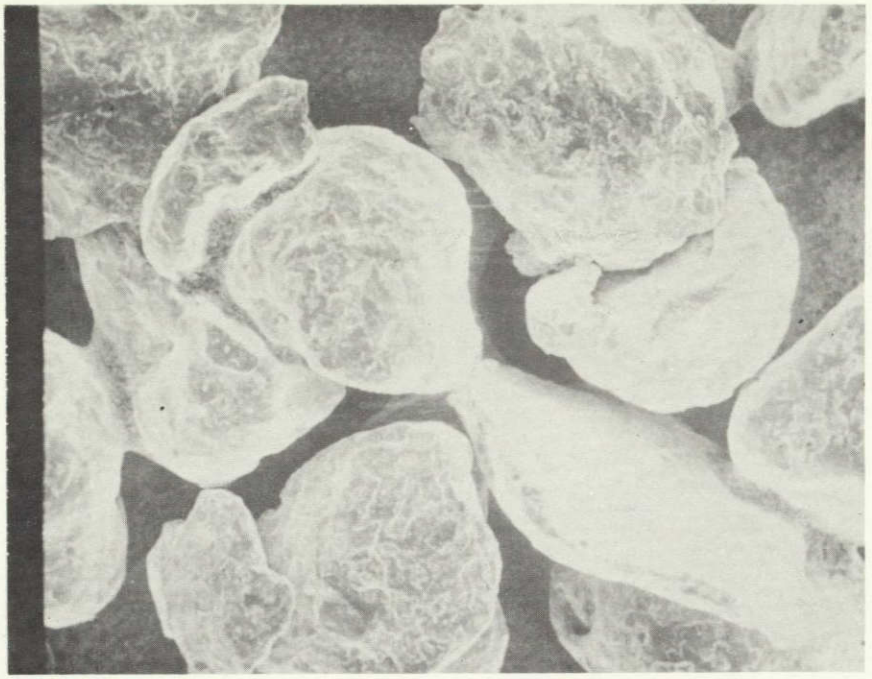

Figure 3: Scanning electron micrograph of Heat No. AT-196 as-attrited powder - 50X

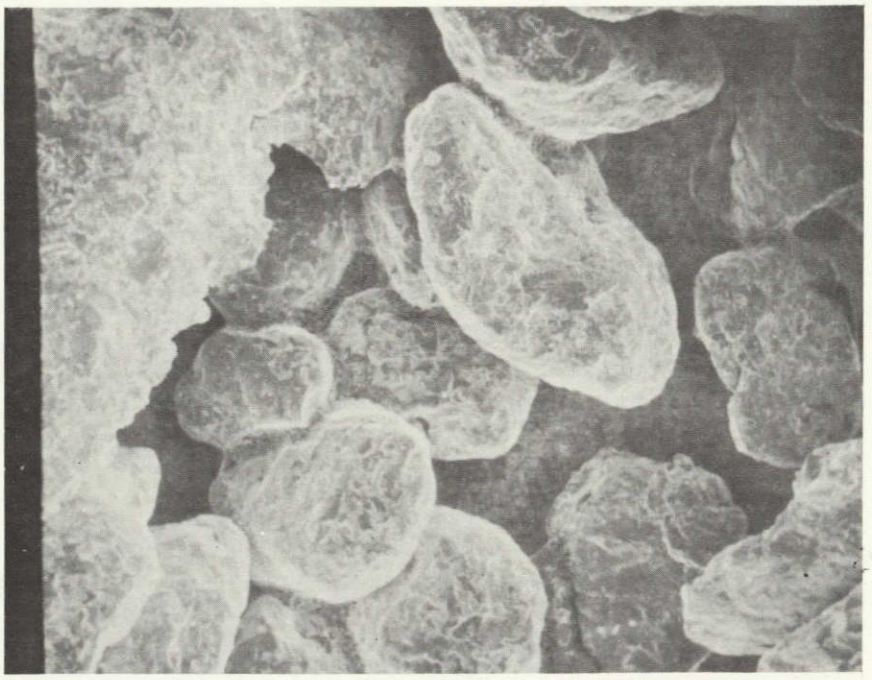

Figure 4: Scanning electron micrograph of Heat No. AT-201 as-attrited powder - 50X

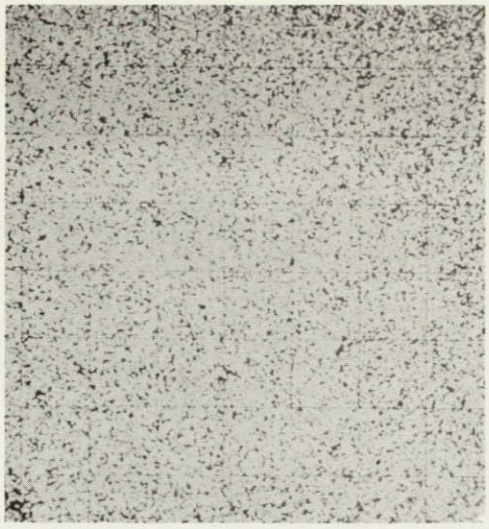

Ni

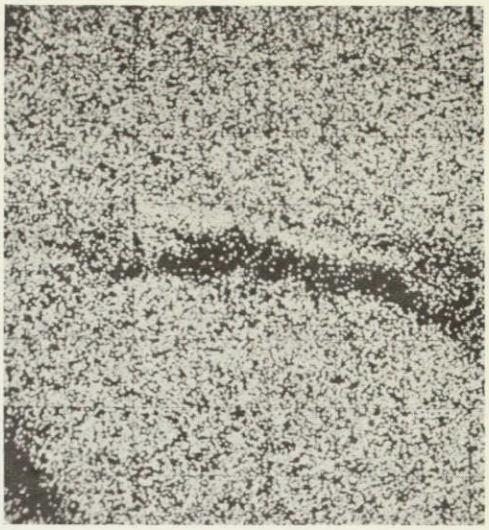

Cr

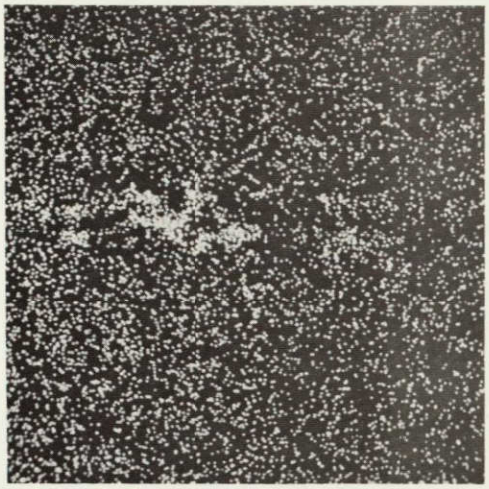

Al

Y

Fe

Figure 5: Elemental distribution mapping of AT-196 as-attrided powder. Nominal composition Ni-16Cr-4Al-0.8 Y_2O_3. Area measures .12 mm x .12 mm.

Ni

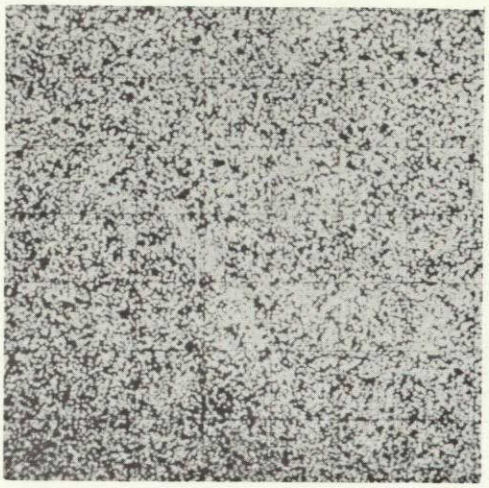

Cr

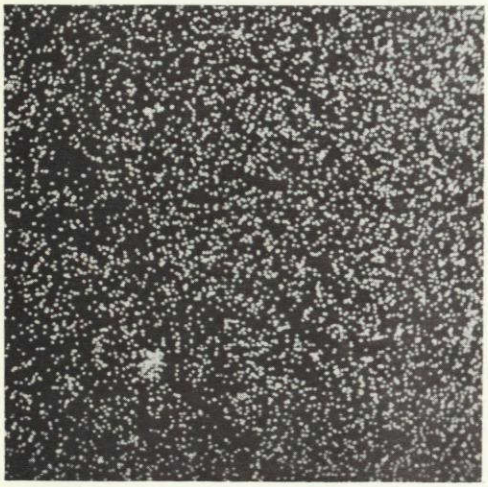

Al

Y

Fe

Figure 6: Elemental distribution mapping of AT-197 as-attrited powder. Nominal composition Ni-16Cr-4Al-1.2 Y_2O_3. Area measures .12 mm x .12 mm.

Ni

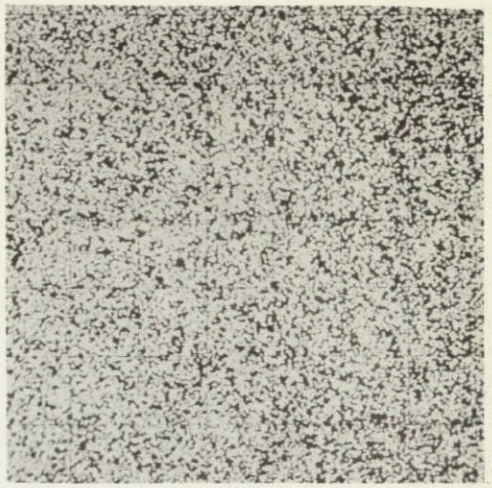

Cr

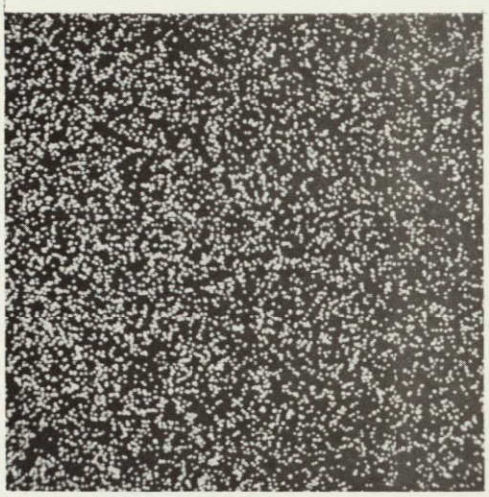

Al

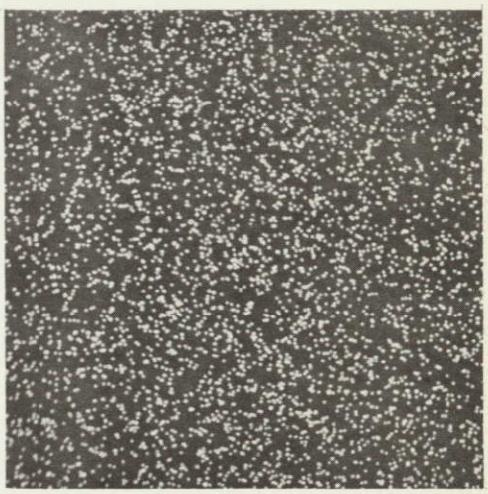

Y

Fe

Figure 7: Elemental distribution mapping of AT-198 as-attrided powder. Nominal composition Ni-16Cr-5Al-1.2Y_2O_3. Area measures .12 mm x .12 mm.

Ni

Cr

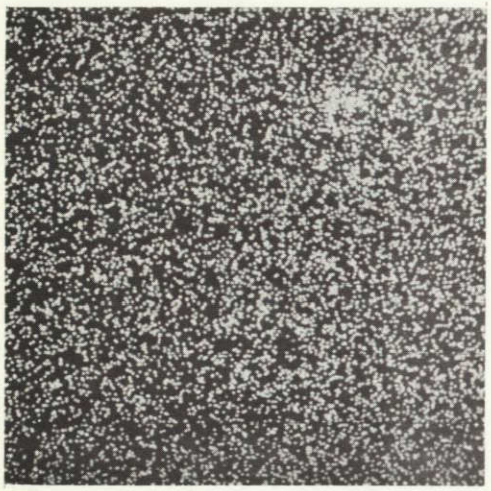

Al

Y

Fe

Figure 8: Elemental distribution mapping of AT-199 as-attrited powder. Nominal composition Ni-16Cr-5Al-0.8Y_2O_3. Area measures .12 mm x .12 mm.

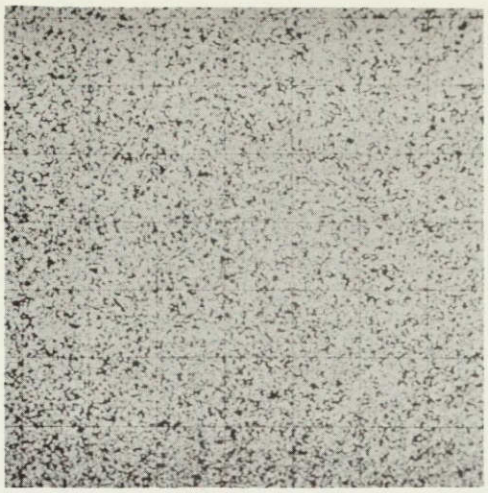

Ni

Cr

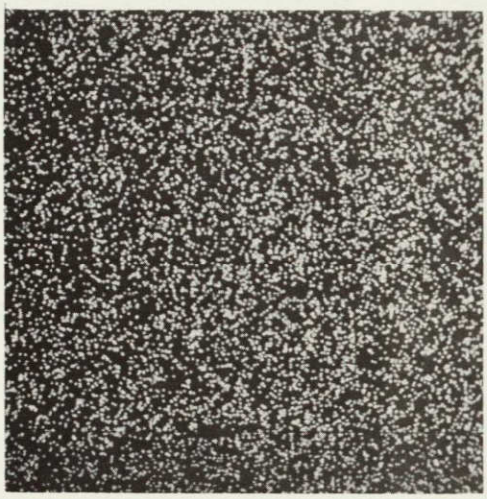

Al

Y

Fe

Figure 9: Elemental distribution mapping of AT-200 as-attrited powder. Nominal composition Ni-16Cr-6Al-0.8Y_2O_3. Area measures .12 mm x .12 mm.

Ni

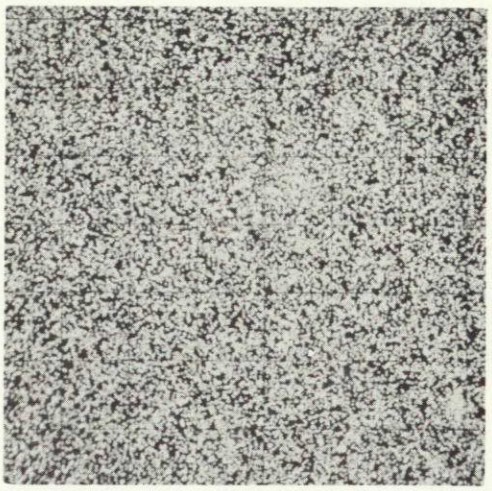

Cr

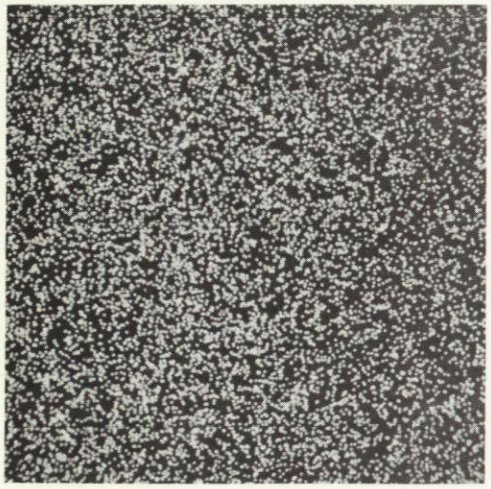

Al

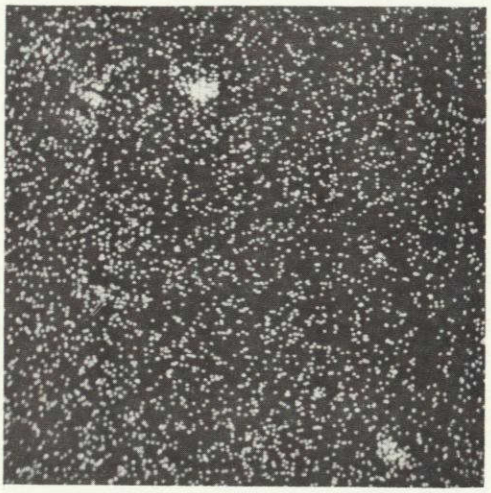

Y

Fe

Figure 10: Elemental distribution mapping of AT-201 as-attrited powder. Nominal composition Ni-16Cr-6Al-1.2Y_2O_3. Area measures .12 mm x .12 mm.

Figure 11: Mild Steel Extrusion Can

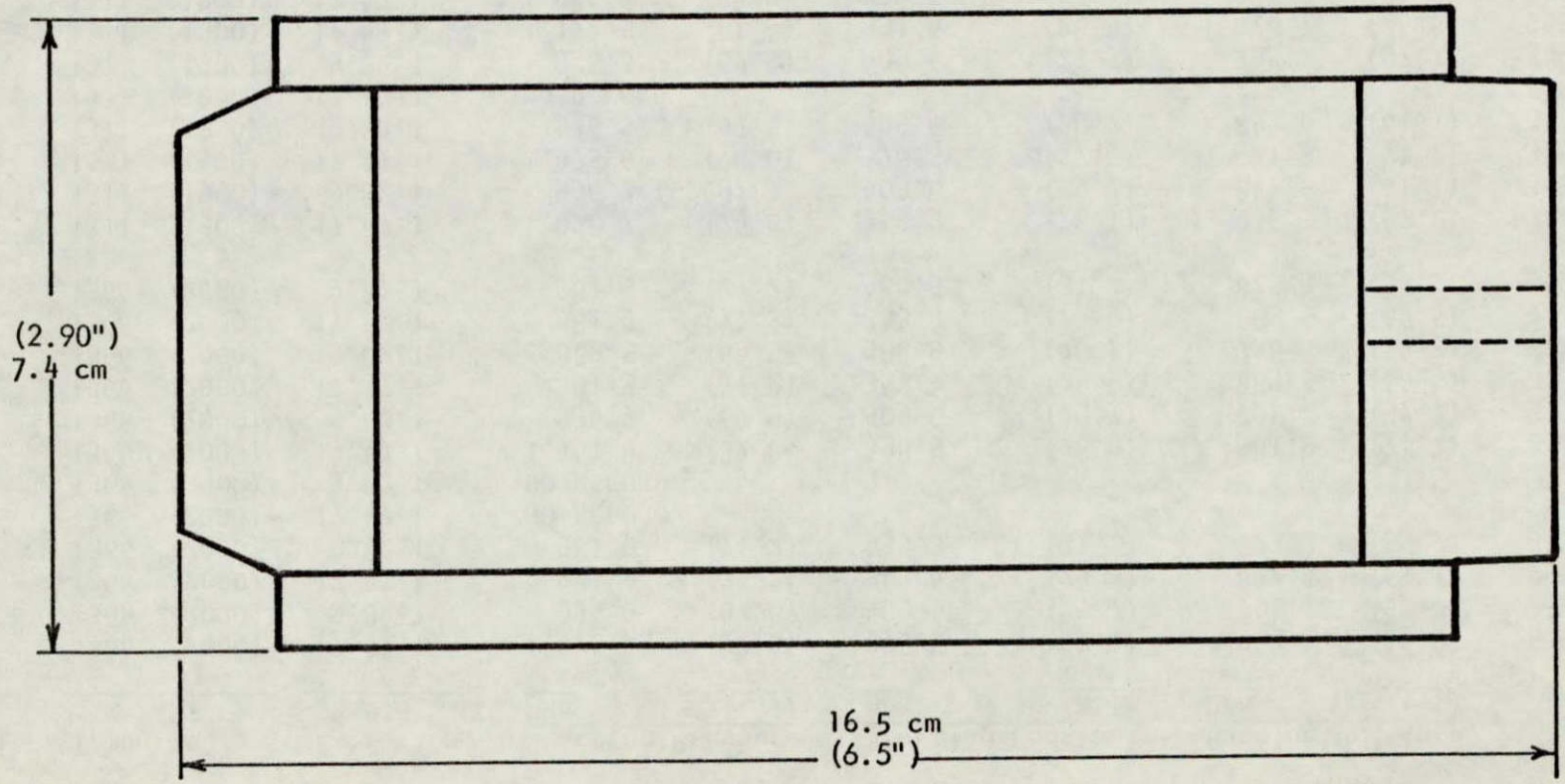

16.5 cm (6.5") long, 7.4 cm (2.90") diameter
Nose plug - 2.54 cm (1") long with 45° on front 1.27 cm (1/2")
Tail plug - 2.54 cm (1") long with .64 cm (1/4") diameter
evacuation hole

TABLE 4

SUMMARY OF TASK II EXTRUSION DATA

Extrusion No.	Temperature °K	(°F)	Extrusion Ratio	Starting Pressure MPa	(tsi)	Starting Constant MPa	(tsi)	Running Pressure MPa	(tsi)	Running Constant MPa	(tsi)
196HC	1366	(2000)	17.47:1	1,075.6	(78.0)	376.5	(27.3)	963.2	(69.9)	336.5	(24.4)
196LC	1366	(2000)	9.82:1	935.0	(67.8)	409.6	(29.7)	795.7	(57.7)	347.5	(25.2)
197HC	1366	(2000)	17.47:1	981.9	(71.2)	343.4	(24.9)	842.6	(61.1)	295.1	(21.4)
197LC	1366	(2000)	9.82:1	981.9	(71.2)	430.3	(31.2)	823.3	(59.7)	359.9	(26.1)
198HC	1366	(2000)	17.47:1	NO RECORD							
198LC	1366	(2000)	9.82:1	NO RECORD							
199HC	1366	(2000)	17.47:1	1,141.8	(82.8)	398.5	(28.9)	981.9	(71.2)	343.4	(24.9)
199LC	1366	(2000)	9.82:1	936.3	(67.9)	409.6	(29.7)	795.7	(57.7)	347.5	(25.2)
200HC	1366	(2000)	17.47:1	981.9	(71.2)	343.4	(24.9)	889.5	(64.5)	311.7	(22.6)
200LC	1366	(2000)	9.82:1	889.5	(64.5)	388.9	(28.2)	748.8	(54.3)	328.2	(23.8)
201HC	1366	(2000)	17.47:1	981.9	(71.2)	343.4	(24.9)	889.5	(64.5)	311.7	(22.6)
201LC	1366	(2000)	9.82:1	981.9	(71.2)	430.3	(31.2)	823.3	(59.7)	359.9	(26.1)
196HB	1311	(1900)	17.47:1	1,028.7	(74.6)	359.9	(26.1)	936.3	(67.9)	326.8	(23.7)
196LB	1311	(1900)	9.82:1	936.3	(67.9)	409.6	(29.7)	842.6	(61.1)	368.2	(26.7)
197HB	1311	(1900)	17.47:1	1,075.6	(78.0)	376.5	(27.3)	981.9	(71.2)	343.4	(24.9)
197LB	1311	(1900)	9.82:1	936.3	(67.9)	409.6	(29.7)	842.6	(61.1)	368.2	(26.7)
198HB	1311	(1900)	17.47:1	NO RECORD							
198LB	1311	(1900)	9.82:1	936.3	(67.9)	409.6	(29.7)	795.7	(57.7)	347.5	(25.2)
199HB	1311	(1900)	17.47:1	1,122.5	(81.4)	391.6	(28.4)	1,028.7	(74.6)	359.9	(26.1)
200HB	1311	(1900)	17.47:1	1,075.6	(78.0)	376.5	(27.3)	981.9	(71.2)	343.4	(24.9)
200LB	1311	(1900)	9.82:1	981.9	(71.2)	430.3	(31.2)	889.5	(64.5)	388.9	(28.2)
201HB	1311	(1900)	17.47:1	1,169.4	(84.8)	408.2	(29.6)	1,075.6	(78.0)	376.5	(27.3)
201LB	1311	(1900)	9.82:1	NO RECORD							

(continued)

TABLE 4 (continued)

Extrusion No.	Temperature °K	(°F)	Extrusion Ratio	Starting Pressure MPa	(tsi)	Starting Constant MPa	(tsi)	Running Pressure MPa	(tsi)	Running Constant MPa	(tsi)
196HA	1255	(1800)	17.47:1	1,075.6	(78.0)	376.5	(27.3)	1,010.8	(73.3)	353.0	(25.6)
196KA	1255	(1800)	9.82:1	936.3	(67.9)	409.6	(29.7)	795.7	(57.7)	347.5	(25.2)
197HA	1255	(1800)	17.47:1	1,075.6	(78.0)	376.5	(27.3)	981.9	(71.2)	343.4	(24.9)
197LA	1255	(1800)	9.82:1	936.3	(67.9)	409.6	(29.7)	842.6	(61.1)	368.2	(26.7)
198HA	1255	(1800)	17.47:1	1,975.6	(78.0)	376.5	(27.3)	981.9	(71.2)	343.4	(24.9)
198LA	1255	(1800)	9.82:1	936.3	(67.9)	409.6	(29.7)	795.7	(57.7)	347.5	(25.2)
199HA	1255	(1800)	17.47:1	1,975.6	(78.0)	376.5	(27.3)	1,010.8	(73.3)	353.0	(25.6)
199LA	1255	(1800)	9.82:1	981.9	(71.2)	430.3	(31.2)	766.7	(55.6)	335.1	(24.3)
200HA	1255	(1800)	17.47:1	1,159.7	(81.4)	391.6	(28.4)	1,028.7	(74.6)	359.9	(26.1)
200LA	1255	(1800)	9.82:1	936.3	(67.9)	409.6	(29.7)	842.6	(61.1)	368.2	(26.7)
201HA	1255	(1800)	17.47:1	1,975.6	(78.0)	376.5	(27.3)	981.9	(71.2)	343.4	(24.9)
201LA	1255	(1800)	9.82:1	917.0	(66.5)	401.3	(29.1)	842.6	(61.1)	368.2	(26.7)

analysis by fast neutron activation. The results are listed in Table 5. By comparing these values to the results on the corresponding powders, it can be concluded there was no additional oxygen pick-up. The fact that the powders have higher reported values is probably due to the degassing procedures. That is, the analyzed powder samples were cold degassed whereas the powders contained in the billets were hot degassed prior to extrusion consolidation.

Melting Ranges

The melting temperature range of each alloy composition was determined using furnace annealing treatments in combination with metallographic examination. Sections were cut from the centers of the extruded bars after the mild steel canning material had been removed by acid pickling. A sample of each material was then placed in a closely controlled furnace at a temperature which was estimated to be at or near its melting temperature and held for 30 minutes to establish thermal equilibrium. If the sample remained intact, it was withdrawn and rapidly cooled to room temperature. The sample was then prepared metallographically and examined for signs of incipient melting. If no signs of melting were observed, the experiment was repeated at a temperature 14°K (25°F) higher than the previous temperature. This procedure was followed until positive signs of melting were observed. If melting occurred in the initial experiment, the annealing temperature was lowered in 14°K (25°F) increments in subsequent trials until a temperature below the solidus was reached.

The results of the study are summarized in Table 6. The approximate melting temperatures for the nominal 4%, 5% and 6% aluminum levels were determined to be 1659°K (2525°F), 1644°K (2500°F) and 1630°K (2475°F), respectively. Thus, the temperature for the incipient melting was found to decrease with increasing aluminum content as was anticipated based on the general effect of aluminum additions on the melting points of other alloys.

Recrystallization Behavior

Based on the results of the melting range study, it was decided to carry out recrystallization heat treatments at 1616°K (2450°F) for Heats 196 through 199 and at 1588°K (2400°F) for Heats 200 and 201. A preliminary experiment was performed with several of the 1311°K (1900°F) extrusions to determine their response to a slow heat treatment: in furnace at 1478°K (2200°F) then raise the temperature to the maximum temperature and hold for one hour. After metallographic preparation, the specimens were electrolytically etched in a solution composed of 70 ml methanol, 48 ml glycerine and 10 ml nitric acid. Typical microstructures developed by this schedule are shown in Figures 12 and 13. In both examples, recrystallization did not go to 100% completion. Incomplete recrystallization appeared to be promoted by high oxide and high aluminum levels. Samples of the same extrusions were also given a rapid heat treatment which consisted of placing the material directly into a furnace set at the maximum recyrstallization temperature and holding for one hour. Comparison

TABLE 5

OXYGEN ANALYSIS OF TASK II EXTRUDED BAR
BY FAST NEUTRON ACTIVATION

Sample No.	Oxygen, ppm
196LA	3675
197LA	4175
198LA	4545
199LA	4085
200LA	4330
201LA	4385

TABLE 6

MELTING RANGE STUDY ON TASK II EXTRUDED BARS

Sample Heat No.	% Al Analyzed	Annealing Temperature (30 minute holding time) 1602°K (2425°F)	1616°K (2450°F)	1630°K (2475°F)	1644°K (2500°F)	1658°K (2525°F)
AT-196HB	4.16	No melting	No melting	No melting	No melting	Melted
AT-197HB	4.18	No melting	No melting	No melting	No melting	Melted
AT-198HB	4.82	No melting	No melting	No melting	Melting at G.B.	Melted
AT-199HB	5.00	No melting	No melting	No melting	Melting at G.B.	Melted
AT-200HB	5.69	No melting	No melting	No melting	Melted	--
AT-201HB	6.09	No melting	No melting	Melting at G.B. and grain interior	Melted	--

G.B. Grain Boundary

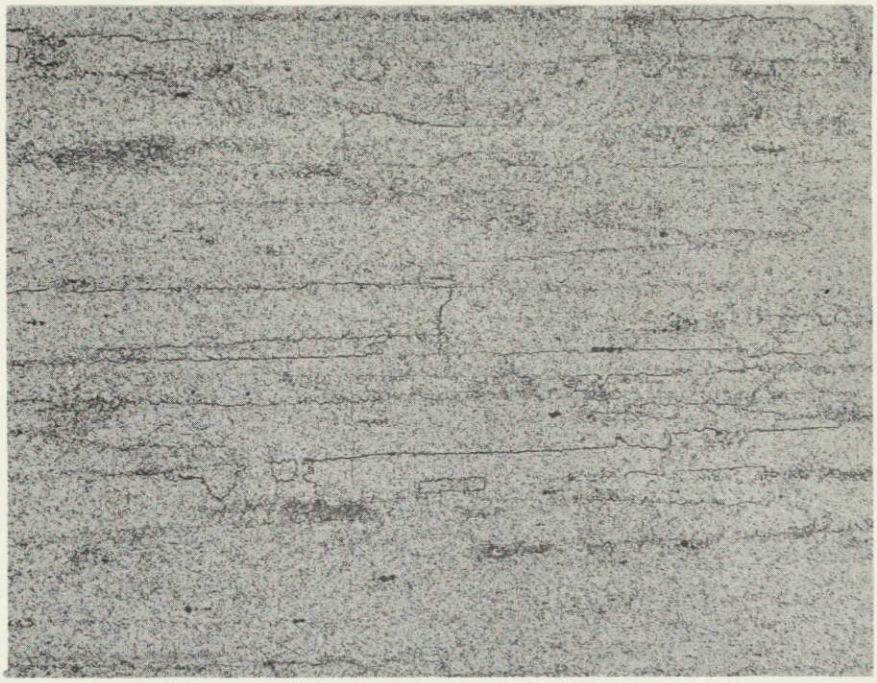

Figure 12: 196HB - furnace recrystallized - in at 1478°K (2200°F) → 1616°K (2450°F)/1 hour - magnification 100X

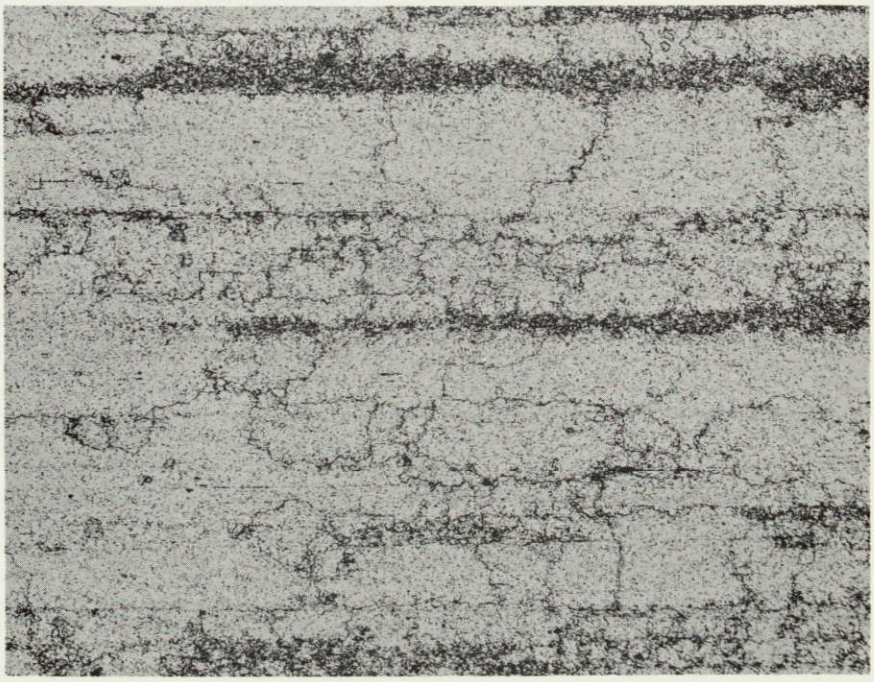

Figure 13: 199HB - furnace recrystallized - in at 1478°K (2200°F) → 1616°K (2450°F)/1 hour - magnification 100X

micrographs which illustrate the grain structures resulting from this procedure are given in Figures 14 and 15. In both cases, complete recrystallization was obtained.

The recrystallized structures obtained contained grains of differing shape to the extent that it was considered to be an over-simplification to ascribe a particular aspect ratio to a given structure. No attempt was made, therefore, in this or in subsequent metallographic evaluations, to characterize the materials in terms of grain aspect ratios.

To complement the initial recrystallization study, the longitudinal dynamic sonic moduli were determined for samples given both types of heat treatment. The specimens were 5.58 mm (.220 inch) diameter by 76.2 mm (3.0 inch) longitudinal, centerless ground pins as illustrated in Stellite Drawing No. 533463-05 in Appendix A. The results are listed in Table 7. Only the low oxide level, 4% Al extrusion developed a texture having a modulus within the desired low range, and this occurred via the slow heat treatment procedure. All other samples developed non-<100> textures for both heat treatment schedules as judged from the high modulus values obtained.

In view of the preliminary modulus findings, only extrusions of Heat AT-196 were given the slow heat treatment in completing the recrystallization study. A summary of the modulus values obtained is presented in Table 8. These results in conjunction with metallographic analysis bore out the conclusions of the initial study: slow heat treatment promoted a low modulus value but less than complete recrystallization while fast heat treatment gave the opposite results. Auxiliary experiments were also carried out to determine whether secondary working of the materials would enable the development of a fully recrystallized grain structure with a low longitudinal elastic modulus. Samples of the low ratio, 1366°K (2000°F) extrusions of each alloy composition were given a 20% reduction in thickness in one rolling pass at a temperature of 1311°K (1900°F). Metallographic analysis of the heat treated samples again revealed that only a fast heat treatment procedure provided complete recrystallization.

As the result of technical discussions held with the NASA Program Manager, eight of the extrusions were selected for mechanical property evaluation with the rapid heat treatment specified as the method of recrystallization. These materials are listed in Table 9. This selection afforded the evaluation of extrusions from each alloy composition having approximately the same modulus values in the high end of the range as well as two extrusions of differing aluminum contents in the low end of the modulus range. A summary of the recrystallized grain structures obtained in the extrusions selected is presented in Figures 14-21.

Observation of Dispersoid

Transmission electron microscopy was used to examine the dispersoid in the six Task II alloy compositions. The extrusions used for this purpose were among those selected for mechanical property evaluation. All specimens were examined in the fully recrystallized condition. Due to difficulties in retaining the dispersoid in the thin film because of its solubility in the polishing medium and difficulties in resolving particles at the fine end of the particle size range, no attempt was made to quantitatively determine

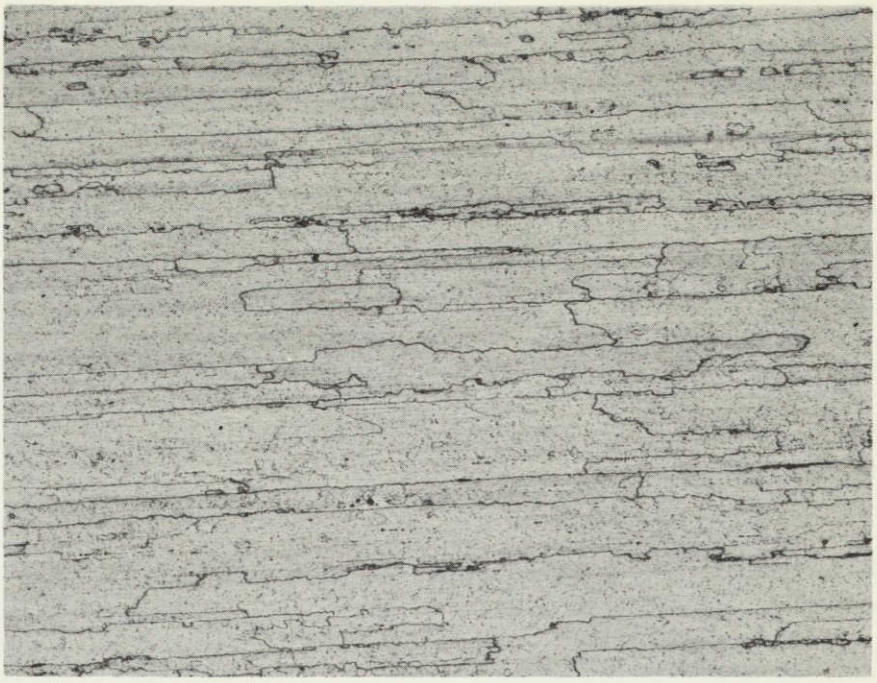

Figure 14: 196HB - furnace recrystallized - in at 1616°K (2450°F)/ 1 hour - magnification 100X

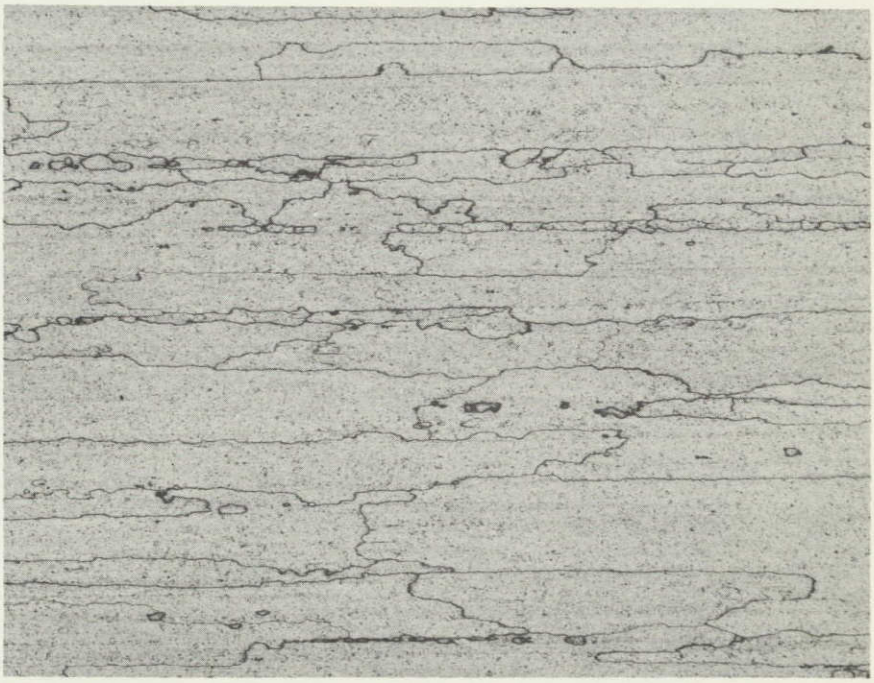

Figure 15: 199HB - furnace recrystallized - in at 1616°K (2450°F)/ 1 hour - magnification 100X

TABLE 7

ROOM TEMPERATURE DYNAMIC SONIC MODULI OF SELECTED TASK II EXTRUSIONS AS A FUNCTION OF HEAT TREATMENT SCHEDULE

Sample No.	Longitudinal Modulus of Elasticity, GPa (psi)	
	Slow H.T.	Rapid H.T.
196HB	146.17 (21.2×10^6)	188.23 (27.3×10^6)
197LB	170.99 (24.8×10^6)	209.60 (30.4×10^6)
199HB	172.37 (25.0×10^6)	170.30 (24.7×10^6)
200HB	217.18 (31.5×10^6)	199.26 (28.9×10^6)
201HB	243.38 (35.3×10^6)	222.01 (32.2×10^6)

TABLE 8

ROOM TEMPERATURE SONIC MODULI FOR TASK II EXTRUSIONS

Sample No.	Longitudinal Modulus of Elasticity GPa (psi)
196HA	177.88 (25.8 x 10^6)
196HC	149.62 (21.7 x 10^6)
196LA	202.02 (29.3 x 10^6)
196LB	153.06 (22.2 x 10^6)
196LC	155.13 (22.5 x 10^6)
197HA	151.00 (21.9 x 10^6)
197HC	184.09 (26.7 x 10^6)
197LA	193.05 (28.0 x 10^6)
197LB	193.05 (28.0 x 10^6)
197LC	193.05 (28.0 x 10^6)
198HA	193.74 (28.1 x 10^6)
198HB	168.92 (24.5 x 10^6)
198HC	189.61 (27.5 x 10^6)
198LA	207.53 (30.1 x 10^6)
198LB	188.23 (27.3 x 10^6)
198LC	189.61 (27.5 x 10^6)
199HA	173.75 (25.2 x 10^6)
199HC	188.23 (27.3 x 10^6)
199LA	206.15 (29.9 x 10^6)
199LB	197.88 (28.7 x 10^6)
199LC	195.12 (28.3 x 10^6)
200HA	203.40 (29.5 x 10^6)
200HC	189.61 (27.5 x 10^6)
200LA	211.67 (30.7 x 10^6)
200LB	211.67 (30.7 x 10^6)
200LC	200.64 (29.1 x 10^6)
201HA	200.64 (29.1 x 10^6)
201HC	195.12 (28.3 x 10^6)
201LA	217.10 (31.5 x 10^6
201LB	219.25 (31.8 x 10^6)
201LC	211.67 (30.7 x 10^6)

TABLE 9

TASK II EXTRUSIONS SELECTED FOR MECHANICAL PROPERTY EVALUATION

Extrusion No.	Longitudinal R.T. Modulus of Elasticity GPa (psi)
196HB	188.23 (27.3×10^6)
197LA	193.05 (28.0×10^6)
198HB	168.92 (24.5×10^6)
198LB	188.23 (27.3×10^6)
199HB	170.30 (24.7×10^6)
199LC	195.12 (28.3×10^6)
200HC	189.61 (27.5×10^6)
201HC	195.12 (28.3×10^6)

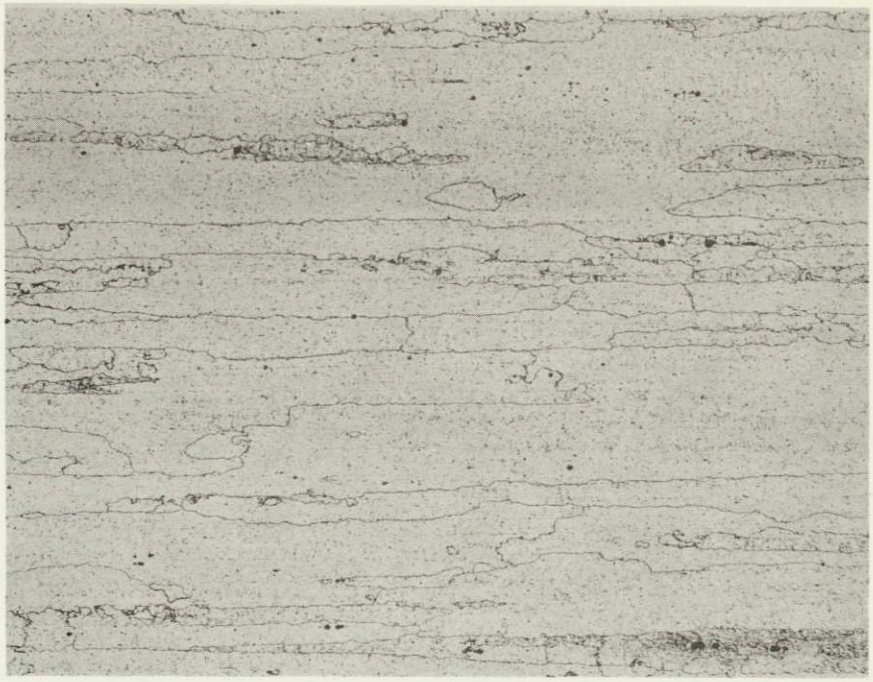

Figure 16: 197LA - furnace recrystallized - in at 1616°K (2450°F)/ 1 hour - magnification 100X

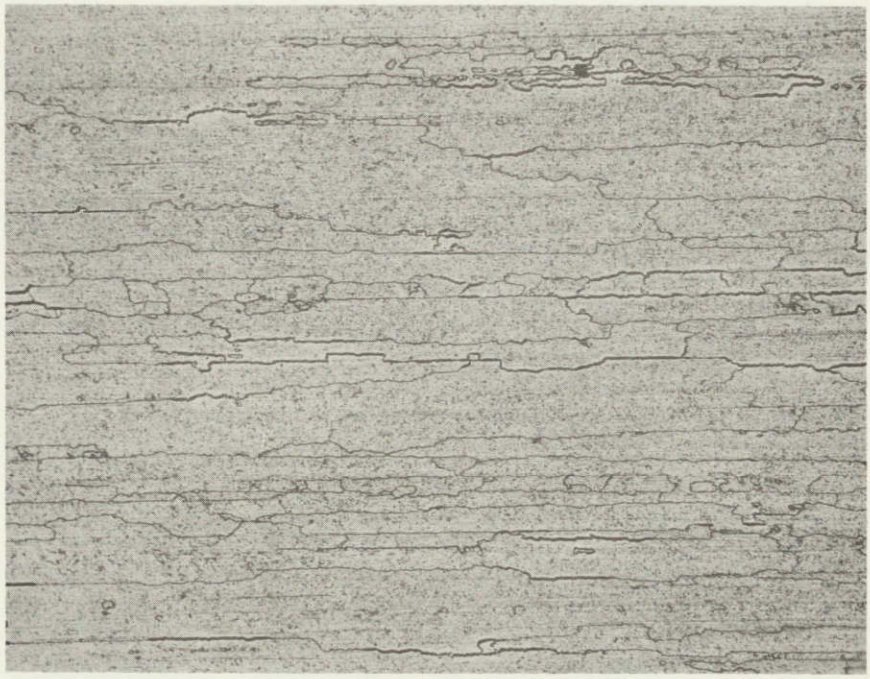

Figure 17: 198HB - furnace recrystallized - in at 1616°K (2450°F)/ 1 hour - magnification 100X

Figure 18: 198LB - furnace recrystallized - in at 1616°K (2450°F)/ 1 hour - magnification 100X

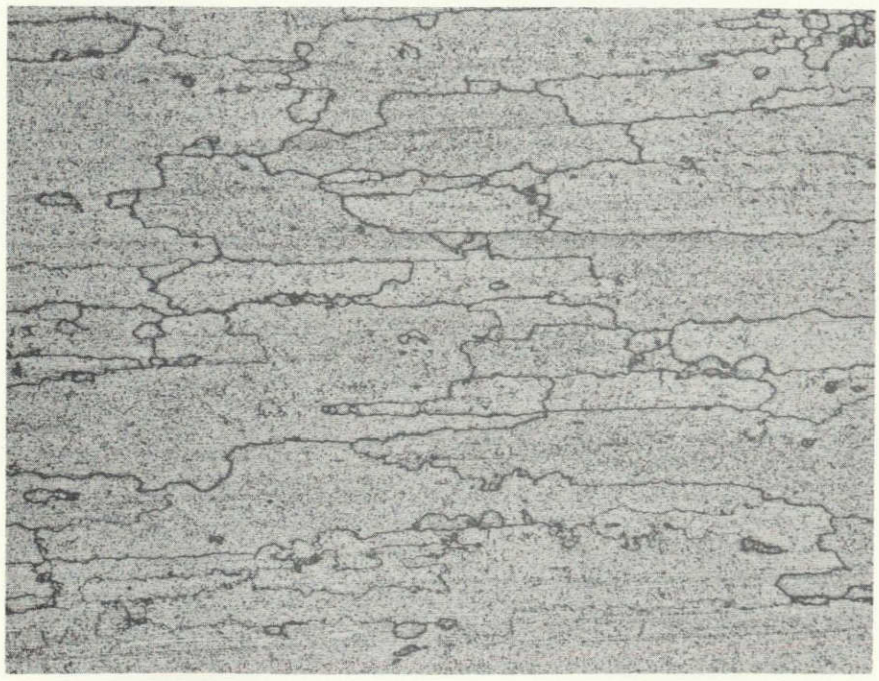

Figure 19: 199LC - furnace recrystallized - in at 1616°K (2450°F)/ 1 hour - magnification 100X

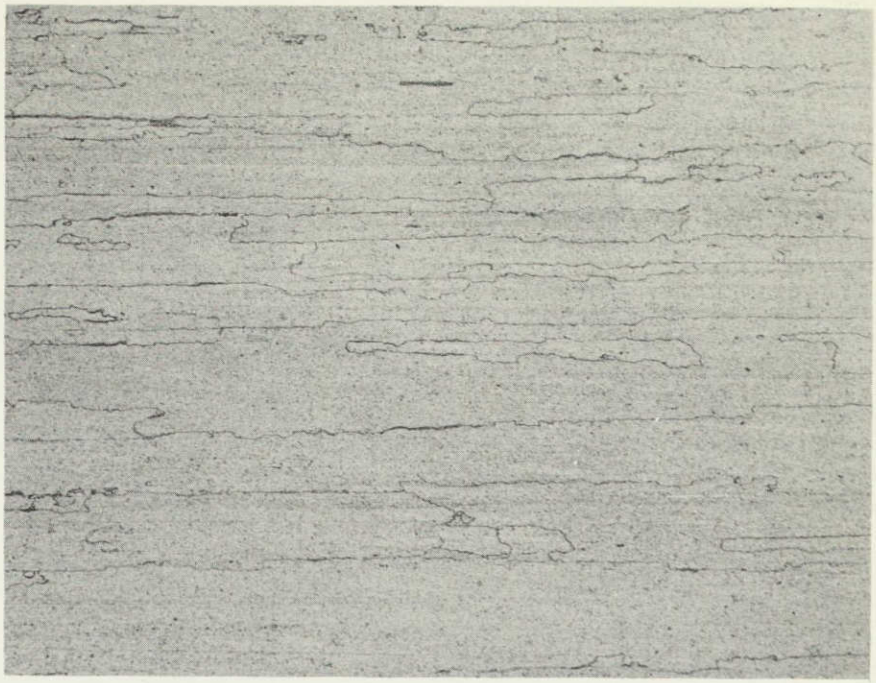

Figure 20: 200HC - furnace recrystallized - in at 1588°K (2400°F)/ 1 hour - magnification 100X

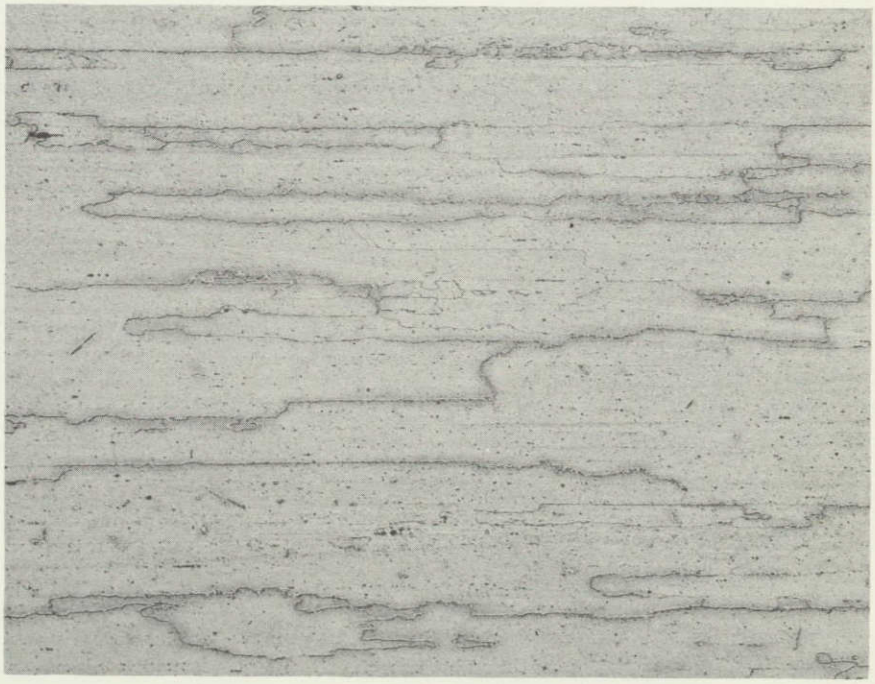

Figure 21: 201HC - furnace recrystallized - in at 1588°K (2400°F)/ 1 hour - magnification 100X

particle size distribution. However, the average particle size appeared to be approximately 250-500 Å. Typical electron micrographs of the dispersoid observed in the various alloys are given in Figures 22-27. The dispersoid was found to be uniformly distributed throughout each sample. The dislocation density was also observed to be very low.

Gamma Prime Phase Formation

Three samples representing the three different aluminum levels were investigated in terms of their tendencies to form the gamma prime phase. The selected samples were subjected to a heat treatment of 1144°K (1600°F) for 24 hours. Replicas of the heat treated samples were then examined in the electron microscope. Micrographs of typical areas in each sample are illustrated in Figures 28-30. The gamma prime phase was observed to form at each aluminum level, and the amount present increased with increasing aluminum content.

Tensile Properties

Duplicate longitudinal tensile tests were carried out at room temperature, 1144°K (1600°F) and 1366°K (2000°F) on the selected extrusions in the furnace recrystallized condition. The specimen configuration employed was that given in Stellite Drawing No. 561170 which is illustrated in Appendix A. The test results are summarized in Table 10. Generally, strength values tended to increase and ductility values decrease with increasing aluminum content. The largest differences were observed at the 1144°K (1600°F) test temperature. This was most likely due to the increasing amount of the gamma prime phase with aluminum content as noted in the previous section. At the 1366°K (2000°F) test temperature, all extrusions exhibited tensile strengths on the order of 103-124 MPa (15-18 ksi), and the differences between alloy compositions were not as great as those observed at the two lower temperatures. No noticeable differences in strength were observed with respect to differences in longitudinal elastic moduli.

Stress Rupture Properties

Stress rupture testing was carried out at 1366°K (2000°F) on duplicate longitudinal and transverse specimens in the furnace recrystallized condition. The longitudinal and transverse specimen configurations were in conformance with Stellite Drawings No. 561170 and 560274-209904, respectively, which are illustrated in Appendix A. The results are presented in Table 11. Some large variations time to rupture occurred for replicate tests in the transverse direction. This may have been due to difficulties in testing the necessarily miniaturized specimens. The best combination of longitudinal and transverse strength was achieved by extrusion 196HB which exceeded 82.7 MPa (12 ksi)/20 hours and 41.4 MPa (6 ksi)/20 hours in those respective directions. Strength values tended to degrade slightly with increasing aluminum content. However, the values attained at the 6% Al level which exceed 82.7 MPa (12 ksi)/20 hours in the longitudinal direction and 34.5 MPa (5 ksi)/20 hours in the transverse direction are still quite good. The longitudinal strengths obtained did not appear to be related to elastic modulus within the range studied.

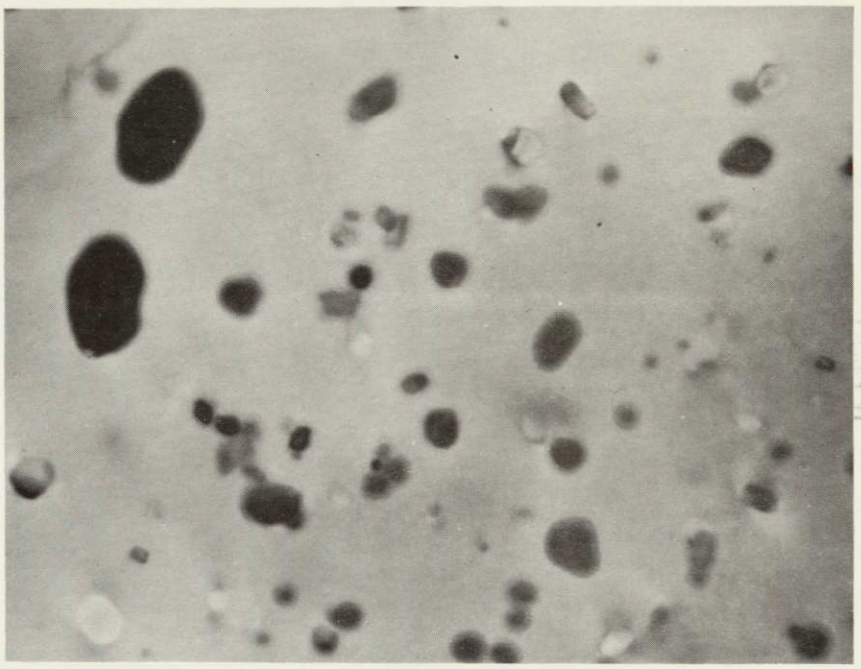

Figure 22: Dispersoid observed in extrusion 196HB - nominal composition Ni-16Cr-4Al-0.8Y_2O_3 - magnification 20,000X

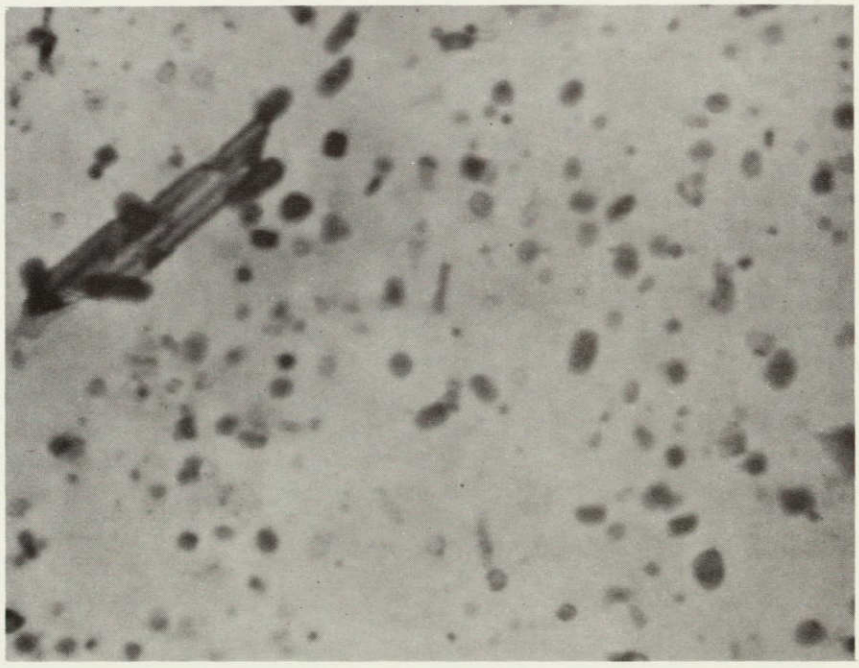

Figure 23: Dispersoid observed in extrusion 197LA - nominal composition Ni-16Cr-4Al-1.2Y_2O_3 - magnification 20,000X

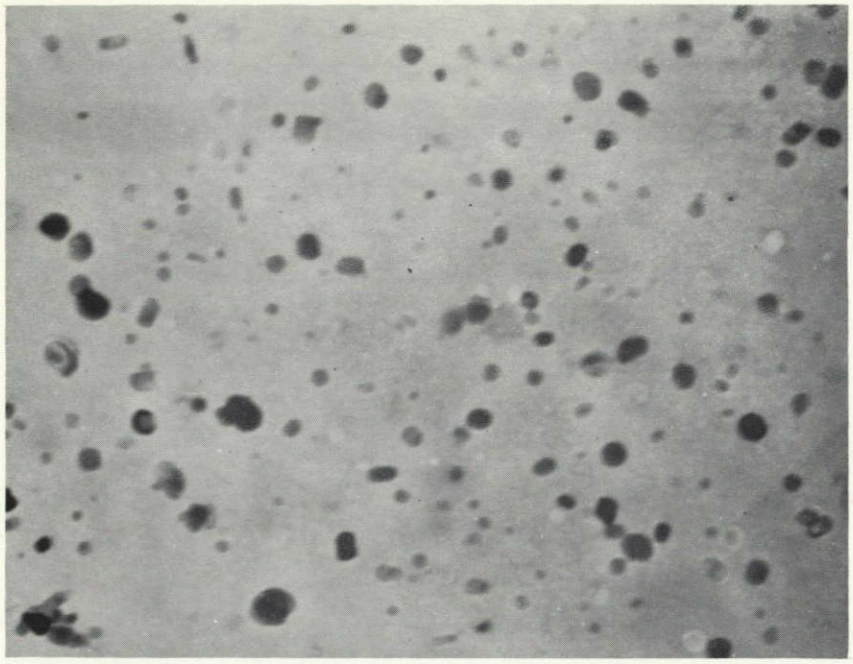

Figure 24: Dispersoid observed in extrusion 198LB - nominal composition Ni-16Cr-5Al-1.2Y_2O_3 - magnification 20,000X

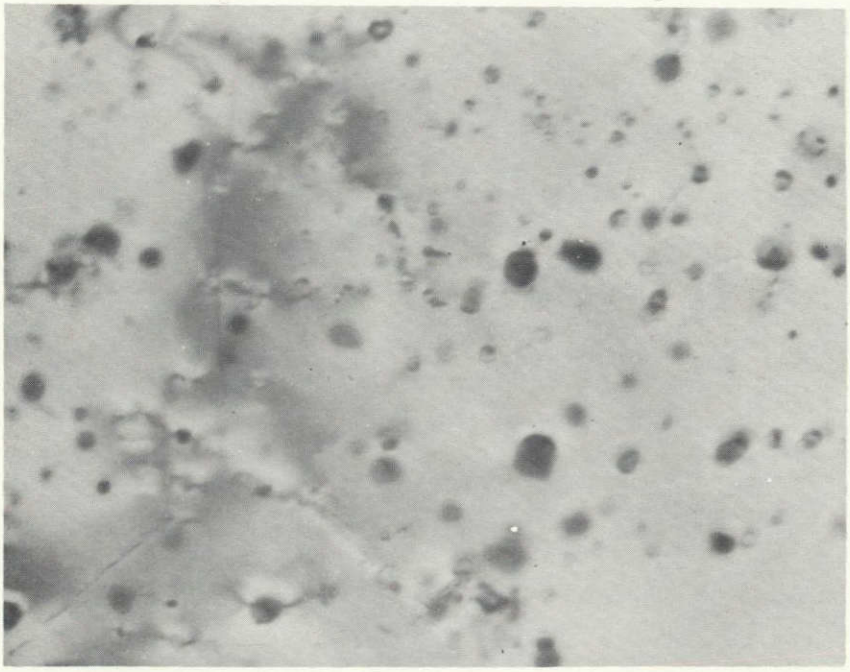

Figure 25: Dispersoid observed in extrusion 199HB - nominal composition Ni-16Cr-5Al-0.8Y_2O_3 - magnification 20,000X

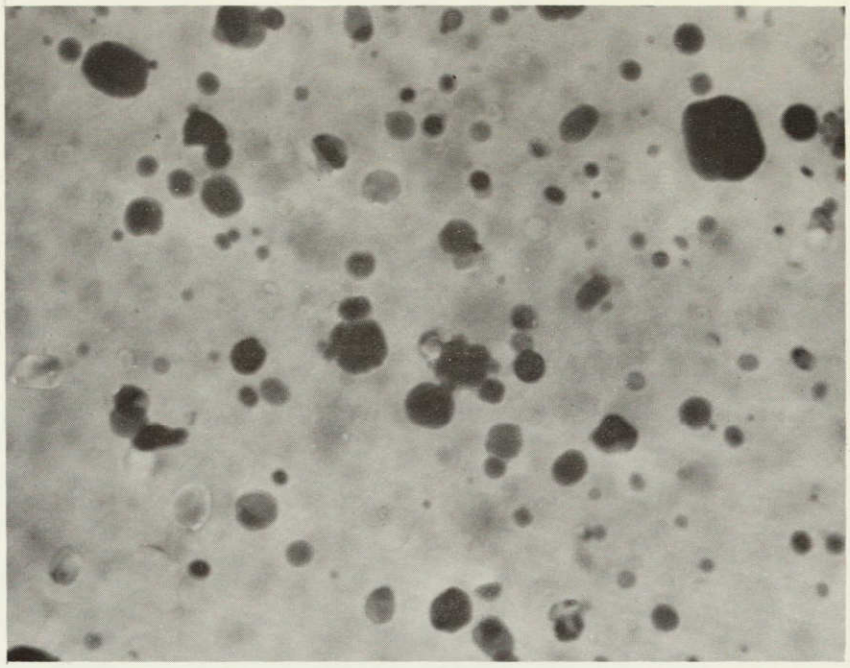

Figure 26: Dispersoid observed in extrusion 200HC - nominal composition Ni-16Cr-6Al-0.8Y_2O_3 - magnification 20,000X

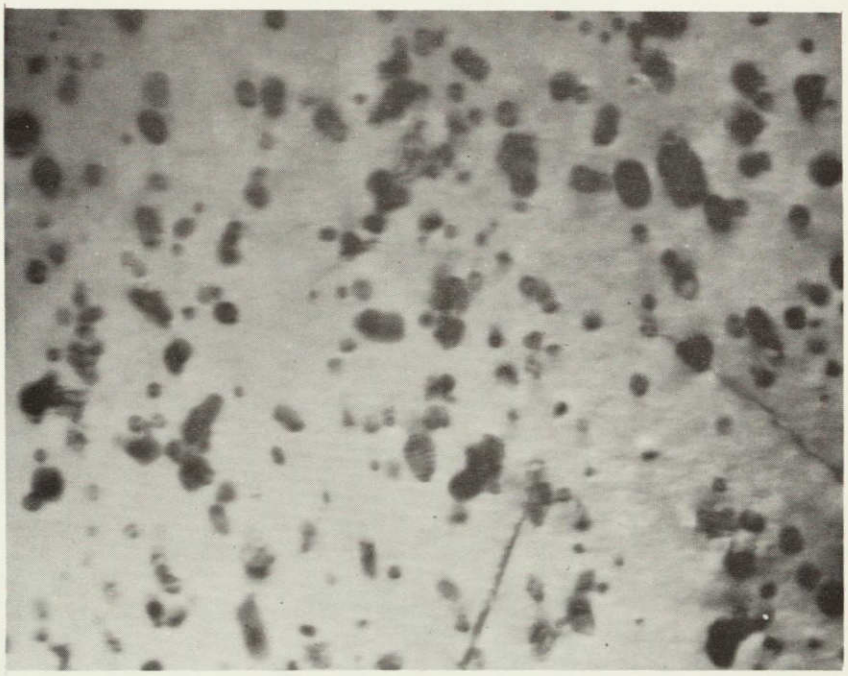

Figure 27: Dispersoid observed in extrusion 201HC - nominal composition Ni-16Cr-6Al-1.2Y_2O_3 - magnification 20,000X

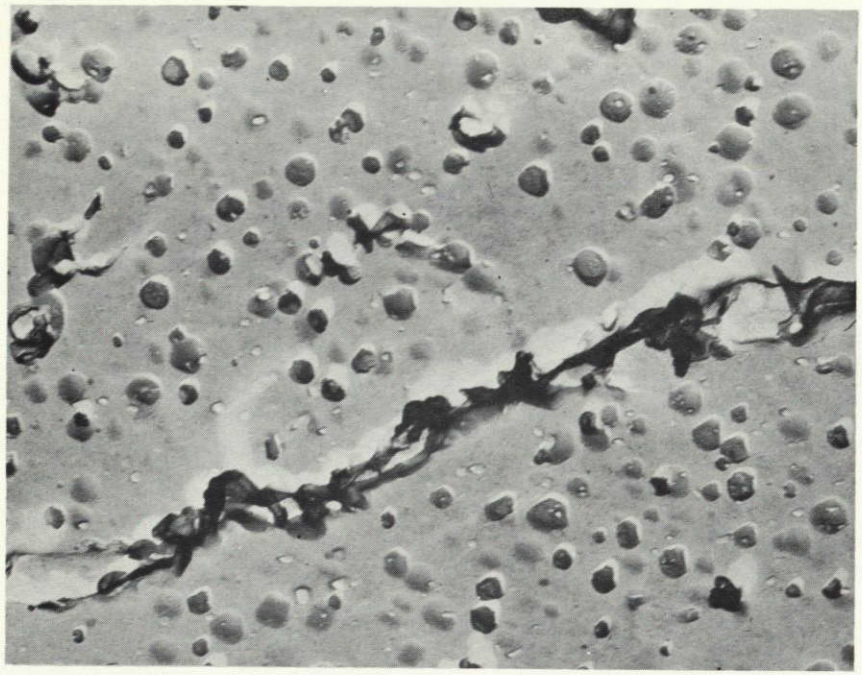

Figure 28: Gamma prime formation in extrusion 196HB - nominal aluminum level 4% - magnification 10,000X

Figure 29: Gamma prime formation in extrusion 199HB - nominal aluminum level 5% - magnification 10,000X

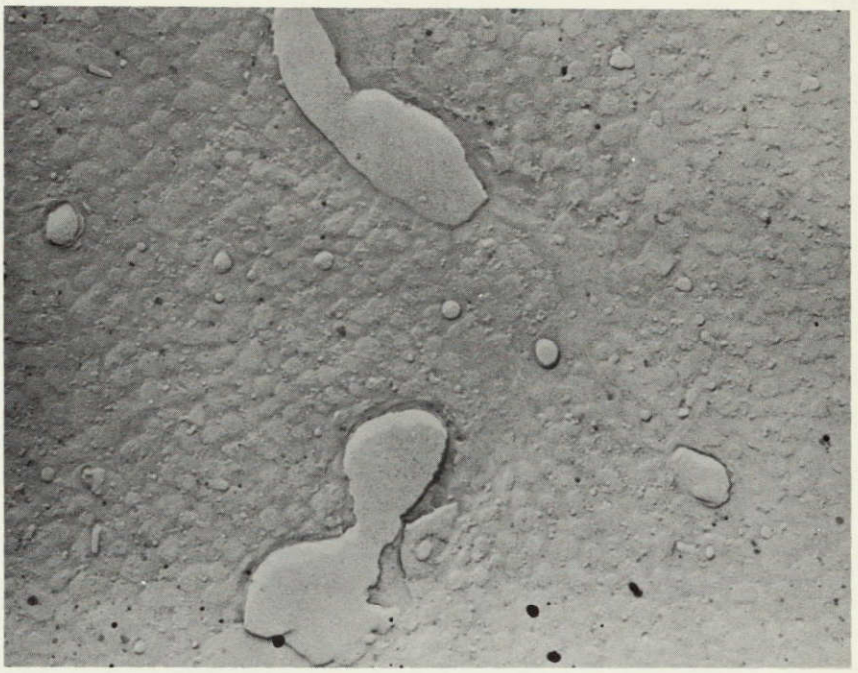

Figure 30: Gamma prime formation in extrusion 201HB - nominal aluminum level 6% - magnification 10,000X

TABLE 10

LONGITUDINAL TENSILE TEST RESULTS FOR SELECTED TASK II EXTRUSIONS

Extrusion No.	0.2% YS MPa	0.2% YS (ksi)	UTS MPa	UTS (ksi)	Elong. %	R.A. %
			Room Temperature			
196HB	760.5	(110.3)	1,085.9	(157.5)	18.3	22.0
	742.6	(107.7)	1,096.3	(159.0)	18.4	18.5
197LA	787.4	(114.2)	1,082.5	(157.0)	18.5	17.9
	777.0	(112.7)	1,077.0	(156.2)	18.9	16.9
198HB	884.6	(128.3)	1,150.0	(166.8)	14.4	14.0
	859.1	(124.6)	1,149.4	(166.7)	13.6	14.4
198LB	828.7	(120.2)	1,130.7	(164.0)	14.8	13.4
	869.4	(126.1)	1,125.2	(163.2)	14.4	10.0
199HB	855.6	(124.1)	1,158.3	(168.0)	10.4	10.5
	838.4	(121.6)	1,157.6	(167.9)	11.7	10.9
199LC	850.8	(123.4)	1,127.3	(163.5)	14.4	16.3
	868.0	(125.9)	1,128.7	(163.7)	14.4	18.7
200HC	851.5	(123.5)	1,131.4	(164.1)	12.0	10.1
	878.4	(127.4)	1,153.5	(167.3)	12.0	13.6
201HC	857.7	(124.4)	1,121.1	(162.6)	10.9	9.0
	870.1	(126.2)	1,098.3	(159.3)	9.9	9.0
			1144°K (1600°F)			
196HB	188.9	(27.4)	196.5	(28.5)	14.9	30.2
	174.4	(25.3)	185.5	(26.9)	16.5	27.5
197LA	207.5	(30.1)	213.0	(30.9)	8.7	15.4
	255.1	(37.0)	255.1	(37.0)	7.2	10.0
198HB	360.6	(52.3)	365.4	(53.0)	7.5	11.8
	370.2	(53.7)	383.3	(55.6)	6.4	7.0
198LB	379.2	(55.0)	382.0	(55.4)	5.5	6.0
	404.7	(58.7)	404.7	(58.7)	5.3	6.0
199HB	329.6	(47.8)	331.6	(48.1)	4.3	7.5
	308.2	(44.7)	310.3	(45.0)	6.3	5.9
199LC	352.3	(51.1)	354.4	(51.4)	7.5	14.3
	380.6	(55.2)	382.7	(55.5)	9.3	13.4

(continued)

TABLE 10 (continued)

Extrusion No.	0.2% YS MPa	0.2% YS (ksi)	UTS MPa	UTS (ksi)	Elong. %	R.A. %
		1144°K (1600°F) continued				
200HC	386.8	(56.1)	393.0	(57.0)	6.5	9.0
	424.0	(61.5)	457.1	(66.3)	6.4	10.1
201HC	442.6	(64.2)	466.1	(67.6)	3.9	4.0
	439.9	(63.8)	447.5	(64.9	4.1	2.8
		1366°K (2000°F)				
196HB	101.4	(14.7)	106.9	(15.5)	9.5	13.0
	99.3	(14.4)	107.6	(15.6)	8.4	11.5
197LA	125.5	(18.2)	125.5	(18.2)	5.5	2.5
	121.3	(17.6)	121.3	(17.6)	4.1	3.5
198HB	125.5	(18.2)	125.5	(18.2)	6.4	8.5
	121.3	(17.6)	122.7	(17.8)	6.7	7.5
198LB	115.1	(16.7)	115.1	(16.7)	5.9	5.5
	111.0	(16.1)	111.0	(16.1)	4.9	2.5
199HB	111.7	(16.2)	114.5	(16.6)	4.7	6.0
	116.5	(16.9)	121.3	(17.6)	5.7	7.5
199LC	103.4	(15.0)	109.6	(15.9)	9.2	21.4
	111.7	(16.2)	117.2	(17.0)	8.5	14.3
200HC	110.3	(16.0)	114.5	(16.6)	6.8	11.1
	111.7	(16.2)	115.1	(16.7)	8.7	11.1
201HC	108.9	(15.8)	113.1	(16.4)	7.5	6.8
	122.0	(17.7)	137.6	(18.5)	8.1	10.1

TABLE II

1366°K (2000°F) STRESS RUPTURE DATA FOR SELECTED TASK II EXTRUSIONS

Extrusion No.	Specimen Orientation	Time at Stress to Rupture Hours/MPa (ksi)	Elong. %
196HB	L	43.2/82.7 (12.0)	4.9
	L	45.7/82.7 (12.0)	6.5
	T	100/34.5 (5.0) + B.O.L.*/41.4 (6.0)	Void**
	T	47.9/41.4 (6.0)	Void
197LA	L	1.7/89.6 (13.0)	6.3
	L	17.1/82.7 (12.0)	4.8
	T	135.7/34.5 (5.0) + 24/41.4 (6.0) + 21.2/48.3 (7.0)	Void
	T	122.5/34.5 (5.0) + 42.8/41.4 (6.0) + 22/48.3 (7.0)	Void
198HB	L	41.1/82.7 (12.0)	11.2
	L	8.3/82.7 (12.0)	4.5
	T	118.9/34.5 (5.0) + 24/41.4 (6.0) + 0.3/48.3 (7.0)	Void
	T	59.3/34.5 (5.0)	Void
198LB	L	11.5/82.7 (12.0)	6.5
	L	7.7/82.7 (12.0)	4.0
	T	117.9/34.5 (5.0) + 24.1/41.4 (6.0) + 10.3/48.3 (7.0)	Void
	T	117.8/34.5 (5.0) + 23.4/41.4 (6.0) + 6.2/48.3 (7.0)	39.2
199HB	L	1.3/82.7 (12.0)	Void
	L	8.4/75.8 (11.0)	5.1
	T	18.2/34.5 (5.0)	Void
	T	160.1/34.5 (5.0) + 10.1/41.4 (6.0)	Void
199LC	L	11.2/82.7 (12.0)	6.3
	L	Discontinued after 88.6/75.8 (11.0)***	-
	T	38.8/34.5 (5.0)	29.9
	T	119.7/34.5 (5.0) + 26.1/41.4 (6.0) + 0.7/48.3 (7.0)	Void
200HC	L	84.4/82.7 (12.0)	7.1
	L	62.0/82.7 (12.0)	5.3
	T	57.4/34.5 (5.0)	20.8
	T	69.7/34.5 (5.0)	Void

TABLE 11 (continued)

Extrusion No.	Specimen Orientation	Time at Stress to Rupture Hours/MPa (ksi)	Elong. %
201HC	L	26.3/82.7 (12.0)	4.8
	L	16.1/82.7 (12.0)	3.3
	T	53.6/34.5 (5.0)	Void
	T	66.4/34.5 (5.0)	Void

* Broke on uploading

** Void due to multiple fracture

*** Discontinued due to failure of sample threads

Alloy Stability

As a check on alloy stability, duplicate tensile tests were carried out at 1366°K (2000°F) on samples which had been furnace recrystallized and then aged at 1589°K (2400°F) for 100 hours. The test results are presented in Table 12. In comparison to the data listed in Table 10, all the aged samples indicated a degradation in strength on the order of 34.5-55.2 MPa (5-8 ksi) which was accompanied by an increase in ductility. Metallographic examination of the broken tensile bars revealed the presence of small, nodular formations which were usually associated with grain boundaries. Judging from the lack of etching response, the matrix in the immediate vicinity of the nodules was depleted of dispersoid. Electron microprobe analysis indicated the presence of areas within the nodules having high levels of both aluminum and yttrium. An elemental scan of such an area is presented in Figure 31. This would tend to indicate that reactions to form various yttrium aluminate compounds occurred during aging. Electron microscopic examination of the sample representing the highest aluminum level (201HC) also revealed the presence of rod-shaped particles which were not noted to any appreciable extent in the unaged samples. An example of the particles observed is presented in Figure 32.

Although the results of the aging study indicated that a degradation in strength did occur, it should be noted that the test conditions were quite severe. The aging temperature selected was within approximately 55°K (100°F) of the respective incipient melting temperatures and the material was held at that temperature for an extended period of time. The data are certainly of interest from a design limitation point of view; however, the conditions imposed would probably never be encountered in the life of an actual engine. To gain a more realistic insight to aging capability, samples of extrusion 198HB were recrystallized and aged at 1477°K (2200°F) for 100 hours then stress rupture tested in the longitudinal direction at 1366°K (2000°F). The results are listed in Table 13. Although the values obtained were less than those reported in Table 11 for the unaged material, it can be concluded that the degradation in rupture strength was very minor.

Stellite Dynamic Oxidation Testing

Dynamic oxidation testing of the Task II alloy extrusions was carried out at Stellite using a flame tunnel type rig which provided a gas velocity of Mach 0.3. The combustible mixture was composed of air and No. 2 fuel oil in a weight ratio of approximately 54:1. The tests were carried out for 100 hours at temperatures of 1255°K (1800°F) and 1422°K (2100°F). Centerless ground pins previously used to measure the dynamic sonic moduli were used as the test specimens. One specimen of HAYNES alloy No. 188 was included in each test as a standard for comparison. The specimens were subjected to cycles of 30 minutes in the test chamber followed by a 2 minute air quench throughout the 100 hour test duration. Periodically, the specimens were removed and weighed to document weight changes. At the conclusion of each test, the specimens were sectioned, nickel plated and prepared metallographically to determine oxidation penetration. The definitions of the parameters determined by this examination are schematically illustrated in Figure 33.

TABLE 12

1366°K (2000°F) TENSILE TEST RESULTS FOR SELECTED TASK II EXTRUSIONS FURNACE RECRYSTALLIZED AND AGED AT 1589°K (2400°F) FOR 100 HRS

Sample No.	0.2% YS MPa	0.2% YS (ksi)	UTS MPa	UTS (ksi)	Elong. %	R.A. %
196HB	62.1	(9.0)	67.6	(9.8)	12.3	17.1
	67.6	(9.8)	72.4	(10.5)	13.3	14.6
197LA	71.0	(10.3)	74.5	(10.8)	8.0	10.9
	69.9	(10.1)	72.4	(10.5)	8.3	8.0
198LB	64.8	(9.4)	68.3	(9.9)	9.7	7.5
	66.9	(9.7)	73.1	(10.6)	9.5	11.1
199LC	62.1	(9.0)	66.2	(9.6)	13.2	19.0
	61.4	(8.9)	65.5	(9.5)	12.0	20.6
200HC	64.1	(9.3)	70.3	(10.2)	11.2	12.6
	66.9	(9.7)	70.3	(10.2)	10.7	12.6
201HC	58.6	(8.5)	63.4	(9.2)	11.7	12.6
	66.2	(9.6)	71.0	(10.3)	10.1	13.6

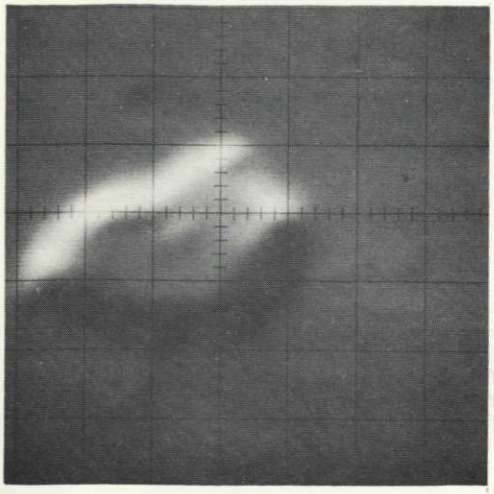

BSE

Ni

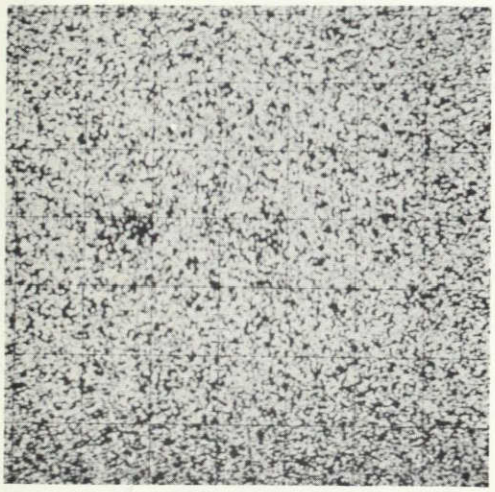

Cr

Fe

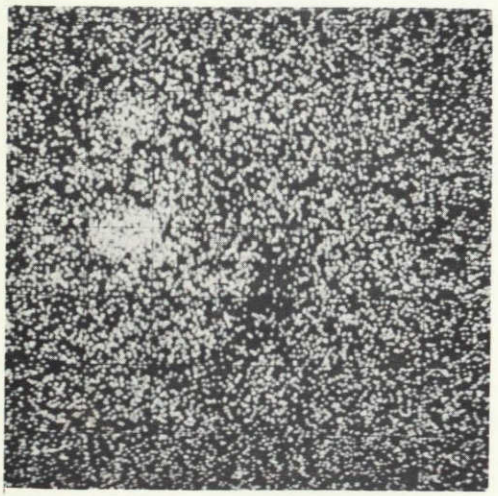

Al

Y

Figure 31: Elemental distribution scan of nodular formation in extrusion 201HC after aging at 1589°K (2400°F) for 100 hours.

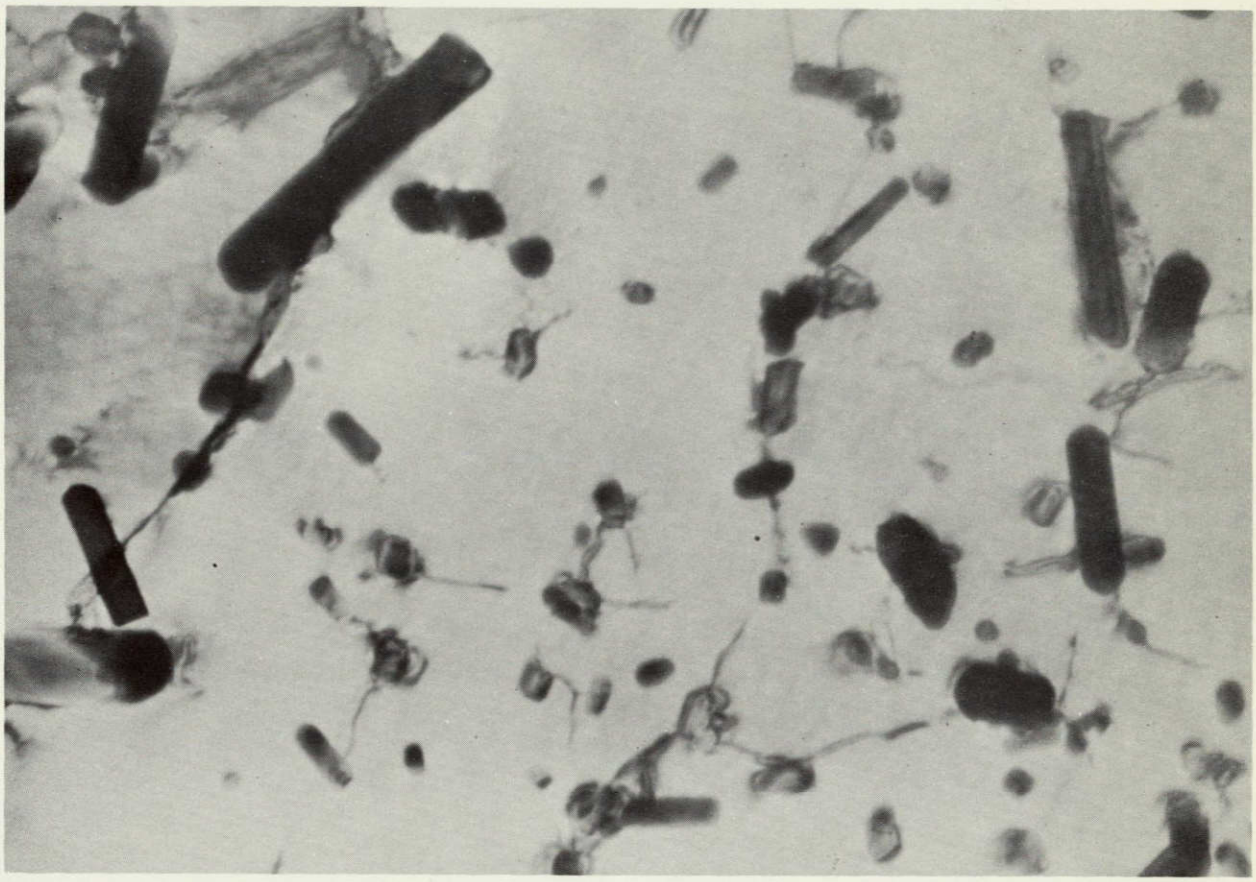

Figure 32: Rod shaped particles observed in extrusion 201HC aged at 1589°K (2400°F) for 100 hours - magnification 40,000X

TABLE 13

LONGITUDINAL STRESS RUPTURE TEST RESULTS AT 1366°K (2000°F) FOR EXTRUSION 196HB FURNACE RECRYSTALLIZED AND AGED AT 1477°K (2200°F) FOR 100 HOURS

Stress		Rupture Life	Elong.	R.A.
MPa	(ksi)	Hours	%	%
82.7	(12.0)	8.5	5.7	3.5
82.7	(12.0)	12.3	4.9	2.5
82.7	(12.0)	36.3	3.3	1.0

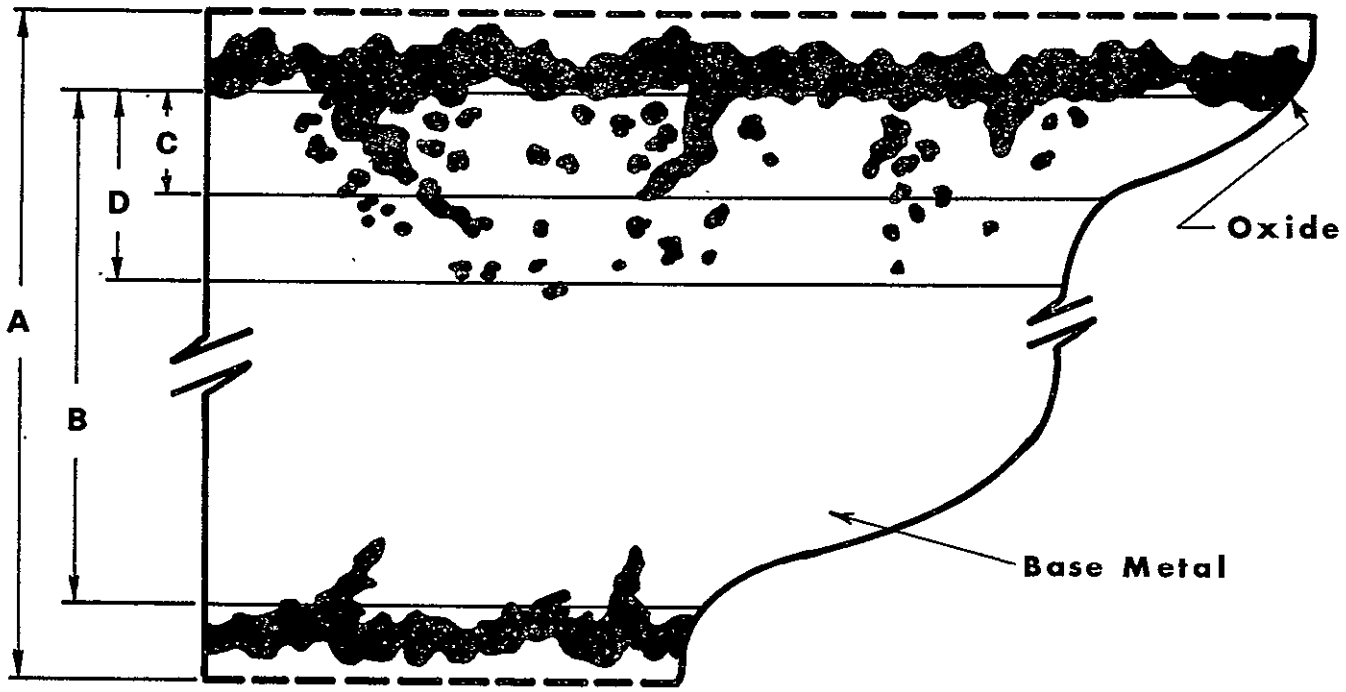

1. Metal Loss (mils/side), $[(A-B)/2]$

2. Continuous Penetration (mils/side), $[C]$

3. Maximum Penetration (mils/side), $[D]$

4. Total Metal Affected (mils/side), $[((A-B)/2) + D]$

Figure 33

Schematic Of Metallographic Measurement Technique

Results for the 1422°K (2100°F)/100 hour test are listed in Table 14. The averages of the weight change data for extrusions having the same analyzed aluminum level are presented graphically in Figure 34. The total weight loss after 100 hours was found to decrease with increasing aluminum content.

The level of aluminum was also observed to affect the sense of curvature of the plots. Below 5% Al the curves are concave upwards and have a decreasing slope with time, i.e., they tend to level off. Above 5% Al, the curves are concave downwards and exhibit an initial weight gain followed by a trend to weight loss. The standard comparison sample of HAYNES alloy No. 188 was found to lose less weight than the ODS samples containing 4.2% Al for approximately 60 hours, at which time the rate of weight loss underwent a substantial increase. By the conclusion of the test, the HAYNES alloy No. 188 suffered a weight loss significantly greater than any of the ODS alloys. The metallographic parameters determined on the samples after test also supported the beneficial effects of increasing aluminum content and the general superiority of the ODS alloys over HAYNES alloy No. 188. Oxide scale thickness and the amount of metal loss per side tended to decrease with increasing aluminum level and were much less than that observed in the HAYNES alloy No. 188 sample.

Results of the test carried out at 1255°K (1800°F) for 100 hours are listed in Table 15. A graphical presentation of the weight change data is given in Figure 35. Both the magnitude and the range of the data was much smaller due to the lower test temperature. The oxidation resistance of the ODS alloys was again found to improve with increasing aluminum level. Samples with less than 5% aluminum experienced an eventual weight loss while the samples having higher than 5% Al gained weight throughout the test. The weight change data recorded for the HAYNES alloy No. 188 standard was at the upper end of the range defined by the ODS alloys. Data for surface oxidation indicated a general improvement with increasing aluminum content while the data for metal loss per side indicated the opposite effect. The performance of the ODS alloys was comparable to or slightly better than HAYNES alloy No. 188. In comparison, the metallographic parameters obtained were generally greater than those obtained for the 1422°K (2100°F) test temperature. This can be associated with the difficulties in establishing a protective alumina scale at the lower temperature.

NASA-Lewis Dynamic Oxidation Testing

Mach 1, 1366°K (2000°F) dynamic oxidation tests of 500 hour duration were carried out on the Task II alloys at the NASA-Lewis Research Center, Cleveland, Ohio. The specimens measured 10.16 cm long x 2.54 cm wide x 0.64 cm thick (4 inches by 1 inch by 0.25 inch) and had a 45 degree tapered leading edge with a 0.81 mm (.032 inch) radius in the tip. Two oxidation rigs were used (ref. 2): one fueled by natural gas and another fueled by A-1 jet fuel. Each test was carried out with duplicate specimens of TD Ni-16Cr-4.6Al as the standard material for comparison. The specimens were subjected to cycle of 1 hour in a Mach 1, 1366°K (2000°F) gas stream, followed by 3 minutes in a Mach 1, ambient air stream. The temperature of the specimens was approximately 298°K (77°F) upon completion of the air quench. Since a separate report providing all test details will be issued by NASA-Lewis, only the salient results of the tests will be presented in this section.

TABLE 14

1422°K (2100°F) DYNAMIC OXIDATION DATA FOR TASK II EXTRUSIONS

Material	Weight Change, mg/cm^2				Ox. Penetration Continuous with Surface		Metal Loss/ Side	
	20 Hrs.	41 Hrs.	63 Hrs.	100 Hrs.	mm	(Mils)	mm	(Mils)
196LB	-.426	-1.11	-1.66	-2.30	.0043	(0.17)	.0202	(0.80)
196HA	-.346	-1.03	-1.60	-2.24	.0056	(0.22)	.0165	(0.65)
197LB	-.562	-1.47	-1.99	-2.64	.0061	(0.24)	.0089	(0.35)
197HB	-.919	-2.89	-4.03	-5.04	.0061	(0.24)	.0165	(0.65)
198HA	-.273	-.679	-.923	-1.36	.0038	(0.15)	.0102	(0.40)
198LB	-.281	-.727	-.984	-1.43	.0038	(0.15)	.0127	(0.50)
199HA	+.054	-.163	-.325	-.705	.0033	(0.13)	.0191	(0.75)
199LB	-.089	-.415	-.644	-1.19	.0043	(0.17)	.0089	(0.35)
200HA	+.316	+.341	+.474	-.199	.0038	(0.15)	.0114	(0.45)
200LB	+.291	+.268	+.268	-.429	.0030	(0.12)	.0127	(0.50)
201LB	+.308	+.178	-.113	-.624	.0030	(0.12)	.0064	(0.25)
201LC	+.332	+.249	+.007	-.506	.0033	(0.13)	.0114	(0.45)
HA188	+.099	-.685	-1.59	-8.91	.0516	(2.03)	.0610	(2.40)

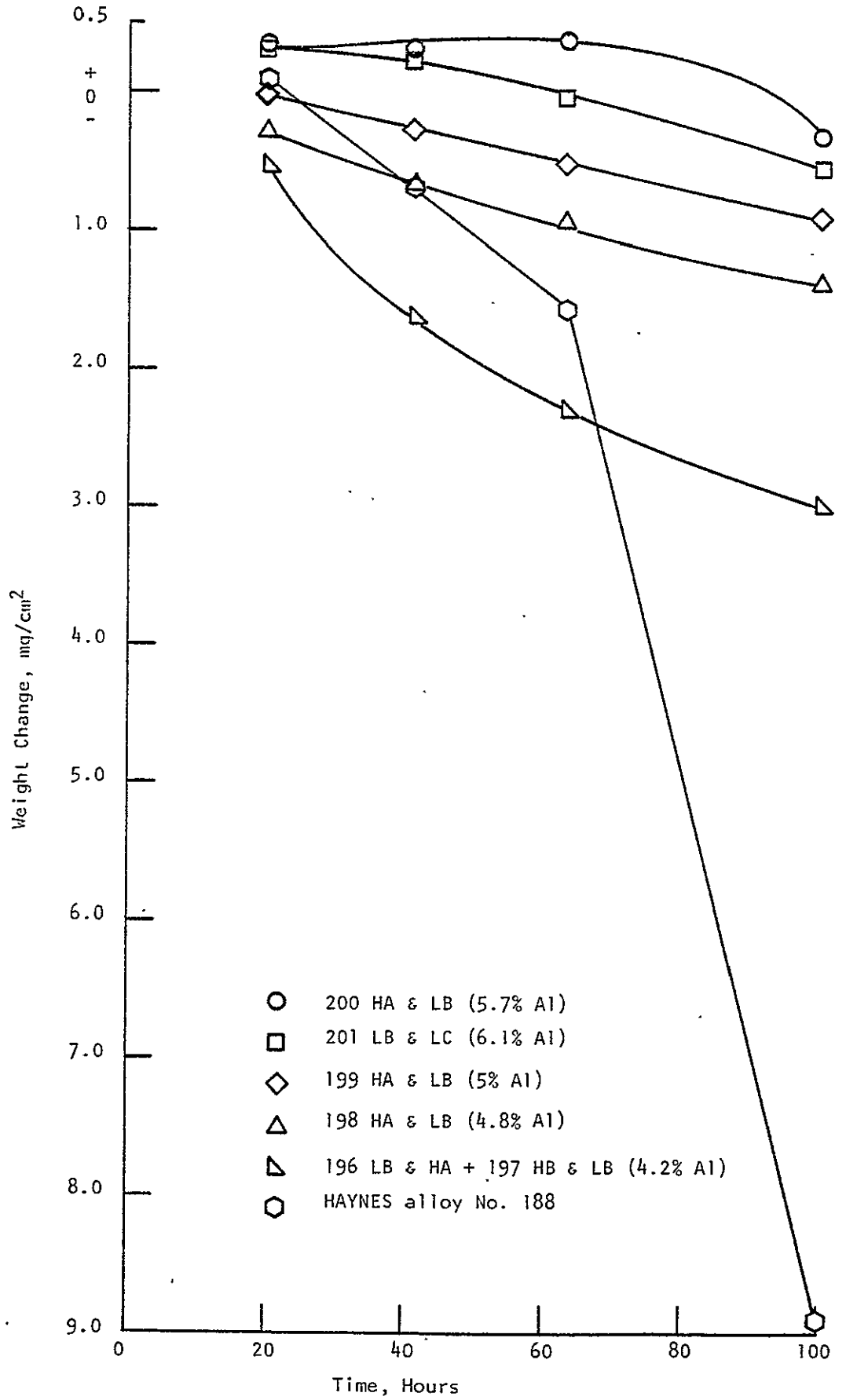

Figure 34: 1422°K (2100°F) dynamic oxidation behavior for selected Task II extrusions

TABLE 15

1255°K (1800°F) DYNAMIC OXIDATION DATA FOR TASK II EXTRUSIONS

Material	Weight Change, mg/cm^2			Ox. Penetration Continuous with Surface		Metal Loss/Side	
	21 Hrs.	55 Hrs.	100 Hrs.	mm	(Mils)	mm	(Mils)
196HB	+.064	+.048	-.088	.0109	(0.43)	.0229	(0.90)
196LC	+.064	+.064	-.064	.0064	(0.25)	.0178	(0.70)
197HA	+.095	+.119	+.024	.0109	(0.43)	.0178	(0.70)
197LB	+.055	-.016	-.191	.0170	(0.67)	.0241	(0.95)
198HC	+.087	+.114	-.052	.0086	(0.34)	.0203	(0.80)
198LC	+.119	+.135	+.039	.0069	(0.27)	.0203	(0.80)
199LC	+.135	+.150	+.119	.0046	(0.18)	.0203	(0.80)
199HB	+.119	+.142	+.103	.0056	(0.22)	.0254	(1.00)
200LC	+.127	+.143	+.191	.0030	(0.12)	.0254	(1.00)
200HB	-.562	-.618	-.618	.0038	(0.15)	.0343	(1.35)
201HA	*	-	-	.0038	(0.15)	.0432	(1.70)
201HB	+.127	+.189	+.222	.0028	(0.11)	.0216	(0.85)
HA188	+.172	+.165	+.129	.0074	(0.29)	.0330	(1.30)

* Void due to presence of steel canning material

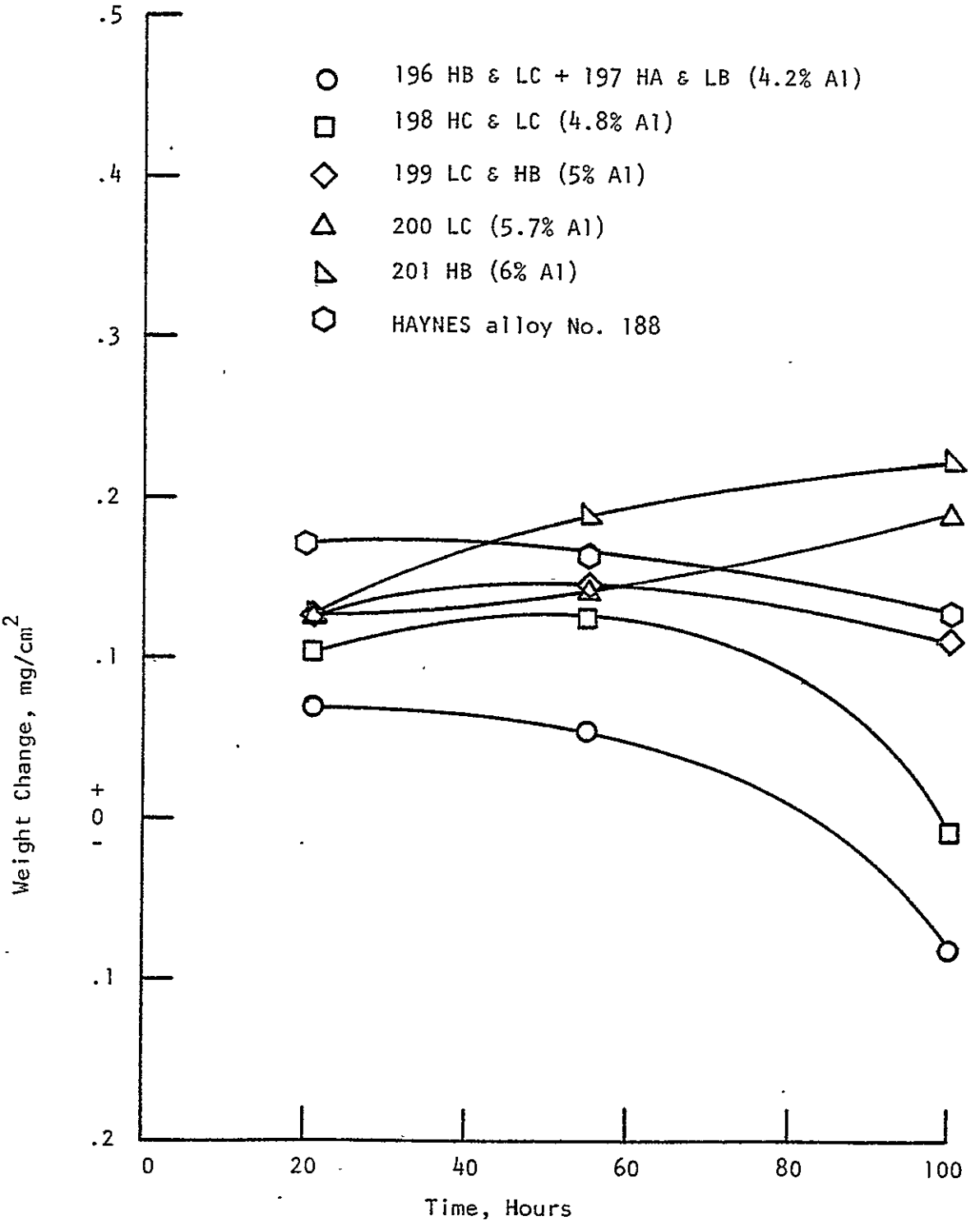

Figure 35: 1255°K (1800°F) dynamic oxidation behavior for selected Task II extrusions

A summary of the weight change data obtained for the two test runs is given in Figures 36-38. For the Task II alloys, weight losses tended to be greater in the test run with jet fuel. The differences were especially large for samples containing nominally 4% Al. In agreement with Stellite results, both tests indicated that weight losses decreased with increasing aluminum level. No relationship was observed between Y_2O_3 content and oxidation resistance. The high aluminum alloys were found to perform as well as or slightly better than the TD Ni-Cr-Al standard. Due to the much longer duration of the NASA tests, another characteristic was noted in the weight change curves. As in the Stellite test at 1422°K (2100°F), weight losses tended to level off after approximately 100 hours which is indicative of a tight alumina scale formation. However, after about 350-400 hours, the weight loss rates underwent a large increase. This might have been due to the gradual depletion of aluminum in the surface layers of the samples. That is, an aluminum level was eventually reached at which a protective alumina scale could no longer form. Based on metallographic observations of the oxidation attack along the parallel sides of the samples, the amount of metal recession for all of the alloy compositions was found to be very small and judged to be less than .0025 mm (.0001 inch). Thus all of the alloys met the program goal for dynamic oxidation resistance.

The NASA investigators also noted an increase tendency for thermal fatigue cracking with increasing alumina content. After 500 hours, crack lengths for samples containing 4-5% Al were in the range of 1-4 mm (.039-.157 inch). Samples containing nominally 6% Al had thermal fatigue cracks 6-10 mm (.236-.394 inch) long. It should be noted, however, that the materials tested had high longitudinal elastic moduli so that their resistance to thermal fatigue cracking was not optimum. Even so, this was the first series of materials tested by NASA-Lewis to have withstood the full 500 hours of testing at Mach 1, 1366°K (2000°F) without cracking apart, or bending over as did the TD Ni-Cr-Al standard samples.

TASK III - PRELIMINARY SCALE-UP EVALUATION

Selection of Compositions and Processing Parameters

The primary purpose of Task II was to define an optimum alloy composition and the processing conditions that offered the best potential for meeting engine vane material requirements. When the results of the evaluation of the Task II alloy compositions were compared against the original program goals, the primary factor of descrimination was oxidation resistance. From this point of view, a 4% aluminum content was clearly not optimum. The 6% Al level, representing overall maximum oxidation resistance, was also judged not to be optimum based on secondary considerations of melting point penalty and tendency to thermal fatigue cracking. The nominal 5% Al level, therefore, appeared to represent the best selection. Of the two heats involved, the heat which was analyzed to actually contain 4.7-4.8% aluminum was judged to be slightly better with respect to thermal fatigue cracking resistance. Consequently, the optimum aluminum content was set at 4.75%.

The major shortcoming of the Task II extrusions was their failure to achieve the required combination of strength and low longitudinal modulus of elasticity. However, other studies on various ODS alloys carried out by Stellite indicated that this goal could be achieved using a

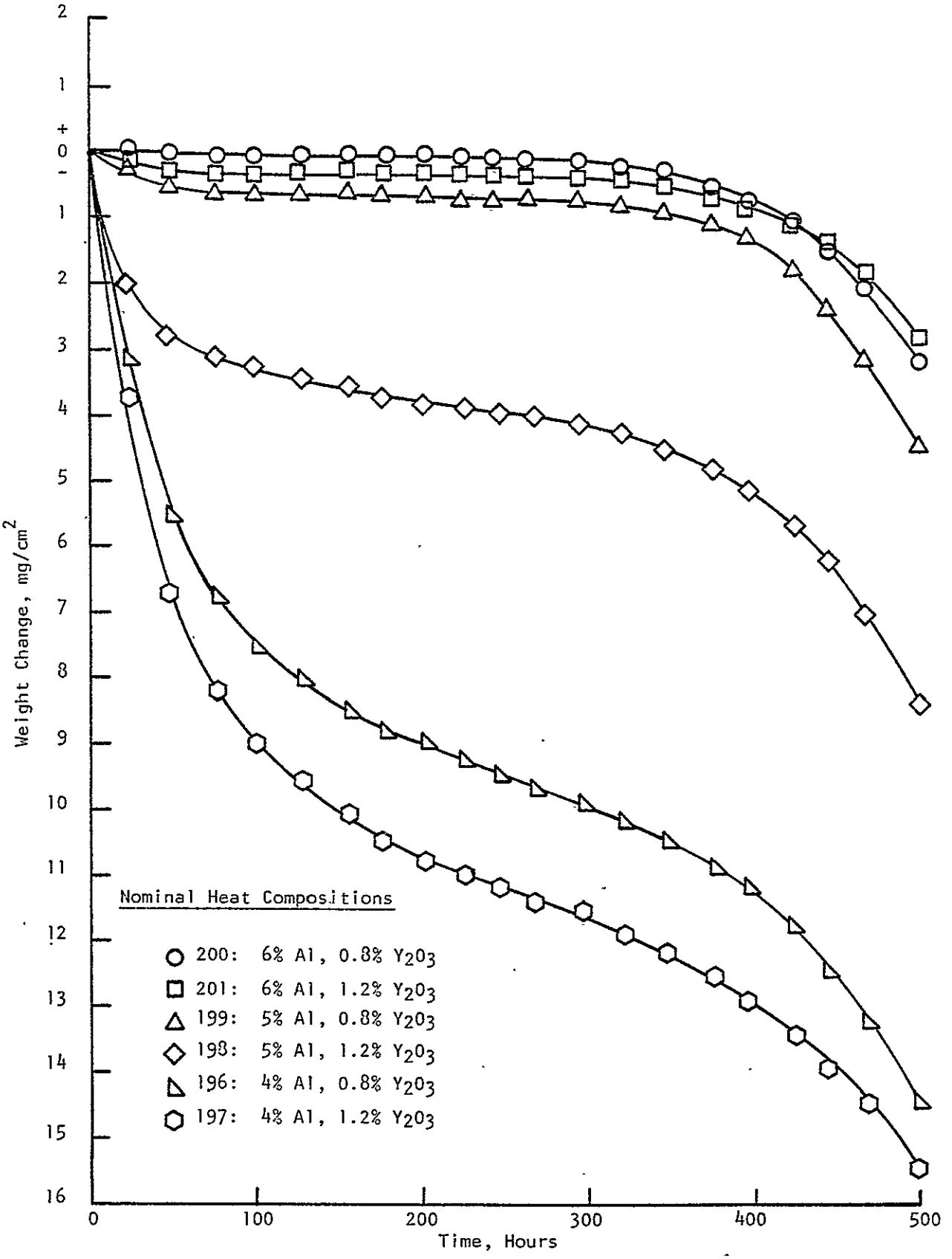

Figure 36: Mach. 1, 1366°K (2000°F) dynamic oxidation behavior (jet fuel) - courtesy of NASA-Lewis Research Center

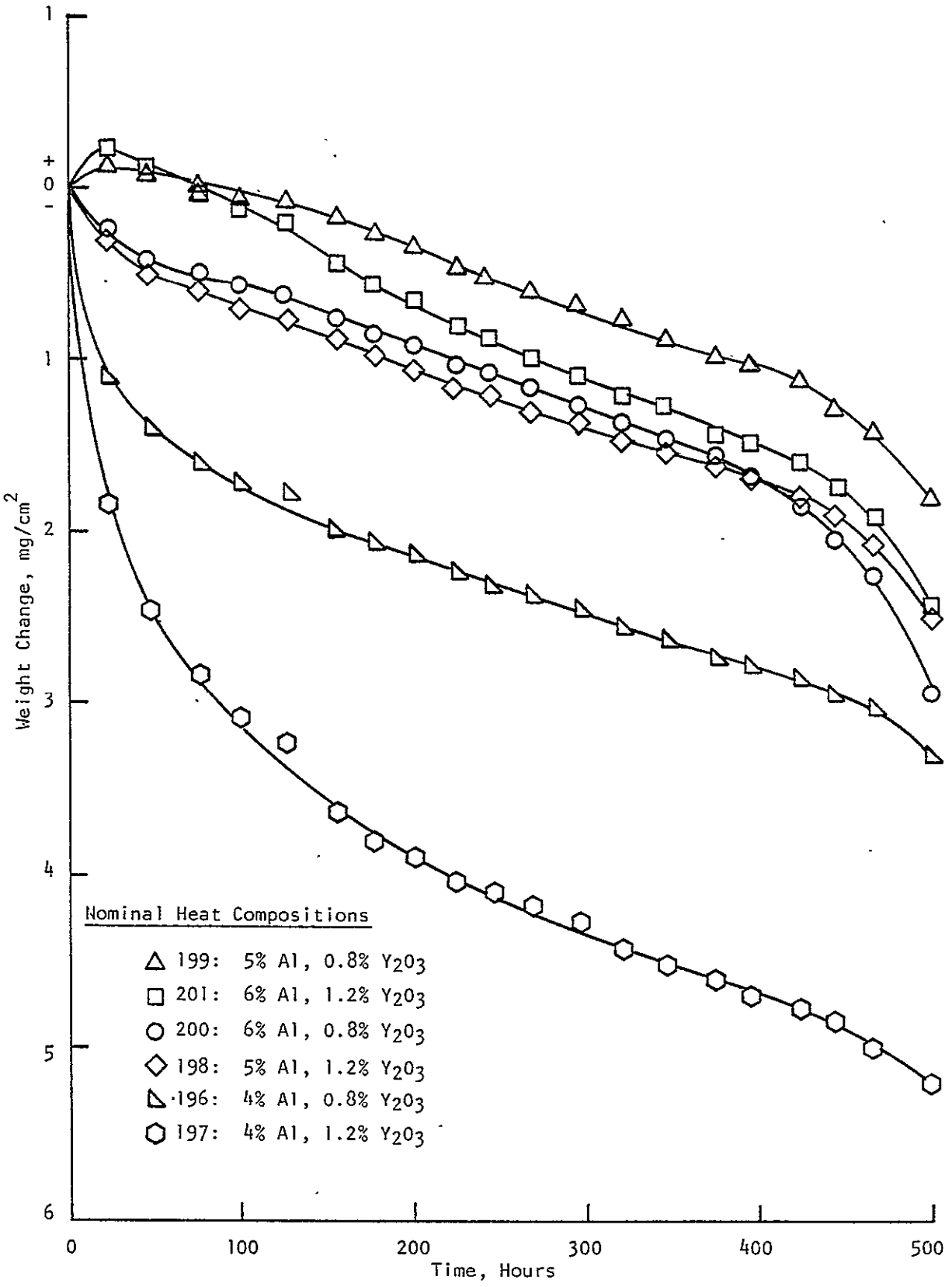

Figure 37: Mach. 1, 1366°K (2000°F) dynamic oxidation behavior (natural gas) - courtesy of NASA-Lewis Research Center

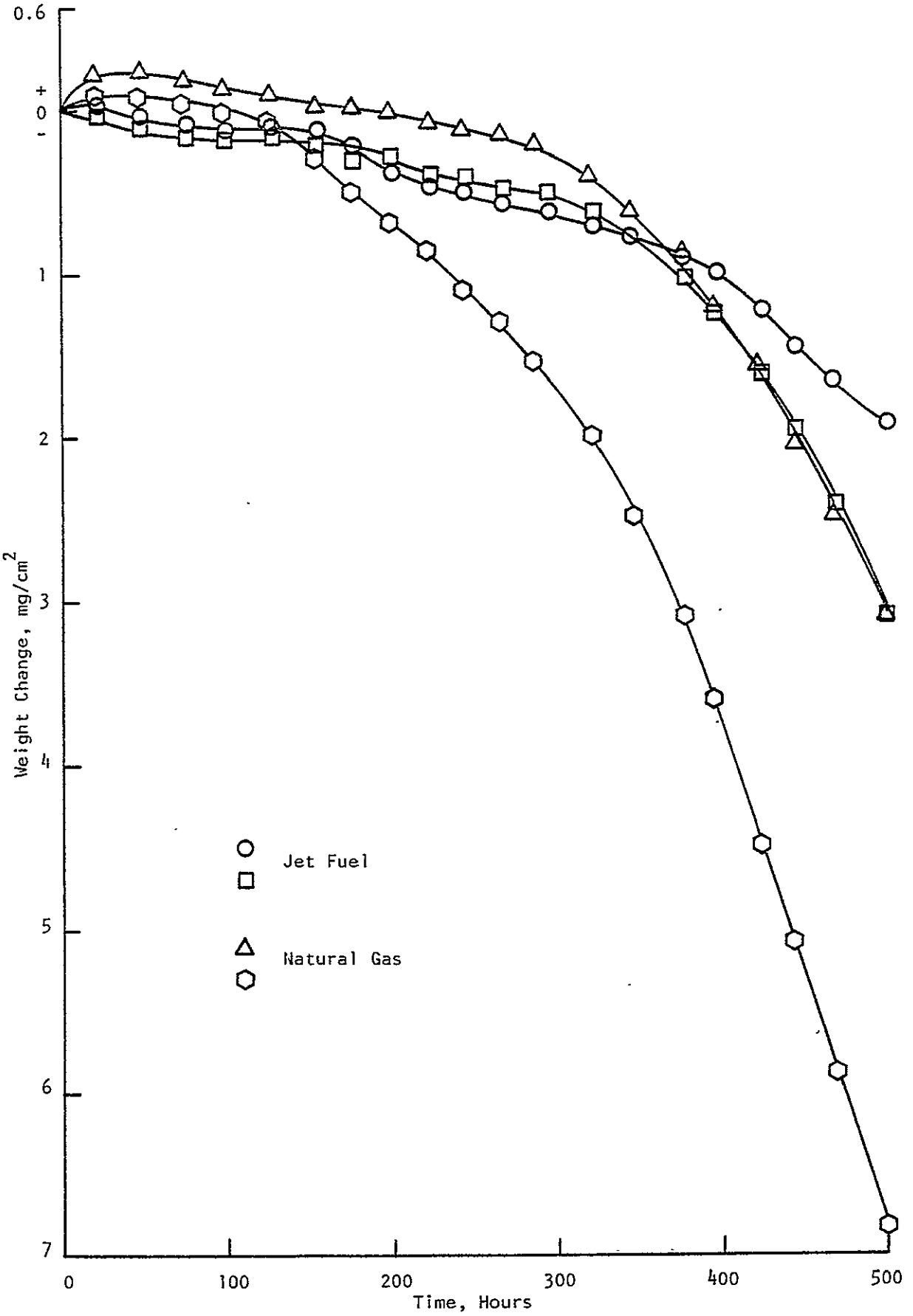

Figure 38: Mach. 1, 1366°K (2000°F) dynamic oxidation behavior of TD Ni-16Cr-4.6Al - courtesy of NASA-Lewis Research Center

modified powder making method with an Y_2O_3 level in the range of 1.8-2%. It was, therefore, decided to produce the Task III powders using this adjusted approach.

Another factor considered in the selection of the Task III alloy compositions was the build-up of grain boundary chromium carbides observed in some of the samples subjected to cyclic dynamic oxidation testing. Although no detrimental effects on mechanical properties had been linked to the presence of such carbides, it was decided in technical discussions with the NASA Program Manager to attempt to control their formation through the introduction of a refractory metal carbide former in two experimental heats. Tantalum was chosen for this purpose based on a review of data which indicated that it was a strong carbide former which would not adversely affect dynamic oxidation resistance nor interfere with the dispersoid chemistry of the base alloy. One heat would contain a tantalum level in excess of that required to combine with all the carbon present (up to 1.8 w/o) and another heat would contain tantalum at a lower level (up to 0.9 w/o).

Task III was finalized to consist of the study of four, full size, rectangular extrusions. Two heats would contain nominally Ni-16Cr-4.75Al-2Y_2O_3 to permit the study of property reproducibility in the optimum alloy composition and two heats would contain nominally Ni-16Cr-4.75Al-2Y_2O_3 with additions of 0.9 Ta and 1.8 Ta in an effort to control carbide formation as discussed above. Based on previous Stellite experience, the extrusion would be carried out using the 18.1 cm (7-1/8 inch) diameter liner size which would provide a reduction ratio of approximately 14.4:1 for a 7.44 cm x 2.41 cm (2.93 inch x 0.95 inch) rectangle. The extrusion temperature selected was 1311°K (1900°F), and the ram speed was set at 254 cm/min (100 in/min).

Attrition of Task III Powders

The Task III powders were prepared by mechanical attrition in approximately 45.4 kg (100 pound) lots using a 100S attritor. The two heats containing tantalum were prepared on a best efforts basis because of their experimental nature, and no wash heats were employed to obtain close agreement with the target compositions set for tantalum. After attrition, each powder lot was screened and only the -30 mesh fraction was characterized and used.

Analysis of Attrited Powders

Results of chemical analyses performed on the attrited powder lots are presented in Table 16. The aluminum levels attained in all of the heats were reasonably close to the 4.75% Al target level. Chromium contents were all within the original recommended compositional limits of Task I. Based on the yttrium analyses, the Y_2O_3 levels achieved were in the range of 1.83-1.88 weight percent. The tantalum levels in the experimental tantalum containing heats were reasonably close to the levels desired. Agreement between the actual and target levels was much better in the

TABLE 16

CHEMICAL ANALYSES OF TASK III ATTRITED POWDERS
(Weight %)

Wt. %	AT-262	AT-264	AT-265	AT-266
Al	4.60	4.71	4.84	4.71
C	.05	.05	.05	.05
Cr	16.53	16.04	15.80	16.48
Fe	.20	.20	.24	.23
N	.029	.032	.032	.032
Ni	75.92	74.98	73.87	74.76
O (ppm)	6035	6205	6290	6200
S	<.002	<.002	<.002	<.002
Ta	<.01	<.01	1.72	1.23
Y	1.48	1.44	1.48	1.48

Nominal Compositions: AT-262 - Ni-16Cr-4.75Al-2Y_2O_3

AT-264 - Ni-16Cr-4.75Al-2Y_2O_3

AT-265 - Ni-16Cr-4.75Al-1.8Ta-2Y_2O_3

AT-266 - Ni-16Cr-4.75Al-0.9Ta-2Y_2O_3

case of the high tantalum heat. Powder contaminants such as carbon, iron, nitrogen and sulfur were all at low levels. In addition to the routine chemical analyses, a sample of each powder lot was also examined with the electron microprobe to determine the distribution of the major elements within randomly selected powder particles. No indication of significant chemical inhomogeneity was observed in any of the four powder lots. Typical elemental distribution scans for each powder lot are presented in Figures 39-42.

An approximately 454 gm (1 pound) sample of -30 mesh powder from each of the first two powder lots was sieve analyzed. The results are listed in Table 17. The particle size distributions obtained were very similar to the Task I powders in that over 50% of the sample weight was in the size range of -30/+60 mesh, and at least 99% was in the -30/+200 mesh range. Particle size and shape was also examined by means of metallography. Typical photomicrographs of the four powder lots are illustrated in Figures 43-46.

Extrusion of Task III Powders

The extrusion billets prepared for the Task III powder were a scaled up version of the design illustrated in Figure 11. Maximum dimensions were held to 17.7 cm O.D. x 50.8 cm length (6.95 inch O.D. x 20 inch length) to accommodate the liner size. Each billet contained approximately 43.1 kg (95 pounds) of powder. Billet loading and evacuation procedures were the same as those employed in Task II. Extrusion of the billets was carried out at the RMI Company, Ashtabula, Ohio, using a 39.14 MN (4400 ton) capacity press. A coating of Markal Ceramic CRN-53* was applied to the billets to protect them during furnace heat up. On extrusion, Fiske 604D** lubricant was applied to the die and liner. The follower block employed was of mild steel. A summary of the extrusion data is given in Table 18.

Evaluation of Task III Extrusions

Chemical Analysis

A decanned section of each extrusion was submitted for a routine chemical analysis. The results are listed in Table 19. Agreement of the values obtained with those determined for the as-attrited powders is good and within experimental error with the exception of oxygen. The higher oxygen values obtained for the powders is most likely due to differences in degassing procedures employed for chemical analysis of the powders and the preparation of billets containing the powders as previously discussed. A sample of AT-262 extruded bar was also submitted for mass spectrographic

* T.M. Markal Company, Chicago, Illinois

** T.M. Fiske Brothers Refining Company, Toledo, Ohio

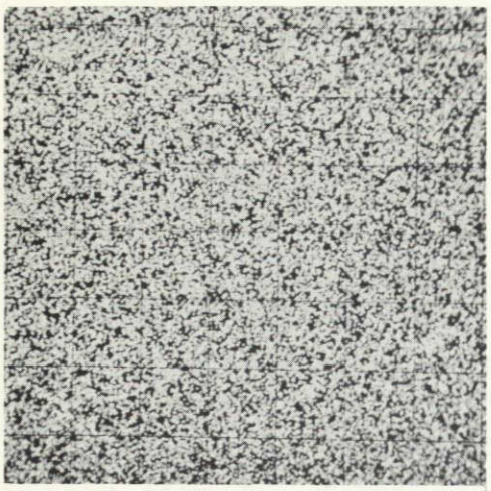

Ni

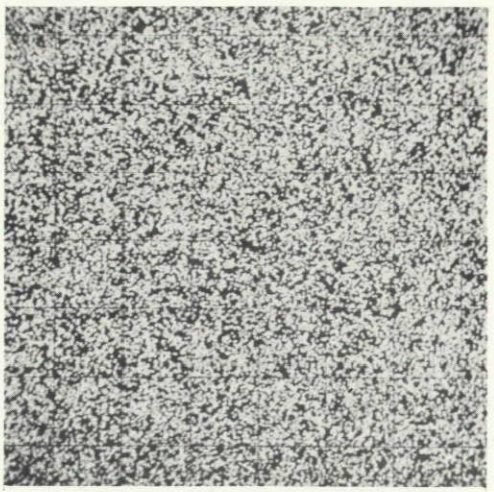

Cr

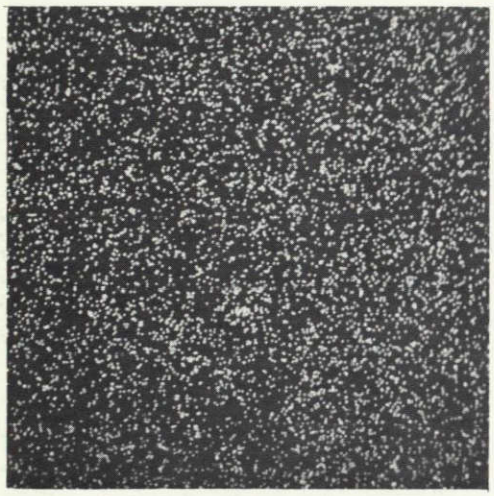

Al

Y

Fe

Figure 39: Elemental distribution mapping of AT-262 as-attrited powder - nominal composition Ni-16Cr-4.75Al-2Y_2O_3 - area measures .12 mm x .12 mm

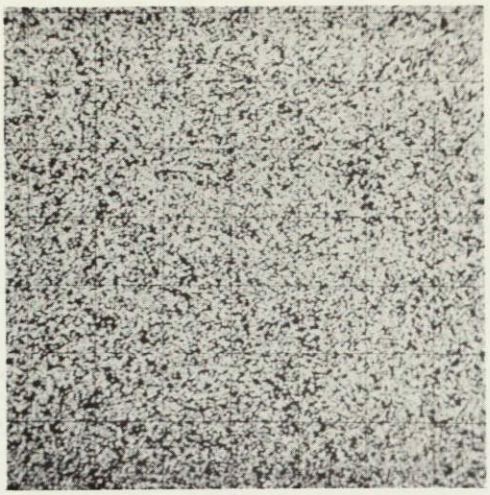

Ni

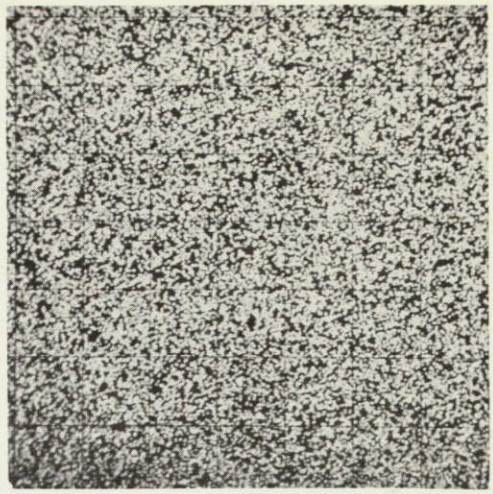

Cr

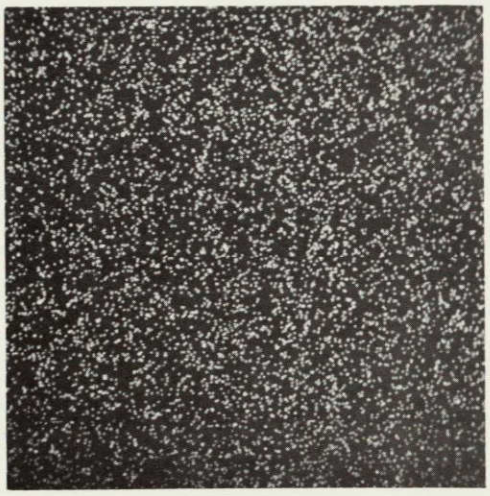

Al

Y

Fe

Figure 40: Elemental distribution mapping of AT-264 as-attrited powder - nominal composition Ni-16Cr-4.75Al-2Y_2O_3 - area measures .12 mm x .12 mm

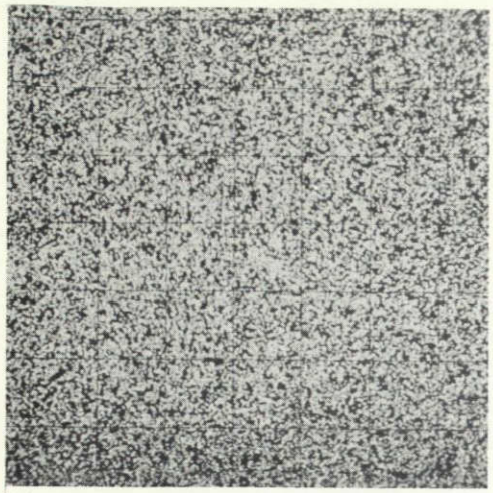

Ni

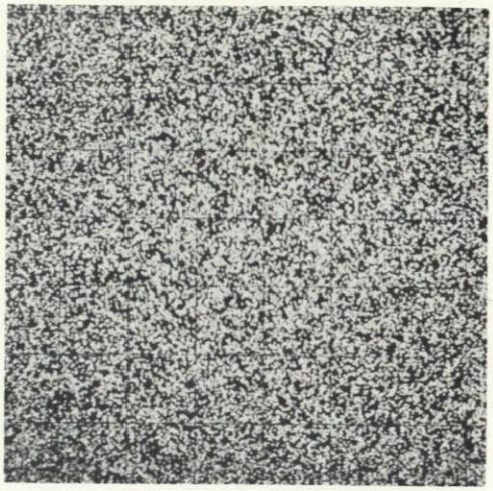

Cr

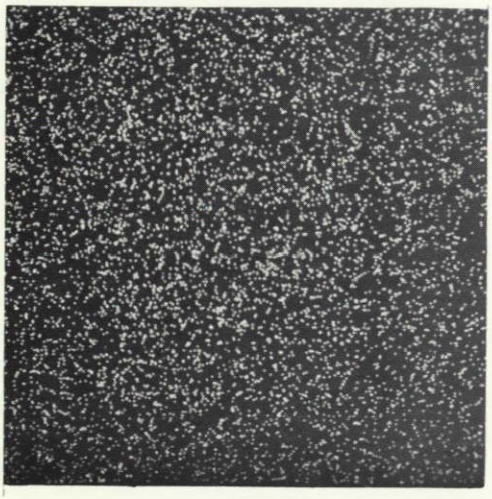

Al

Y

Fe

Figure 41: Elemental distribution mapping of AT-265 as-attrited powder - nominal composition Ni-16Cr-4.75Al-1.8Ta-2Y_2O_3 - area measures .12 mm x .12 mm

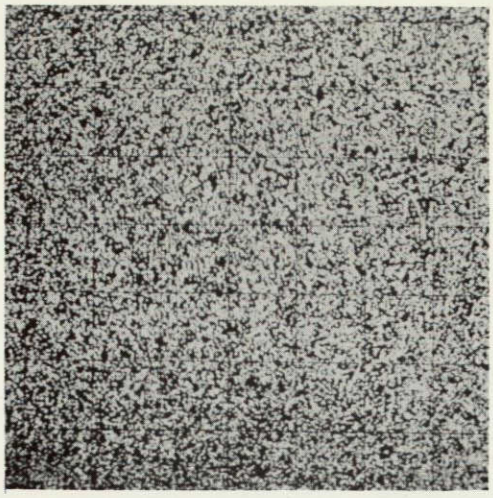

Ni

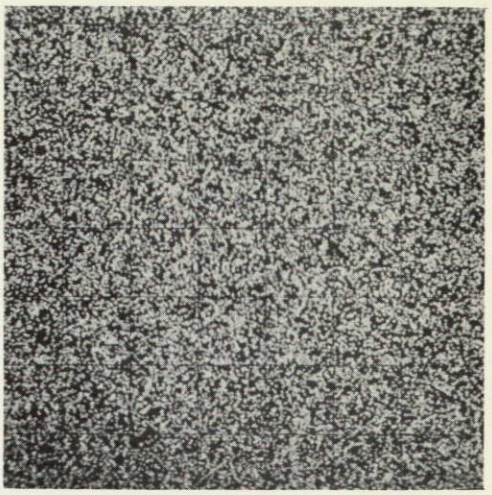

Cr

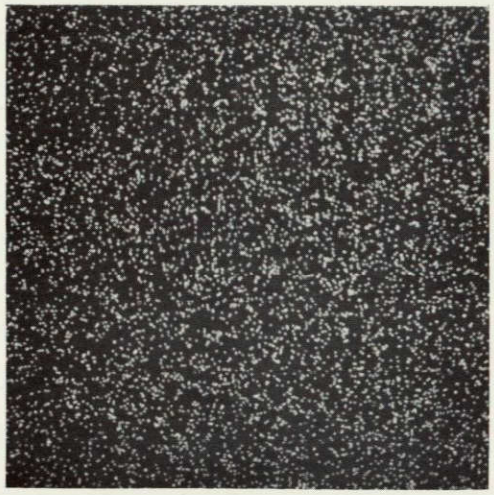

Al

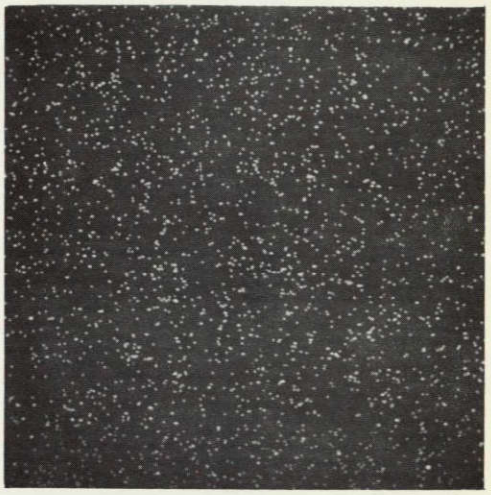

Y

Ta

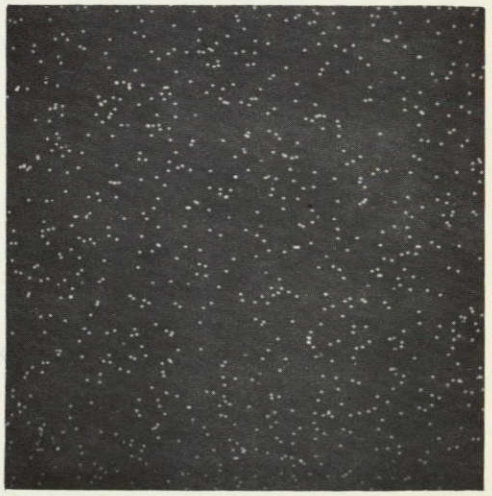

Fe

Figure 42: Elemental distribution mapping of AT-266 as-attrited powder - nominal composition Ni-16Cr-4.75Al-0.9Ta-2Y_2O_3 - area measures .12 mm x .12 mm

TABLE 17

PARTICLE SIZE ANALYSES OF -30 MESH TASK III ATTRITED POWDERS
(454 gm sample weight)

U.S. Mesh No.	AT-262		AT-264	
	Wt. %	Cum. %	Wt. %	Cum. %
60	56.8	56.8	57.0	57.0
100	35.0	91.9	36.4	93.4
200	7.3	99.1	6.4	99.8
270	0.7	99.8	0.2	100.0
325	0.2	100.0	Trace	100.0
-325	Trace	100.0	Trace	100.0

Figure 43: Heat AT-262 as-attrited powder - as polished - magnification 100X

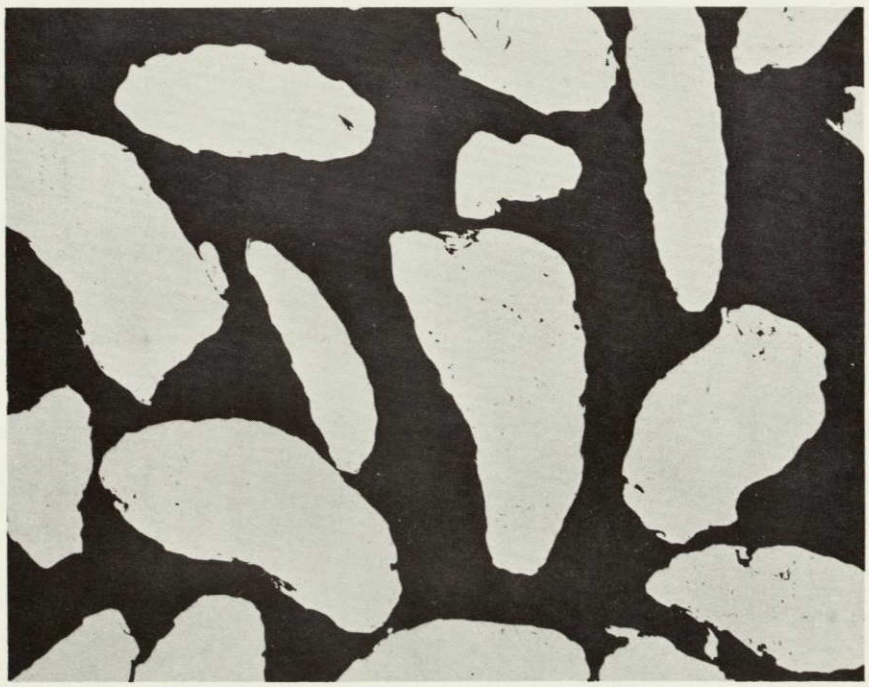

Figure 44: Heat AT-264 as-attrited powder - as polished - magnification 100X

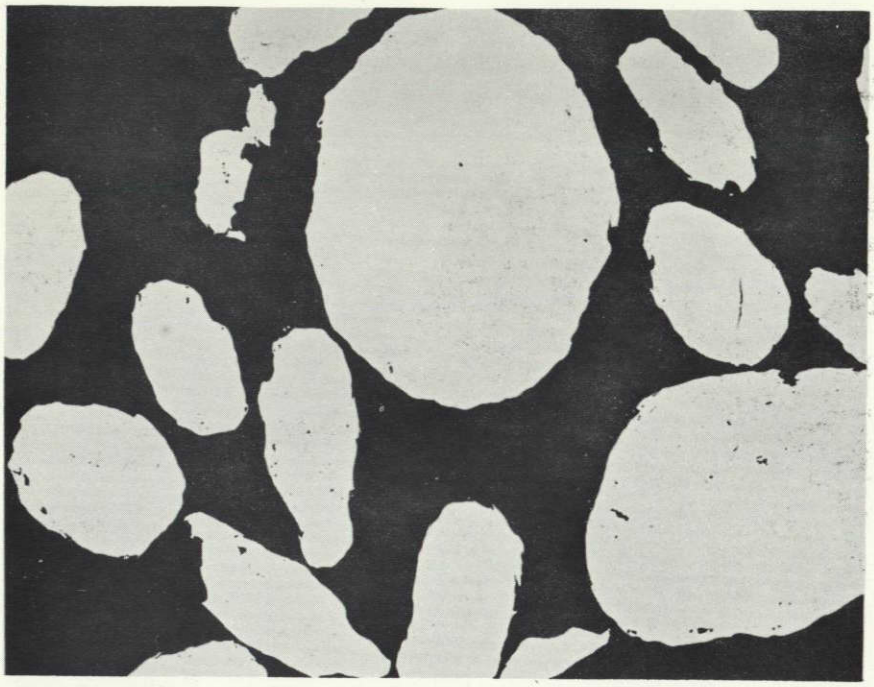

Figure 45: Heat AT-265 as-attrited powder - as polished - magnification 100X

Figure 46: Heat AT-266 as-attrited powder - as polished - magnification 100X

TABLE 18

SUMMARY OF TASK III EXTRUSION DATA

Extrusion No.	Temperature °K	(°F)	Extrusion Ratio	Starting Pressure MPa	(tsi)	Starting Constant MPa	(tsi)	Running Pressure MPa	(tsi)	Running Constant MPa	(tsi)
AT-262	1311	(1900)	14.4:1	1,036.3	(75.2)	388.6	(28.2)	855.7	(62.1)	321.1	(23.3)
AT-264	1311	(1900)	14.4:1	1,011.5	(73.4)	379.0	(27.5)	847.5	(61.5)	316.9	(23.0)
AT-265	1311	(1900)	14.4:1	971.5	(70.5)	363.8	(26.4)	821.3	(59.6)	307.3	(22.3)
AT-266	1311	(1900)	14.4:1	1,019.7	(74.0)	381.7	(27.7)	811.6	(58.9)	304.5	(22.1)

TABLE 19

CHEMICAL ANALYSES OF TASK III EXTRUDED BARS

Wt. %	AT-262	AT-264	AT-265	AT-266
Al	4.61	4.61	4.69	4.77
C	.05	.05	.05	.05
Cr	15.78	15.65	15.80	15.90
Fe	.28	.64	.24	.23
N	.032	.032	.032	.031
Ni	74.75	74.94	73.27	74.04
S	<.002	<.002	<.002	<.002
Ta	<.01	<.01	1.76	1.25
Y	1.52	1.52	1.50	1.52
O (ppm)	5345	5507	5165	5270

Nominal Compositions: AT-262 - Ni-16Cr-4.75Al-$2Y_2O_3$

AT-264 - Ni-16Cr-4.75Al-$2Y_2O_3$

AT-265 - Ni-16Cr-4.75Al-1.8Ta-$2Y_2O_3$

AT-266 - Ni-16Cr-4.75Al-0.9Ta-$2Y_2O_3$

of trace elements. The results of this analysis are given in Table 20. The only contaminant found to be present in an amount above a trace level was cobalt. Based on the previously reported chemical analyses, the amount of cobalt is estimated to be on the order of 1%. Its presence is undoubtedly due to the prior use of the 100S attritor to produce ODS cobalt-base alloys rather than contamination present in any of the starting powders employed.

Melting Range

The melting temperature range of each Task III was determined using furnace annealing treatments in conjunction with metallographic analysis as required. The procedure was the same as that employed for the Task II extrusions except that the temperature intervals were in steps of 5.6°K (10°F). The results of the study are presented in Table 21. The two tantalum-free extrusions showed signs of melting in the temperature range of 1649.8-1655.4°K (2510-2520°F) with the temperature for incipient melting close to 1649.8°K (2510°F). The two tantalum-containing extrusions melted in the temperature range of 1633.2-1638.7°K (2480-2490°F). Judging from metallographic observations, the temperature for incipient melting for the high tantalum composition would be less than 1633.2°K (2480°F), and close to 1633.2°K (2480°F) for the low tantalum composition.

Recrystallization Behavior

Decanned sections of each extrusion were given a slow recrystallization heat treatment which consisted of placing the material into a furnace set at 1478°K (2200°F) then raising the temperature over a 2 hour period to 1616°K (2450°F) and holding for one hour. This heat treatment method was selected in order to promote the development of a low longitudinal modulus of elasticity. Photomicrographs of typical areas in each extrusion are illustrated in Figures 47-50. All the extrusions underwent complete secondary recrystallization to produce a grain structure which was elongated in the extrusion direction. The two tantalum-containing materials were found to possess grains which were wider in the transverse directions.

A transverse section of each extrusion was also prepared and macroetched in a solution composed of 90% hydrochloric acid and 10% hydrogen peroxide to examine variations in grain structure and to qualitatively assess crystallographic texture variations over the cross section. The latter determination is based on the fact that grains having a <100> direction perpendicular to the plane of section will etch with a dull, matte finish. Those grains having a non-<100> orientation will become shiny on macroetching. Photographs of the sections prepared from the Task III extrusions are presented in Figures 51-54. Both tantalum-containing extrusions were found to possess a core which was completely composed of large grains having a non-<100> texture. The two tantalum-free extrusions responded to the heat treatment much better, but they possessed a greater than desirable amount of non-<100> oriented grains. These grains were distributed over the cross section in a "salt and pepper" fashion and more heavily concentrated in the center region. Extrusion AT-264 was found to be worse than AT-262 in its degree of non-<100> texturing.

TABLE 20

MASS SPECTROGRAPHIC ANALYSIS OF TASK III - HEAT AT-262 EXTRUDED BAR

(All values in ppm weight)

Uranium		Terbium		Ruthenium		Vanadium	
Thorium	11	Gadolinium		Molybdenum	23	Titanium	38
Bismuth	<0.10	Europium		Niobium	0.15	Scandium	
Lead	1.4	Samarium		Zirconium	1.7	Calcium	
Thallium	<0.10	Neodymium		Yttrium	Maj	Potassium	1.3
Mercury		Praseodymium		Strontium	1.2	Chlorine	270*
Gold		Cerium	18	Rubidium		Sulphur	12
Platinum		Lanthanum	80	Bromine		Phosphorus	NR
Iridium		Barium	39	Selenium	<0.12	Silicon	220
Osmium		Cesium		Arsenic	1.0	Aluminum	Maj
Rhenium		Iodine		Germanium	0.12	Magnesium	3.3
Tungsten	10	Tellurium	0.13	Gallium	1.6	Sodium	0.73
Tantalum	3.7	Antimony	0.30	Zinc	2.2	Fluorine	72*
Hafnium	<1.1	Tin	<2.1	Copper	14	Oxygen	NR
Lutecium		Indium		Nickel	Maj	Nitrogen	NR
Ytterbium		Cadmium	<1.0	Cobalt	Maj	Carbon	NR
Thullium		Silver	<0.10	Iron	840	Boron	8.1
Erbium		Palladium		Manganese	70	Beryllium	
Holmium		Rhodium		Chromium	Maj	Lithium	<0.10
Dysprosium							

Notes: All elements not reported <0.1 ppm weight

NR - Not Reported

* - Determined on assumed sensitivity

TABLE 21

RESULTS OF MELTING RANGE STUDY ON TASK III EXTRUDED BARS

Sample Heat No.	Annealing Temperature (30 Minute Hold Time)					
	1627.6°K (2470°F)	1633.2°K (2480°F)	1638.7°K (2490°F)	1644.3°K (2500°F)	1649.8°K (2510°F)	1655.4°K (2520°F)
AT-262 (Ta free)	--	--	No melting	No melting	Slight signs of melting at G.B.	Obvious melting
AT-264	--	--	No melting	No melting	Melting at G.B.	Obvious melting
AT-265 (High Ta)	No melting	Melting at G.B.	Obvious melting	Obvious melting	--	--
AT-266 (Low Ta)	No melting	Slight signs of melting at G.B.	Obvious melting	Obvious melting	--	--

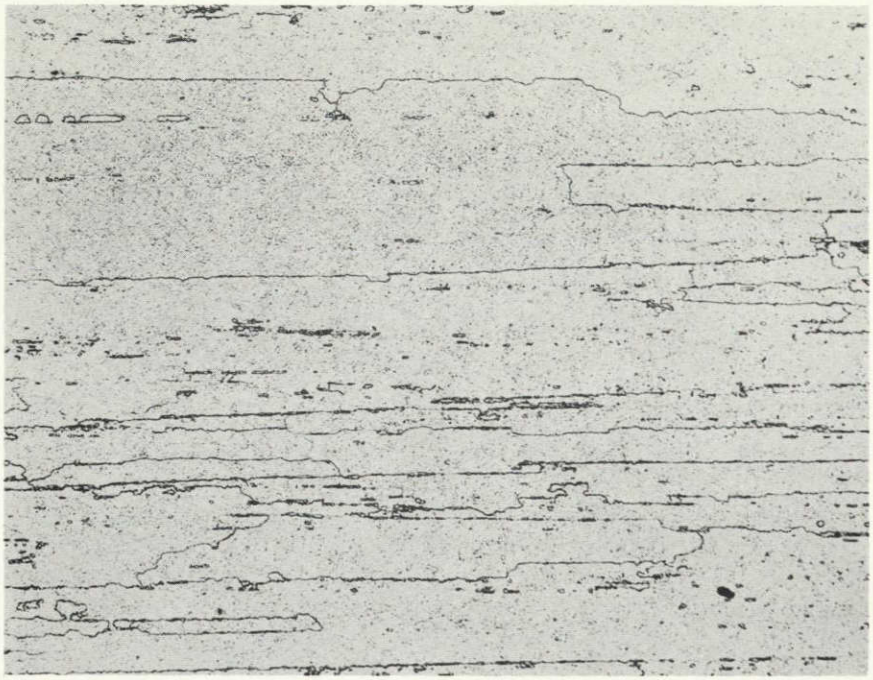

Figure 47: Extrusion AT-262 - furnace recrystallized - in at 1478°K (2200°F) → 1616°K (2450°F)/1 hour - magnification 100X

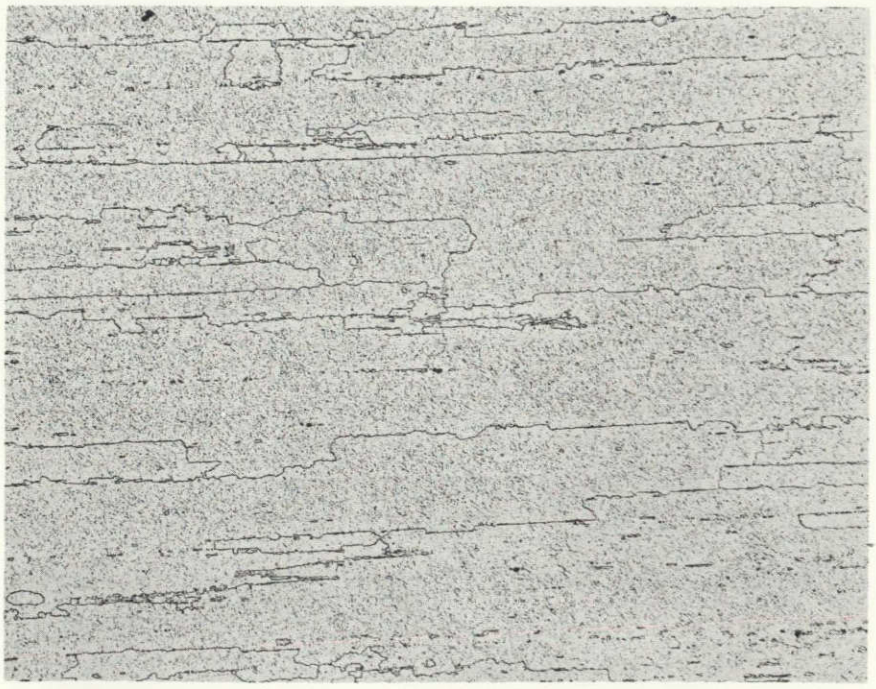

Figure 48: Extrusion AT-264 - furnace recrystallized - in at 1478°K (2200°F) → 1616°K (2450°F)/1 hour - magnification 100X

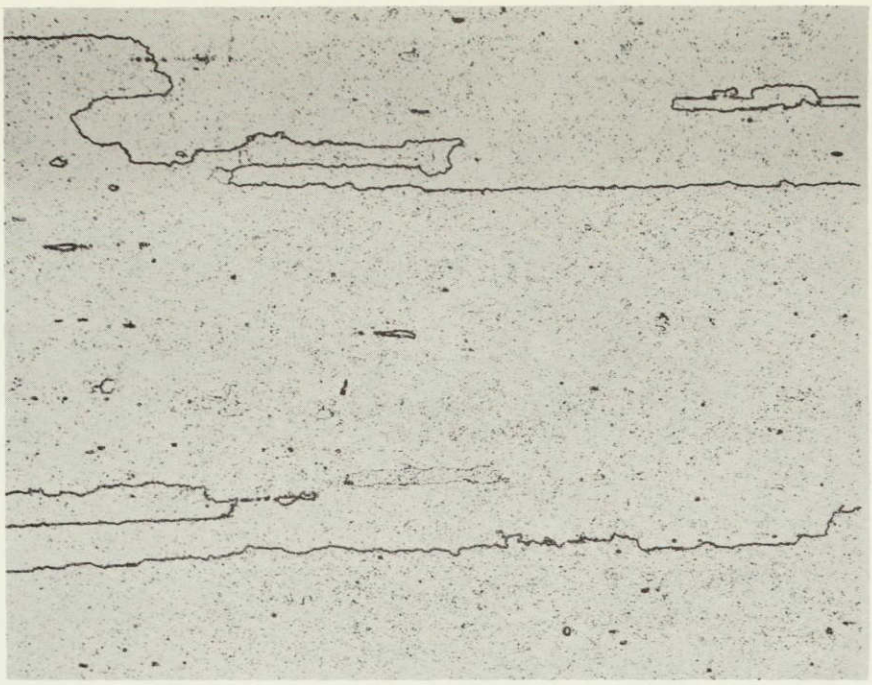

Figure 49: Extrusion AT-265 - furnace recrystallized - in at 1478°K (2200°F) → 1616°K (2450°F)/1 hour - magnification 100X

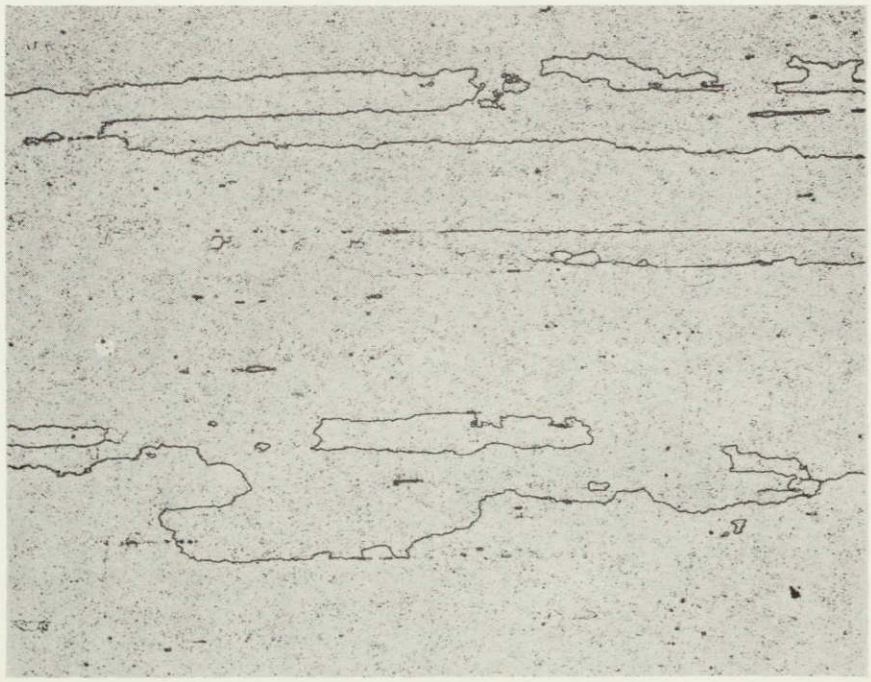

Figure 50: Extrusion AT-266 - furnace recrystallized - in at 1478°K (2200°F) → 1616°K (2450°F)/1 hour - magnification 100X

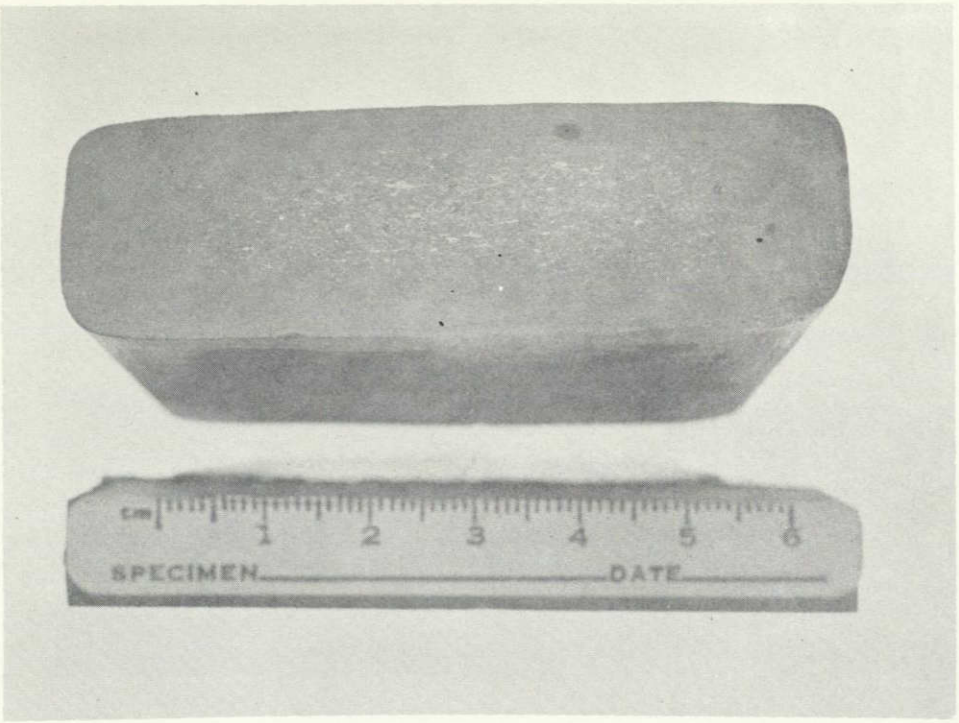

Figure 51: Macroetched transverse cross section of extrusion AT-262 in furnace recrystallized condition

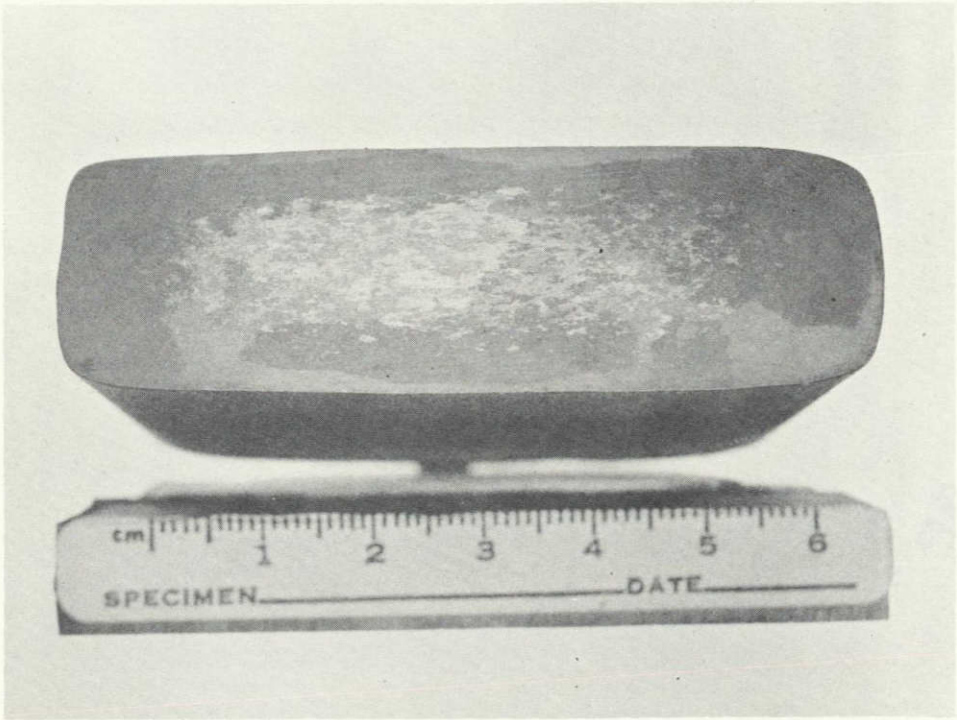

Figure 52: Macroetched transverse cross section of extrusion AT-264 in furnace recrystallized condition

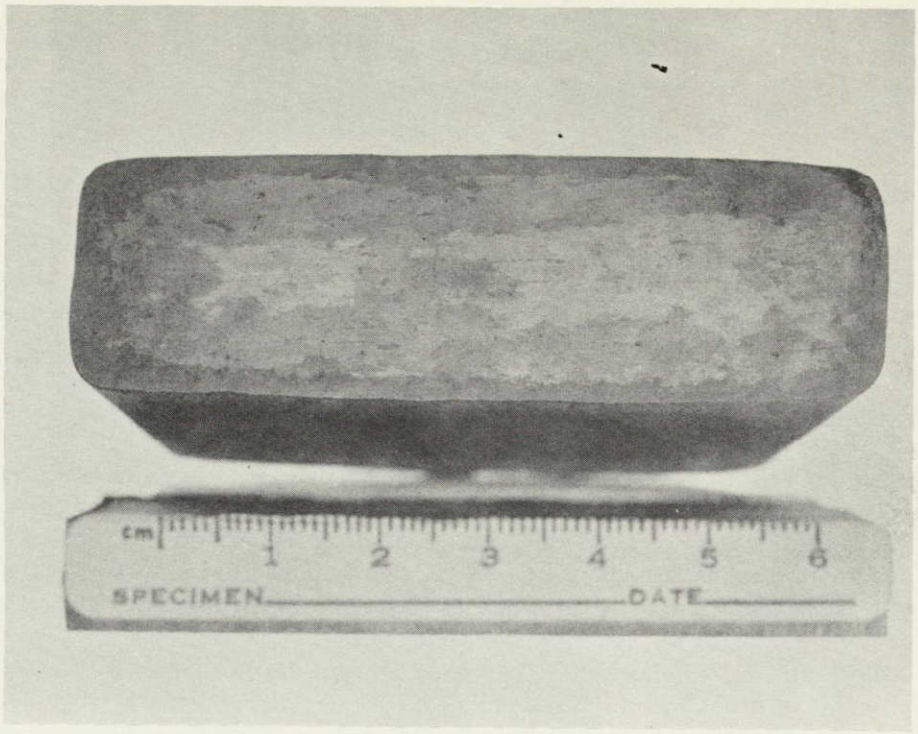

Figure 53: Macroetched transverse cross section of extrusion AT-265 in furnace recrystallized condition

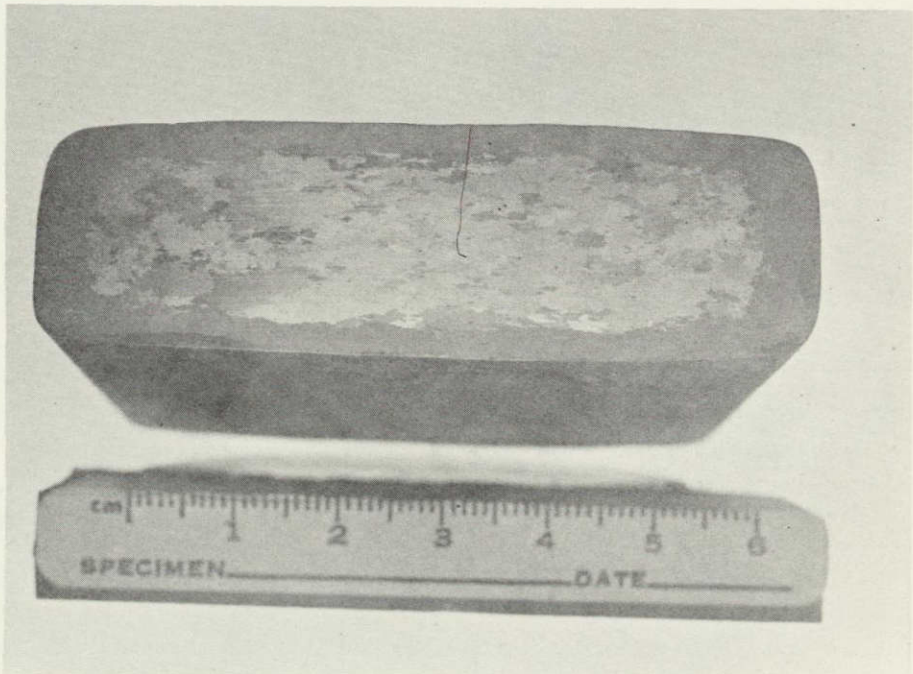

Figure 54: Macroetched transverse cross section of extrusion AT-266 in furnace recrystallized condition

A quantitative evaluation of texture in the recrystallized extrusions was also carried out by determining the room temperature dynamic sonic moduli in the longitudinal direction. The values obtained are listed in Table 22. Both tantalum-free extrusions possessed moduli in the desired low range (~137.9 GPa or 20 x 10^6 psi) while both tantalum containing extrusions had values much higher than desired (~200 GPa or 29 x 10^6 psi). It should be noted that all samples for modulus had been taken near the short side of the rectangular cross section. In light of the structures observed in the macroetched transverse sections, that location was freer of incorrectly oriented grains in the two tantalum free extrusions. Therefore, the moduli in the center of the cross sections of AT-262 and AT-264 were probably higher than the values listed in the table.

The existence of incorrectly textured grains in the center of the cross section of HDA 8077 (Ni-16Cr-4Al-Y_2O_3) extruded vane blanks had been observed in other studies carried out at Cabot Corporation. Alternate heat treatments have recently been developed which minimize their occurrence while also improving stress rupture properties. Specimens of the present extrusions were given one such heat treatment (in furnace at 2200°F, heat to 2300°F over a period of one hour, hold at 2300°F for one hour, heat to 2400°F over a period of one hour, hold one hour, cool) and examined using the macroetching technique. A decrease in the number of incorrectly textured grains was observed in the tantalum-free extrusions while little change was observed in the tantalum-containing materials. While the scope of the present program did not allow for further investigation of heat treatment response, this is a topic which requires further attention.

In the following sections which cover the evaluation of mechanical properties, all materials were recrystallized according to the heat treatment procedure described in the beginning of this section.

Tensile Properties

Duplicate longitudinal tensile tests were carried out on the recrystallized extrusions at room temperature, 1144°K (1600°F) and 1366°K (2000°F). The test results are summarized in Table 23. At room temperature and 1366°K (2000°F), the strength values obtained were roughly the same in all of the extrusions. At 1144°K (1600°F), however, the tantalum containing materials had higher strengths. Aside from this aspect, the tensile properties obtained were quite similar to those of the Task II extrusions containing nominally 5% aluminum.

Stress Rupture Properties

Duplicate 1366°K (2000°F) longitudinal and transverse stress rupture tests were carried out on the recrystallized Task III extrusions at Joliet Metallurgical Laboratories. The test results are summarized in Table 24. The data contain scatter which can be associated with both variations in material properties across the cross section and also with normal statistical fluctuations. The variations across the cross section are associated with the way in which the material flows during extrusion and with the response of the as-extruded material to the recrystallization heat treatment.

TABLE 22

ROOM TEMPERATURE SONIC MODULI FOR TASK III EXTRUSIONS

Sample No.	Longitudinal Elastic Modulus GPa	(psi)
AT-262 (Ta free)	136.52	(19.8×10^6)
	148.93	(21.6×10^6)
AT-264 (Ta free)	142.72	(20.7×10^6)
	135.83	(19.7×10^6)
AT-265 (High Ta)	205.46	(29.8×10^6)
	201.33	(29.2×10^6)
AT-266 (Low Ta)	186.85	(27.1×10^6)
	199.95	(29.0×10^6)

TABLE 23

LONGITUDINAL TENSILE TEST RESULTS FOR TASK III EXTRUSIONS

Extrusion No.	0.2% YS MPa	0.2% YS (ksi)	UTS MPa	UTS (ksi)	Elong. %	R.A. %
			Room Temperature			
AT-262	921.1	(133.6)	1,252.8	(181.7)	5.2	11.9
(Ta free)	894.9	(129.8)	1,145.9	(166.2)	5.2	7.6
AT-264	863.2	(125.2)	1,078.3	(156.4)	5.9	6.5
(Ta free)	860.5	(124.8)	1,118.3	(162.2)	6.1	7.6
AT-265	903.9	(131.1)	1,050.8	(152.4)	5.7	7.6
(High Ta)	861.8	(125.0)	1,060.4	(153.8)	5.7	9.5
AT-266	900.5	(130.6)	1,071.4	(155.4)	6.0	6.5
(Low Ta)	883.2	(128.1)	1,065.2	(154.5)	6.8	8.4
			1144°K (1600°F)			
AT-262	367.5	(53.3)	367.5	(53.3)	12.2	27.6
(Ta free)	422.0	(61.2)	422.0	(61.2)	6.8	14.5
AT-264	349.6	(50.7)	349.6	(50.7)	6.6	16.4
(Ta free)	393.7	(57.1)	393.7	(57.1)	9.2	21.5
AT-265	479.9	(69.6)	479.9	(69.9)	5.9	17.5
(High Ta)	427.5	(62.0)	427.5	(62.0)	6.4	13.5
AT-266	464.7	(67.4)	464.7	(67.4)	5.2	13.5
(Low Ta)	458.5	(66.5)	458.5	(66.5)	6.4	15.6
			1366°K (2000°F)			
AT-262	111.0	(16.1)	111.0	(16.1)	6.5	12.4
(Ta free)	108.9	(15.8)	108.9	(15.8)	6.0	10.5
AT-264	106.9	(15.5)	106.9	(15.5)	7.6	18.5
(Ta free)	110.3	(16.0)	110.3	(16.0)	5.6	10.4
AT-265	104.1	(15.1)	104.1	(15.1)	6.4	22.2
(High Ta)	99.3	(14.4)	99.3	(14.4)	6.6	14.5
AT-266	108.2	(15.7)	108.2	(15.7)	6.9	13.5
(Low Ta)	106.2	(15.4)	106.2	(15.4)	10.5	22.2

TABLE 24

1366°K (2000°F) STRESS RUPTURE DATA FOR TASK III EXTRUSIONS

Extrusion No.	Specimen Orientation	Time at Stress to Rupture Hours/MPa (ksi)	Elong. %	R.A. %
AT-262	L	100/82.7 (12.0) + 9.3/89.6 (13.0)	6.5	12.2
	L	73.4/82.7 (12.0)	2.6	3.9
	T	100/34.5 (5.0) + 0.2/41.4 (6.0)	4.8	3.9
	T	82.7/34.5 (5.0)	4.7	3.5
AT-264	L	100/82.7 (12.0) + 2.8/89.6 (13.0)	5.9	8.6
	L	6.8/82.7 (12.0)	8.2	14.7
	T	65.5/34.5 (5.0)	4.9	4.3
	T	110.3/34.5 (5.0)	14.5	5.3
AT-265	L	55.3/82.7 (12.0)	10.2	22.3
	L	52.7/82.7 (12.0)	4.4	6.4
	T	100/34.5 (5.0) + 0.8/41.4 (6.0)	3.5	2.7
	T	39.7/34.5 (5.0)	2.3	4.4
AT-266	L	52.4/82.7 (12.0)	7.3	9.6
	L	17.1/82.7 (12.0)	4.9	10.3
	T	100/34.5 (5.0) + 24/41.4 (6.0) + 0.1/48.3 (7.0)	4.8	5.9
	T	40.7/41.4 (6.0)		

Allowing for this scatter, the 100 hour strength capability of the two tantalum extrusions is at 82.7 MPa (12 ksi) in the longitudinal direction and 34.5 MPa (5 ksi) in the transverse direction. The stress for 100 hour lives in the longitudinal direction is definitely less than 82.7 MPa (12 ksi) for both tantalum-containing materials and is more likely on the order of 79.2 MPa (11.5 ksi). Extrusion AT-266, which contained the low tantalum addition, has the highest transverse strength. Its stress for a 100 hour life is probably close to 37.9 MPa (5.5 ksi). The high tantalum extrusion, AT-265, appears to have a 100 hour transverse strength capability of 34.5 MPa (5 ksi).

DISCUSSION OF RESULTS

For the purpose of this discussion, the program can be divided into two parts. In the first of these, composed of Task I and Task II, the main aim was to establish the preferred aluminum and oxide contents in the alloy.. In the second part, composed of Task III, the aim was to scale up, to full vane blank size, an alloy with this optimum composition.

The material produced during Task I and Task II was in the form of small scale rectnagular cross sectioned extrusions which nominally contained 4%, 5% or 6% Al and either 0.8 w/o or 1.2 w/o Y_2O_3. With the exception of crystallographic texture, all materials either exceeded or were close to the 100 hour stress rupture goals of 82.7 MPa (12 ksi) in the longitudinal direction and 41.4 MPa (6 ksi) in the transverse direction. None, however, had the required texture. The major differences noted between the alloys became apparent during dynamic oxidation testing and in particular during the 500 hour test carried out by NASA-Lewis at 2000°F using a Mach 1 gas stream. While the optimum dynamic oxidation was observed with the materials containing nominally 6% Al, this resistance was much superior to that of two materials containing between 4.5 and 5% Al. These latter materials also had the advantages of showing less thermal fatigue distress during the oxidation test and of having a higher melting point than the 6% Al material. An aluminum content of 4.75 w/o was, therefore, chosen as the level to be used in the scaled up extrusions.

Two potential problems were observed to exist with the materials examined in Task I and Task II. The first of these was that prolonged aging at 1588°K (2400°F) led to a decrease in 1366°K (2000°F) stress rupture properties, presumably due to dispersoid instability. Although other experiments have indicated that the dispersoid does have adequate stability under even the most extreme of the anticipated use conditions, this point should be further investigated. The second potential problem is that all the materials examined had a higher than desirable elastic modulus in the longitudinal direction. Experience with other dispersion strengthened alloys indicated that this could be avoided by modifying the process used in powder production. The powders used in Task III were, therefore, manufactured by a modification of the process used to produce the earlier powders. The oxide content used was arbitrarily set at 1.8-2 w/o, again on the basis of previous experience.

In Task III two full scale extrusions of nominal composition Ni-16Cr-4.75Al-1.9Y_2O_3 were produced. Two additional full scale extrusions containing small

amounts of Ta were also produced. However, the presence of Ta had a detrimental effect on the texture of the material.

Only a very brief evaluation of the mechanical properties of the two tantalum free extrusions was carried out. All material was recrystallized using a procedure which is now regarded as less than optimum. This involved placing the material in a furnace at 1477°K (2200°F), raising the furnace temperature over a period of approximately two hours to 1616°K (2450°F), holding for one hour, and then cooling.

Stress rupture strengths at 1366°K (2000°F) met the program goal of 100 hours at a stress of 82.7 MPa (12 ksi) in the longitudinal direction but fell short of the transverse goal of 100 hours at a stress level of 41.4 MPa (6 ksi). The rupture capability obtained at a stress level of 34.5 MPa (5 ksi) was still well within the strength range of interest to engine designers, however. An initial evaluation of texture carried out by determining the elastic moduli in longitudinal pins taken near the short sides of the rectangular cross section indicated that the desired texture had been achieved in both extrusions. However, it is now believed that if these pins had been taken from near to the center of the cross section than higher, and possibly unacceptably higher, values would have been observed. Our experience with an alloy which is similar to the above apart from the fact that it contains only 4% Al suggests that improved transverse stress rupture properties and a more correctly textured material could be obtained with no sacrifice in longitudinal strength, by the use of alternate recrystallization heat treatments.

CONCLUDING REMARKS

While the present study has been successful in defining a material with great potential for future application, it should be noted that this material is still not optimized. Areas which require further definition are the effect of variations in the oxide content of the alloy and of the recrystallization heat treatment on the development of crystallographic texture and mechanical properties. Recent studies at Cabot Corporation on a material with a matrix composition of Ni-16Cr-4Al have shown that manipulation of the oxide content and heat treatment are very important to optimizing properties and this technology needs to be applied to the optimized Ni-16Cr-4.75Al matrix.

A further topic requiring additional study is the effect of long time, high temperature exposure on mechanical properties. While the heat treatment which was found to degrade the 1366°K (2000°F) strength properties of the small scale extrusions is more severe than the material is likely to see in actual application, the presence of some form of instability certainly warrants attention being paid to this topic. Material from the four full scale extrusions will be provided to NASA and it is planned that a more detailed evaluation will be carried out.

APPENDIX A

SPECIMEN CONFIGURATIONS

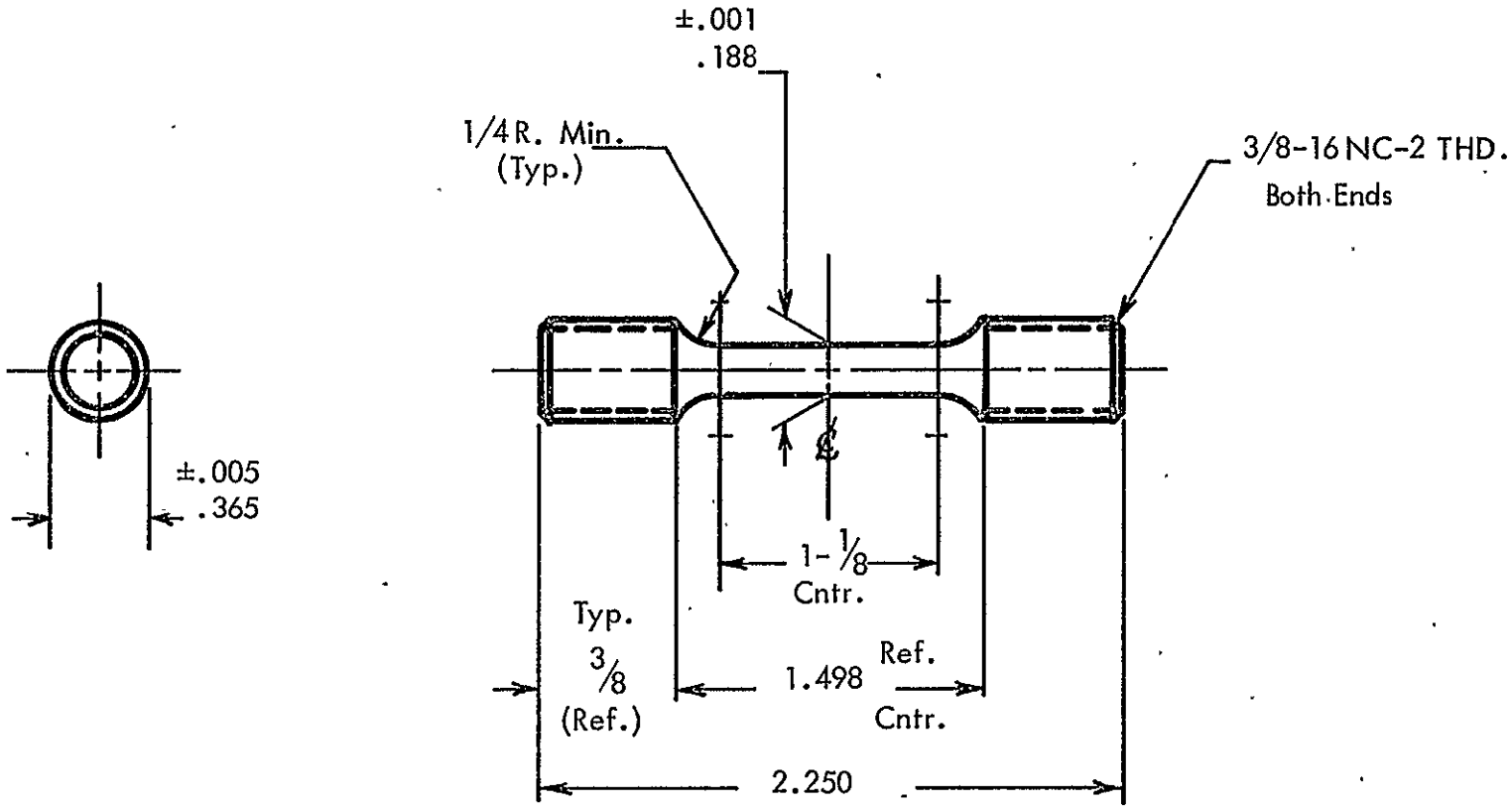

Tensile and Stress Rupture Specimen

(B/P No. 560027)

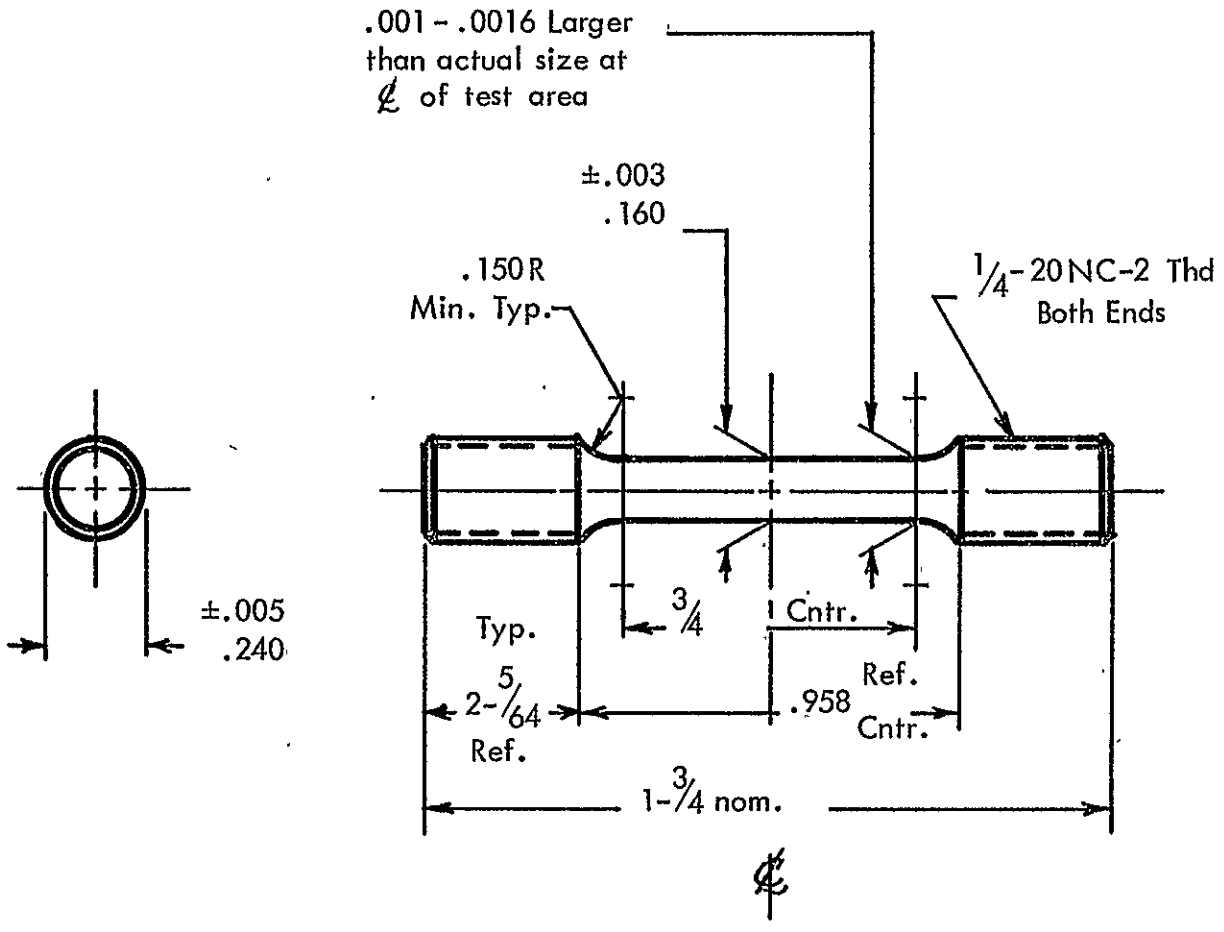

Longitudinal Tensile and Stress Rupture Specimen

(B/P No. 561170)

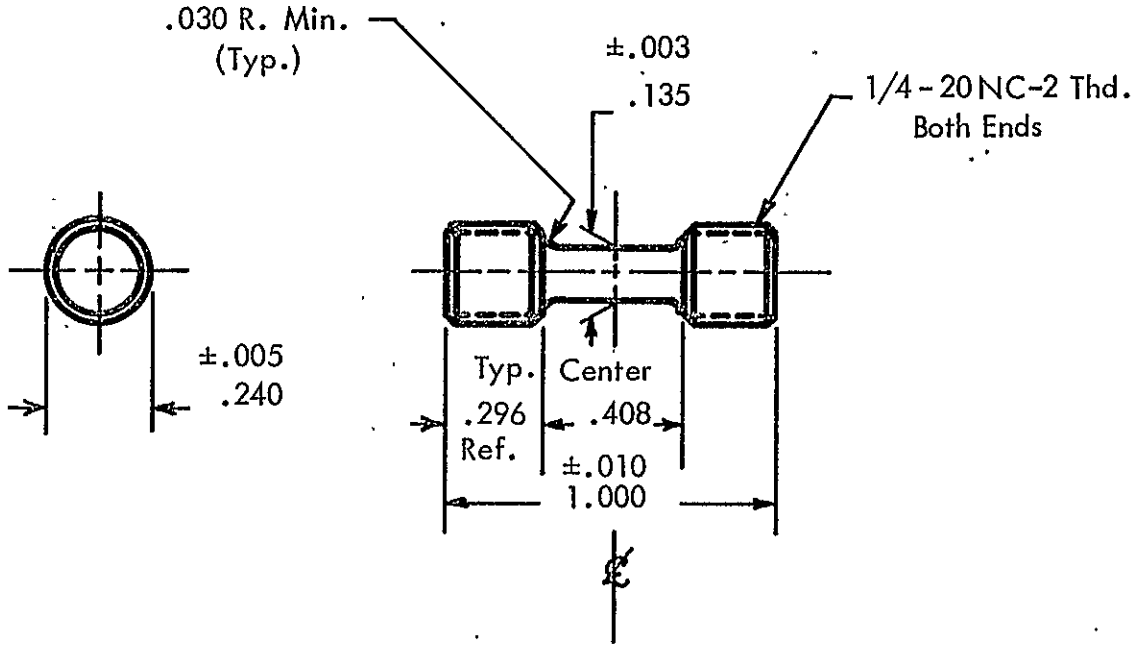

Transverse Stress Rupture Specimen
(B/P No. 560274 - 209904)

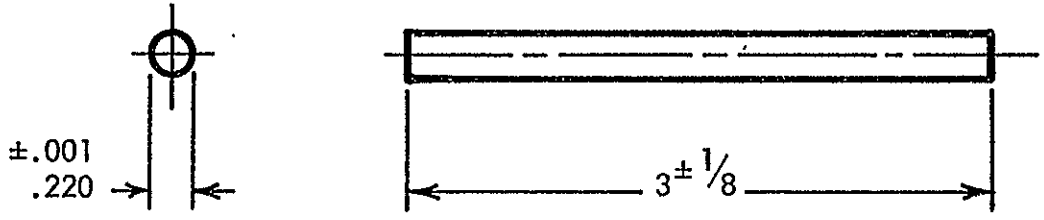

Sonic Modulus and Dynamic Oxidation Specimen

(B/P No. 563463)

REFERENCES

1. Klingler, L. J., Weinberger, W. R., Bailey, P. G., and Baranow, S., "Development of Dispersion Strengthened Nickel-Chromium (Ni-Cr-ThO_2) Sheet for Space Shuttle Vehicles", NASA CR-120796, 1971.

2. Johnston, J. R. and Ashbrook, R. L., "Oxidation and Thermal Fatigue Cracking of Nickel- and Cobalt-Base Alloys in the High Velocity Gas Stream", NASA TN D-5376, 1969.

DISTRIBUTION LIST FOR NASA CR-134901

CONTRACT NAS3-17806

(THE NUMBER IN PARENTHESES SHOWS HOW MANY COPIES IF MORE THAN ONE ARE TO BE SENT TO AN ADDRESS.)

MR. J. ACURIO
MS 77-5
NASA LEWIS RESEARCH CTR.
21000 BROOKPARK ROAD
CLEVELAND, OHIO 44135

MR. A.E. ANGLIN
MS 49-3
NASA LEWIS RESEARCH CTR.
21000 BROOKPARK ROAD
CLEVELAND, OHIO 44135

MR. A. ARIAS
MS 49-3
NASA LEWIS RESEARCH CTR.
21000 BROOKPARK ROAD
CLEVELAND, OHIO 44135

DR. R.L. ASHBROOK
MS 49-3
NASA LEWIS RESEARCH CTR.
21000 BROOKPARK ROAD
CLEVELAND, OHIO 44135

MR. G.M. AULT
MS 3-5
NASA LEWIS RESEARCH CTR
21000 BROOKPARK ROAD
CLEVELAND, OHIO 44135

MR. C.A. BARRETT
MS 49-3
NASA LEWIS RESEARCH CTR.
21000 BROOKPARK ROAD
CLEVELAND, OHIO 44135

MR. C.P. BLANKENSHIP
MS 105-1
NASA LEWIS RESEARCH CTR
21000 BROOKPARK ROAD
CLEVELAND, OHIO 44135

MR. J.C. FRECHE
MS 49-1
NASA LEWIS RESEARCH CTR
21000 BROOKPARK ROAD
CLEVELAND, OHIO 44135

MR. T.K. GLASGOW
MS 49-3
NASA LEWIS RESEARCH CTR.
21000 BROOKPARK ROAD
CLEVELAND, OHIO 44135

MR. S.J. GRISAFFE
MS 49-3
NASA LEWIS RESEAPCH CTR
21000 BROOKPARK ROAD
CLEVELAND, OHIO 44135

MR. R.W. HALL
MS 49-1
NASA LEWIS RESEARCH CTR
21000 BROOKPARK ROAD
CLEVELAND, OHIO 44135

MR. M.H. HIRSCHBERG
MS 49-1
NASA LEWIS RESEARCH CTR.
21000 BROOKPARK ROAD
CLEVELAND, OHIO 44135

MR. C.E. LOWELL
MS 49-3
NASA LEWIS RESEARCH CTR.
21000 BROOKPARK ROAD
CLEVELAND, OHIO 44135

M & S DIVISION FILES
MS 49-1
NASA LEWIS RESEARCH CTR
21000 BROOKPARK ROAD
CLEVELAND, OHIO 44135

RESEARCH LIBRARY
UNITED TECHNOLOGIES CORP
400 MAIN STREET
EAST HARTFORD, CT
06108

DR. M.J. DONACHIE
PRATT & WHITNEY AIRCRAFT
UNITED TECHNOLOGIES CORP
400 MAIN STREET
EAST HARTFORD, CT 06108

DR. M.L. GELL
PRATT & WHITNEY AIRCRAFT
UNITED TECHNOLOGIES CORP
400 MAIN STREET
EAST HARTFORD, CT 06108

DR. R. BEGLEY
WESTINGHOUSE RESEARCH LAB
BEULAH ROAD
PITTSBURGH, PENNSYLVANIA
15235

MR. G.I. FRIEDMAN
NUCLEAR METALS
WHITTAKER CORPORATION
WEST CONCORD, MA
01781

MR. M. QUATINETZ
CONSULTANT
30225 WOLF ROAD
BAY VILLAGE, OH
44140

MR. R.W. FRASER
SHERRITT-GORDON MINES
FORT SASKATCHEWAN
ALBERTA
CANADA

DR. L.F. NORRIS
SHERRITT-GORDON MINES
FORT SASKATCHEWAN
ALBERTA
CANADA

MR. D.H. TIMBRES
SHERRITT-GORDON MINES
FORT SASKATCHEWAN
ALBERTA
CANADA

MR. P.G. BAILEY
AEG/GED
GENERAL ELECTRIC COMPANY
CINCINNATI, OHIO 45215

MR. E. KERZENIK
AEG/GED
GENERAL ELECTRIC COMPANY
CINCINNATI, OHIO 45215

MR. E.S. NICHOLS PT.8 T2B
DETROIT DIESEL ALLISON DV
P.O. BOX 894
INDIANAPOLIS, IN 46206

MR. R.J. NYLEN
HOMOGENOUS METALS INC.
WEST CANADA BLVD
HERKIMER, N.Y. 13350

MR. J.V. LONG
SOLAR DIVISION
INTERNATIONAL HARVESTER
2200 PACIFIC HIGHWAY
SAN DIEGO, CAL. 92112

DR. J. BENJAMIN
INTERNATIONAL NICKEL CO.
MERICA RESEARCH LAB
STERLING FOREST
SUFFERN, NY 10901

MR. J. DEBORD
HUNTINGTON ALLOYS DIV.
INTERNATIONAL NICKEL CO.
HUNTINGTON, WV 25720

MR. T. MILES
KELSEY HAYES CORPORATION
7250 WHITMORE LAKE ROAD
BRIGHTON, MI 48116

TECHNICAL INFORMATION CTR.
MATLS. & SCIENCE LAB.
LOCKHEED RESEARCH LABS
3251 HANOVER STREET
PALO ALTO, CAL. 94304

LIBRARY MSFD
MCDONNELL DOUGLAS CORP.
3000 OCEAN PARK BLVD
SANTA MONICA, CAL. 90406

MR. R. JOHNSON
MCDONNELL DOUGLAS CORP
A3-833 MS 9
HUNTINGTON BEACH, CA
92647

DR. W. KOSTER
METCUT RESEARCH. ASSOC.
3980 ROSSLYN DR.
CINCINNATI, OH 45209

LIBRARY
ROCKWELL INTERNATIONAL
ROCKETDYNE DIVISION
6633 CANOGA AVENUE
CANOGA PARK, CA 91304

DR. S. BARANOW
SPECIAL METALS
CORPORATION
NEW HARTFORD, N.Y. 13413

MR. A.R. KAUFMAN
TEXTRON INC.
WEST CONCORD, MA
01781

DR. H.E. COLLINS
MATERIALS TECHNOLOGY
TRW EQUIPMENT GROUP
23555 EUCLID AVENUE
CLEVELAND, OHIO 44117

MR. R.A. LULA
ALLEGHENY LUDLUM
STEEL CORP.
BRACKENRIDGE, PENNA.
15014

MR. L.J. FIEDLER
AVCO LYCOMING DIV.
550 S.MAIN STREET
STRATFORD, CT 06497

DR. D. WEBSTER
BOEING COMPANY
M.A.S.D.
SEATTLE, WA 98124

DR. R. GRIERSON
STELLITE DIVISION
CABOT CORPORATION
1020 W. PARK AVENUE
KOKOMO, IN 46901

DR. S.T. WLODEK
STELLITE DIVISION
CABOT CORPORATION
1020 W. PARK AVE
KOKOMO, IN 46901

LIBRARY
CABOT CORPORATION
STELLITE DIVISION
P.O. BOX 746
KOKOMO, INDIANA 46901

DR. D.R. MUZYKA
CARPENTER TECHNOLOGY CORP
RES. & DEV. CENTER
P.O. BOX 662
READING, PA 19603

DR. D.L. SPONSELLER
CLIMAX MOLYBDENUM COMPANY
1600 HURON PARKWAY
ANN ARBOR, MICHIGAN 48106

DR. M. ASHBY
FORDON MCKAY LABORATORY
6 OXFORD STREET
CAMBRIDGE, MA 02138

DR. R.F. KIRBY
CHIEF, MATERIALS ENG.
GARPETT AIRESEARCH
402 S. 36TH STREET
PHOENIX, AR 85034

MR. R.T. TORGERSON
CONVAIR AEROSPACE DIV.
GENERAL DYNAMICS CORP.
P.O. BOX 1128
SAN DIEGO, CA 92112

MR. H.H. HIRSCH
CRD
GENERAL ELECTRIC COMPANY
P.O. BOX 8
SCHENECTADY, N.Y. 12301

LIBRARY
ADVANCED TECHNOLOGY LAB
GENERAL ELECTRIC COMPANY
SCHENECTADY, NY 12345

MR. C.T. SIMS
GAS TURBINE PROD.DIV.
GENERAL ELECTRIC COMPANY
SCHENECTADY, N.Y. 12345

MR. G.E. WASIELEWSKI
MATERIALS & PROCESSES LAB
GENERAL ELECTRIC COMPANY
SCHENECTADY, N.Y. 12345

TECHN. INFORMATION CENTER
AEG
GENERAL ELECTRIC COMPANY
CINCINNATI, OHIO 45215

MR. I. MACHLIN AIR-52031B
NAVAL AIR SYSTEMS COMMAND
NAVY DEPARTMENT
WASHINGTON, DC 20361

TECHNICAL REPORTS LIBRARY
ERDA
WASHINGTON, DC
20545

MR. R.W. SWINDEMAN
OAK RIDGE NATIONAL LAB
OAK RIDGE, TN 37830

MR. M.I. COPELAND
DEPT. OF INTERIOR
BUREAU OF MINES
P.O. BOX 70
ALBANY, OR 97321

MR. W.C. MCBEE
DEPT. OF INTERIOR
BUREAU OF MINES
P.O. BOX 70
ALBANY, OR 97321

DR. B.A. WILCOX
NATIONAL SCIENCE
FOUNDATION
WASHINGTON, DC 20550

DR. A.H. CLAUER
BATTELLE MEMORIAL INST.
505 KING AVENUE
COLUMBUS, OHIO 43201

MCIC
BATTELLE MEMORIAL INST.
505 KING STREET
COLUMBUS, OHIO 43201

MR. J.B. MITCHELL
LAWRENCE RADIATION LAB.
UNIVERSITY OF CALIFORNIA
LIVERMORE, CA 94559

PROF. L.J. EBERT
DEPT. OF MET. & MAT. SCI
CASE - WESTERN RESERVE U
CLEVELAND, OH 44106

DR. J.K. TIEN
HENRY KRUMB SCH. OF MINES
COLUMBIA UNIVERSITY
NEW YORK, NY 10027

PROF. N.J. GRANT
DEPT. OF METALLURGY
MASS. INST. OF TECHNOLOG
CAMBRIDGE, MA 02139

PROF. G.S. ANSELL
RENSSELAER POLYTECHNICAL
INSTITUTE
TROY, NY 12100

PROF. O. SHERBY
DEPT. OF MATERIALS SCI.
STANFORD UNIVERSITY
PALO ALTO, CALIF. 94305

DR. J. COLWELL
AEROSPACE CORPORATION
PO BOX 95085
LOS ANGELES, CA 90045

MR. L.E. KINDLIMANN
ALLEGHENY LUDLUM
STEEL CORP.
BRACKENRIDGE, PENNA.
15014

MR. B.A. STEIN MS 188A
NASA
LANGLEY RESEARCH CENTER
LANGLEY FIELD, VA 23365

MR. E. HASEMEYER
NASA SSE-PE-MWM
MARSHALL SPACE FLIGHT
CENTER
HUNTSVILLE, AL 35812

LIBRARY
NASA
MARSHALL SPACE FLIGHT
CENTER
HUNTSVILLE, AL 35812

MR. M.A. SILVEIRA
NASA
JOHNSON SPACE CENTER
HOUSTON, TX 77058

TECHNICAL LIBRARY / JM6
NASA
JOHNSON SPACE CENTER
HOUSTON, TX 77058

LIBRARY - ACQUISITIONS
JET PROPULSION LAB.
4800 OAK GROVE DRIVE
PASADENA, CA 91102

LIBRARY
NASA FLIGHT RESEARCH CTR
P.O. BOX 273
EDWARDS, CALIFORNIA 93523

MR. F. CENTOLANZI
MS 234-1
NASA AMES RESEARCH CENTER
MOFFETT FIELD, CA 94035

LIBRARY - REPORTS
MS 202-3
NASA AMES RESEARCH CENTER
MOFFETT FIELD, CA 94035

ACQUISITIONS BRANCH (10)
NASA SCIENTIFIC & TECHN.
INFORMATION FACILITY
BOX 33
COLLEGE PARK, MD 20740

DEFENCE DOCUMENTATION CTR
CAMERON STATION
5010 DUKE STREET
ALEXANDRIA, VIRGINIA
22314

MR. J.K. ELBAUM
AFML/LP
HEADQUARTERS
WRIGHT PATTERSON AFB,
OH 45433

MR. N. GEYER
AFML/LLP
HEADQUARTERS
WRIGHT PATTERSON AFB,
OH 45433

MR T. NORBUT
AFAPL/TBP
HEADQUARTERS
WRIGHT PATTERSON AFB,
OH 45433

TECHNICAL LIBRARY
AFML/LAM
HEADQUARTERS
WRIGHT PATTERSON AFB.
OH 45433

MR. S.V. ARNOLD AMXMR-XW
ARMY MATERIALS AND
MECHANICS RESEARCH CTR.
WATERTOWN, MA 02172

DR. H.B. PROBST
MS 49-3
NASA LEWIS RESEARCH CTR.
21000 BROOKPARK ROAD
CLEVELAND, OHIO 44135

MR. P.F. SIKORA
MS 49-3
NASA LEWIS RESEARCH CTR.
21000 BROOKPARK ROAD
CLEVELAND, OHIO 44135

DR. J.D. WHITTENBERGER (25)
MS 105-1
NASA LEWIS RESEARCH CTR.
21000 BROOKPARK ROAD
CLEVELAND, OHIO 44135

LIBRARY (2)
MS 60-3
NASA LEWIS RESEARCH CTR
21000 BROOKPARK ROAD
CLEVELAND, OHIO 44135

REPORT CONTROL OFFICE
MS 5-5
NASA LEWIS RESEARCH CTR
21000 BROOKPARK ROAD
CLEVELAND, OHIO 44135

MAJ. F. GASPERICH
AFSC LIAISON MS 501-3
NASA LEWIS RESEARCH CTR
21000 BROOKPARK ROAD
CLEVELAND, OHIO 44135

MR G. C. DEUTSCH / RW
NASA HEADQUARTERS
WASHINGTON, DC
20546

MR. J. MALAMENT / MTG
NASA HEADQUARTERS
WASHINGTON, DC
20546

MR. N.T. SAUNDERS
MS 105-1
NASA LEWIS RESEARCH CTR
21000 BROOKPARK ROAD
CLEVELAND, OHIO 44135

MR. J.W. WEETON
MS 49-3
NASA LEWIS RESEARCH CTR.
21000 BROOKPARK ROAD
CLEVELAND, OHIO 44135

CONTRACTS SECTION B
MS 500-313
NASA LEWIS RESEARCH CTR
21000 BROOKPARK ROAD
CLEVELAND, OH 44135

PATENT COUNSEL
MS 500-113
NASA LEWIS RESEARCH CTR
21000 BROOKPARK ROAD
CLEVELAND, OHIO 44135

TECHNOLOGY UTILIZATION
MS 3-19
NASA LEWIS RESEARCH CTR
21000 BROOKPARK ROAD
CLEVELAND, OHIO 44135

MR. W.S. AIKEN /RT
NASA HEADQUARTERS
WASHINGTON, DC
20546

MR. J. GANGLER / RWM
NASA HEADQUARTERS
WASHINGTON, DC
20546

MR. W.N. GARDNER
JOINT DOT/NASA CARD
IMPLEMENTATION OFFICE
400 7TH AVENUE, SW
WASHINGTON, DC 20590